1986

The structural controls of the Vale Rhinehart Buttes complex, Vale KGRA, Malheur County, Oregon

John Timothy Doerr
Portland State University

ABSTRACT OF THE THESIS OF John Timothy Doerr for the Master of Science in Geology presented November 24, 1986.

Title: The Structural Controls of the Vale Rhinehart Buttes Complex, Vale KGRA, Malheur County, Oregon.

APPROVED BY MEMBERS OF THE THESIS COMMITTEE:

[redacted]

Gilbert T. Benson, Chairman

[redacted]

Ansel G. Johnson

[redacted]

Paul E. Hammond

The Vale KGRA is characterized by high heat flow, two to five times higher than the worldwide average, and by numerous hot springs. The hot springs are aligned along faults. This phenomena is typical of a Basin and Range type geothermal system. The hot geothermal fluids migrate upward along the more permeable, fault planes.

The rocks exposed in the Vale area are the Pliocene Chalk Butte formation and the Pleistocene beds of Captain Keeney Pass. Both units are composed of volcaniclastic siltstones, sandstones and conglomerates. The units are differentiated by color, texture and degree of lithification. About 200 meters of the Chalk Butte formation and 100 meters of the beds of Captain Keeney Pass are exposed in the

area. Silicification is wide spread in the rocks of the Chalk Butte formation.

The structure of the Vale area is dominated by north to northwest trending faults. To the north are the Willow Creek fault and the Bully Creek fault. These two faults have been identified north of the study area and continue through the area. The main faults in the study area are the north trending Rhinehart fault, the northwest trending Willow Creek Fault, and two unnamed northwest trending faults. One of the unnamed faults is located east of Vale Butte and the other is located in the southwest portion of the study area.

The central portion of the Vale horst, the area of Vale Butte and Rhinehart Buttes, contains the Rhinehart fault and the Willow Creek fault and is characterized by many small normal faults. These small faults occur as either en echelon or horst and grabens and are oblique to the main trends in the area.

Rhinehart Buttes is an erosionally resistant fossil hot spring, cored by a silicified zone centered on the north trending Rhinehart fault. Many of the ridges which extend from Rhinehart Buttes are also cored by silicified zones. The silicified rocks are more resistant than the country rocks and the silicified areas adjoining the faults tend to form linear ridges. Vale Butte consists of Chalk Butte formation siltstones interbedded with silicified conglomerates which protect the siltstones from erosion.

The extent and degree of silicification is controlled by both the structure and rock type. The areas of the highest degree of

silicification and secondary mineralization of quartz, calcite and selenite occur at the intersection of faults. The intensity of silicification decreases away from fault intersections. This decrease occurs both along the strike of the fault and perpendicular to the strike. The areal extent of silicification is highest in open framework, clast supported conglomerates. Silicification deceases according to permeability. Coarse grained clast supported sandstones show somewhat lesser silicification while in siltstones the silicification is limited to areas immediately adjoining the faults intersections.

Gravity and magnetic modeling agrees with the interpretation of the major structures of the area. The gravity models depict an upper layer of volcaniclastic sediments of low density, 2.1 g/cm^3 overlying the subsurface Grassy Mountain Basalt at a depth of about 200 meters, which has been offset by a series of small normal faults. A number of these faults appear to have offset the Grassy Mountain Basalt. The locations of these faults found by gravity modeling agree with faults mapped in the field.

Between the north side of Rhinehart Buttes and the Malhuer River, a local hot water aquifer is contained in the recent sediments. The temperature of the water in the aquifer increases toward the southeast. The structure controlling the entrance of geothermal fluids into the acquifer is believed to be a silicified fault trending west northwest at the north end of Rhinehart Butte.

THE STRUCTURAL CONTROLS OF THE VALE RHINEHART BUTTES COMPLEX, VALE KGRA, MALHEUR COUNTY, OREGON

by

JOHN TIMOTHY DOERR

A thesis submitted in partial fulfillment of the requirements for the degree of

MASTER OF SCIENCE
in
GEOLOGY

Portland State University

1986

TO THE OFFICE OF GRADUATE STUDIES AND RESEARCH:

The members of the Committee approve the thesis of John Timothy Doerr presented November 24, 1986.

[redacted]

G. Thomas Benson, Chairman

[redacted]

Ansel G. Johnson

[redacted]

Paul E. Hammond

APPROVED:

[redacted]

Paul E. Hammond, Chairman, Department of Geology

[redacted]

Bernard Ross, Dean of Graduate Studies and Research

ACKNOWLEDGEMENTS

I would like to acknowledge and thank those who have provided me with the support and guidence to complete this study. First I would like to thank the members of Renewable Energy Inc. who have allowed me to use the data. In particular, I would like to thank Mr. Robert O. Walston, the project manager, who aided me in doing so many of the tasks in this project. I would like to thank the members of my advisory committee, Dr. Gilbert T. Benson, Dr. Ansel G. Johnson, and Dr. Paul E. Hammond, for their efforts, advice, and support. I also would like to thank Cindy Stine for her help with the more mundane and unrewarding tasks in preparing the manuscript. Lastly and most importantly I would like to thank my wife, Sharon, for her support, both financial and emotional without which I never would have finished this project.

TABLE OF CONTENTS

LIST OF FIGURES

CHAPTER I

INTRODUCTION

The Vale area has been under investigation to utilize the geothermal potential, since its designation as a Known Geothermal Resource Area (KGRA). The geothermal potential is manifested by an unusually high heat flow and by hot springs located near the base of Rhinehart Buttes (Bowen and Blackwell, 1975). The location of the hot springs is evidence that the upwelling geothermal fluids are being controlled by the geologic structure (Bowen and Blackwell, 1975).

Purpose of the Study

Previous investigations conducted within the Vale KGRA have been primarily on a regional scale, aimed at identifying large scale geologic features. Very little detailed work which would be directly applicable to the commercial utilization of the energy potential which may exist in the Vale KGRA has been published. The purpose of this investigation is to use field mapping, and gravity and magnetic surveys, to delineate the detailed structure of the area around Vale. By investigating and detailing the structures of the Vale area, those which are acting as controls on the upper portion of the geothermal system are also to be delineated. The structural detail found in this investigation when added to previous work enhances our knowledge of

the Vale KGRA.

The purpose of the gravity survey is to define and delineate structures which occur within 500 meters of the suface to define the various fault systems which occur throughout the Vale area.

The magnetic survey is used to detect those structures which extend to the magnetic basement. The depth, orientation, and the amount of offset in the magnetic basement has been obtained through modeling of the data obtained in the magnetic survey.

The field mapping has examined physical evidence for, and delineated those structures which extend to the surface. However, many of these structures may not be detectable through field mapping alone. The use of aerial photographs allows the tracing of many of these fault systems.

The results from each of the study techniques will be first examined separately. The results will then be correlated and compared. The several lines of independant evidence then allow a composite picture of the structure to be developed. The field mapping supplied data for the location of the structures on the surface. Gravity and magnetic surveys supplied data on those structures which extend to various depths beneath the surface.

Geographic Setting

The Vale KGRA is located in eastern Oregon, about 30 kilometers west of the Idaho border, as noted in figure 1. In general, topography in the area is controlled by the resistance of the country rock to

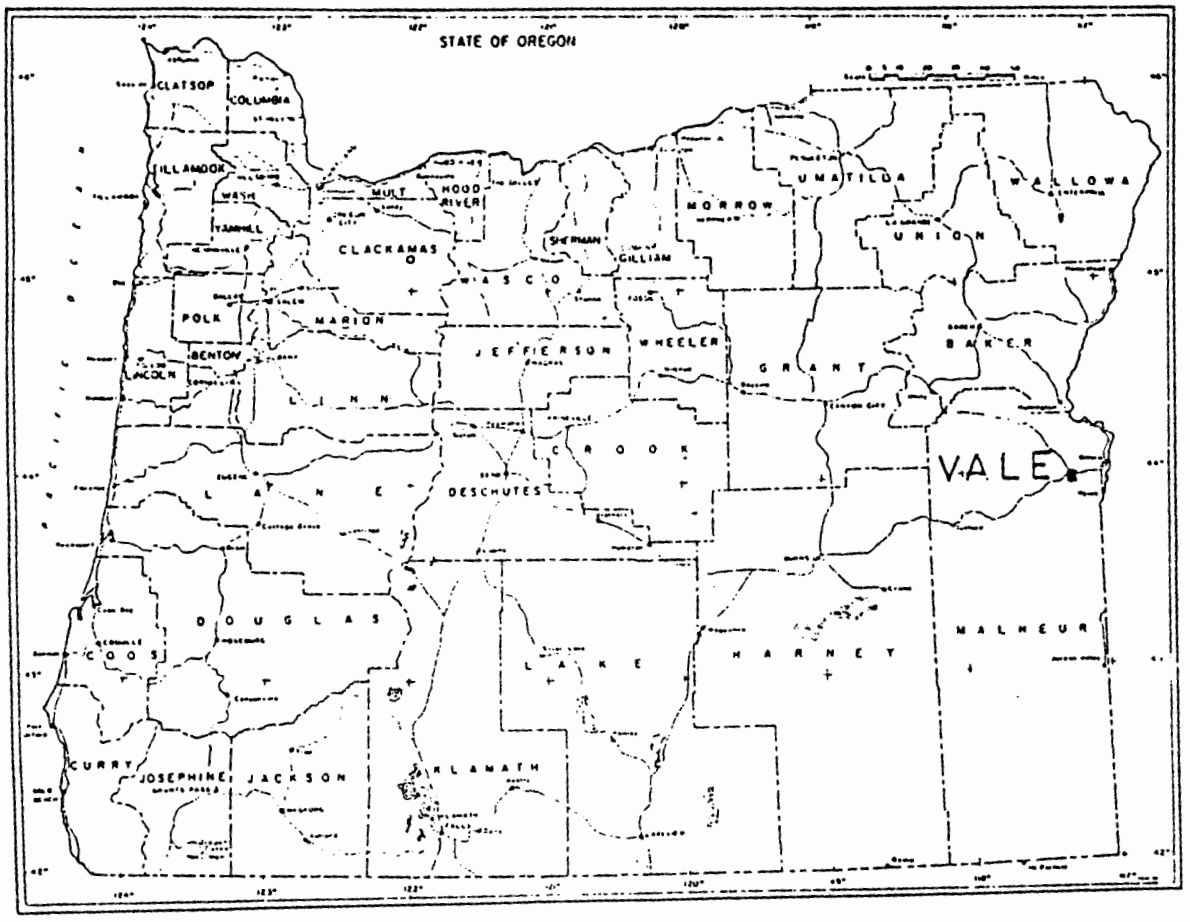

Figure 1. Location diagram of the study area

erosion. Where the country rock is weakly or poorly consolidated the topography consists of rolling hills of low relief. The areas of higher elevation and more rugged relief are generally underlain by more resistant volcanic or intrusive rocks.

The town of Vale is located in the Malheur River valley. The Malheur River flows east and empties into the Snake River near Ontario, Oregon. The area is surrounded on the northern, western, and southern sides with highlands which descend gradually toward the Snake and Malheur Rivers.

Thirty kilometers to the south are the closest upland areas, the Owyhee highlands. The Owyhee highlands are composed of resistant rocks, the Owyhee Basalt and the Idavada Volcanics. The elevations are in excess of 1800 meters. The highlands to the west are similar to the Owyhee area, rising to about the same elevation and composed of resistant igneous rocks. To the north rises the upland of Juniper Mountain, at an elevation of 2000 meters.

The study area is located in the northwest portion of the Vale East 7.5 minute quadrangle. The topography consists generally of rounded hills of moderate relief, with the exception of Rhinehart and Vale Buttes. The Buttes are composed of more resistant rocks and are an area of rugged relief. Vale Butte is the highest elevation in the quadrangle at 965.9 meters. The town of Vale lies at the foot of Rhinehart Buttes with an elevation of about 684 meters, which is the lowest point in the area.

The climate is semi-arid, with an annual precipitation of about 25 cm, is largely confined to winter and early spring. The temperature

varies from a winter minima of -16° C to a summertime maximum of about 30° C (Kittleman, 1967).

Vegetation is sparse and consists of grasses, varieties of sage, and junipers which are found in areas of higher elevation and more precipitation. The vegetation within the study area consists of both long and short grasses and sagebrush. The vegetation was never too thick to impede access, particularly foot travel, and was short enough to ensure ease of surveying, even at long distances cross country.

The region is sparsly populated, and there are few hard surfaced roads. Although there are many unpaved roads and jeep trails these are only seasonably passable and generally only to four wheel drive vehicles. Of historical note, Lytle Boulevard which runs south-east from Vale through the study area follows the route of the Oregon Trail (see, Plate I) which is still visible as deep ruts in some parts of the area.

Previous Work

Cope (1883), compiled the first reconnaissance maps of the area around Vale. Working on what he believed to be the sediments of ancient Lake Idaho, he mapped them in the Vale area and areas to the east in Idaho. The older Payette beds of western Idaho and the Snake River plains of Oregon were mapped by Lindgren (1898).

The area of the Owyhee upland was studied by Bryan (1929) who mapped the Payette and Idaho formations as seperate units. Renick (1930) worked in the eastern part of the Owyhee region. Work by Kirkham (1931) was done mainly in the Snake River plain and summarized

the work of previous authors concerning the Idaho and Payette formations. The units present in the Owyhee upland are not exposed in the study area, but are stratigraphically lower than those exposed around Vale and may underly the Vale area.

In 1953, the Mitchell Butte 30 minute quadrangle was mapped as University of Oregon Master's theses by Corcoran, Doak, Porter, Pritchett and Privrasky. The Vale area is located in the northern central portion of the Mitchell Butte quadrangle. The geologic map prepared by Corcoran et al, was presented in 1962.

Another series of theses, both Ph.d. and Masters were done in the Owyhee region in the early 1960's. Johnson (1961) compiled the stratigraphy of the Deer Butte Formation. Russell, (1961) Green (1962) McMurray (1962) Weeden (1962) and Kittleman (1962) and Hagood (1963) all mapped portions of the Owyhee region. These theses were compiled by Kittleman (Kittleman et al, 1965). The areas mapped all lie south of the Vale area and are stratigraphically lower than those units exposed in the study area. Certainly some of these units underly the Vale area, and some of them such as the Owyhee Basalt are potentially excellent geothermal reservoir rocks.

The stratigraphy of the Western Snake River plain, which includes portions of the Owyhee region was described by Malde and Powers (1962). In 1982 Brown provided a detailed map of the Vale East 7.5 minute quadrangle.

CHAPTER II

REGIONAL GEOLOGY

Regional Geologic History

There are 5400 meters of Cenozoic rocks exposed in south eastern Oregon (Kittleman et al, 1965). The rocks range in age from the late, or possibly middle, Miocene through the Pleistocene. The ages obtained are based both on mammalian fossil assemblages and radiometeric dating techniques (Kittleman et al, 1965). As a whole the stratigraphic sequence can be described as a complex series of lenticular sedimentary deposits with intercalated volcanic flows deformed by both syndepositional and postdepositional Basin and Range style faulting (Kittleman et al, 1965). The volcanic rocks range from effusive basalts to rhyolite and explosive rhyolitic ash flow tuffs. Although there are no volcanic rocks exposed in the study area, some or all of these rocks may underly the area at depth. The sedimentary beds are primarily volcaniclastic in nature, but there are a few units which contain a significant portion of granitic detritus. The sediments were deposited in both fluvial and lacustrine, continental environments in a

series of discreet north trending basins (Kittleman et al 1965).

The oldest rocks exposed in south-eastern Oregon are those of the Sucker Creek Formation. The Sucker Creek Formation is composed of predominantly volcaniclastic sediments with intercalated volcanics. Evernden and James (1964) reported a date of 16.7 my obtained by potassium argon dating from a basalt flow near the base of the formation.

The Sucker Creek Formation is unconformably overlain by the late Miocene Owyhee Basalt. The Owyhee Basalt is a thick multiple flow sequence composed of at least 12 flows (Kittleman et al, 1965). An unconformity marks the contact between the Owyhee Basalt and the overlying Deer Butte Formation. The Deer Butte Formation is primarily volcaniclastic in nature, with some intercalated basalt flows and some widespread conglomerate beds composed primarily of granitic detritus (Johnson, 1962; Kittleman et al, 1965). Kittleman et al (1965) has suggested that the occurrence of the granitic conglomerates is due to the filling of the depositional basin, with the conglomerate beds encroaching from the normal position of peripheral deposition. The Deer Butte Formation is late Miocene to early Pliocene in age (Kittleman et al 1965).

Unconformably overlying the Deer Butte Formation is the Grassy Mountain Formation. Kittleman et al (1965) revised the stratigraphic nomenclature to upgrade the Grassy Mountain Basalt to the Grassy Mountain Formation. This revision was necessitated because the Grassy Mountain unit was not entirely composed of basalt. As part of the revision all post Deer Butte, pre Grassy Mountain Basalt sediments were

included in the Grassy Mountain Formation. This involved the relegation of the Corcoran et al (1962) Kern Basin Formation to the status of a member of the Grassy Mountain Formation. The lower members of the Grassy Mountain Formation, such as the Kern Basin member are primarily volcaniclastic in compostion. The age of the Grassy Mountain Formation is given in Storm (1975) as early to middle Pliocene. The Grassy Mountain Formation does not crop out in the study area, although the basalt member has been encountered in drilling operations (Brown, 1982).

The Grassy Mountain Basalt was described by Bryan (1929) as massive basalt, with flows up to 40 meters thick and intercalated sediments. The total thickness may exceed 350 meters (Newton and Corcoran 1963). Storm (1975) gave an estimated total thickness of 700 meters to 900 meters. The total thickness of the Grassy Mountain Formation was listed as 750 meters to 1050 meters, based on drilling logs by Bowen and Blackwell (1975). The Grassy Mountain Formation unconformably overlies the Deer Butte Formation of Corcoran (1962). The Grassy Mountain Formation, which underlies the Chalk Butte Formation in the Vale area (Brown, 1982) is suggested by Bowen and Blackwell (1975) to contain an excellant geothermal reservoir rock in the Grassy Mountain Basalt member.

Unconformably capping the Grassy Mountain Formation are a series of volcaniclastic beds mapped by Corcoran et al (1962) as the Chalk Butte Formation. The Chalk Butte Formation occurs above the Grassy Mountain Basalt member of the Grassy Mountain Formation, which is the basis of the division between these two formations. The beds of the

Chalk Butte Formation have been assigned an age of Blancan, though Brown (1982) suggested that they may be as old as Hemphillian. The environment of deposition, is fluvial and lacustrine (Corcoran et al 1962). Occuring within the Chalk Butte formation are small scattered intercalated basalt flows. The Chalk Butte Formation, named by Corcoran et al (1962), is of middle Pliocene age, estimated as Hemphillian by J. A. Shotwell, based on vertebrate fossils (Corcoran et al, 1962). The Chalk Butte Formation consists of loosely to poorly consolidated, tuffaecous sandstones, siltstones and conglomerates. These beds were deposited in fluvial and lacustern environments (Corcoran et al, 1962). Also present within the Chalk Butte Formation are thin beds of ash, tuff, fresh water limestones and thin basalt flows. Brown (1982) redescribed the rocks of the Chalk Butte Formation occuring in the Vale East Quadrangle. Capping the entire sequence is Brown's (1982) unit named the sedimentary rocks of Captain Keeney Pass. These rocks are very poorly consolidated tuffaecous siltstones, sandstones and volcanic conglomerates of middle Pliocene to early Pleistocene age.

Following the deposition of the Chalk Butte Formation, the area was subjected to deformation associated with the Snake River Downwarp and Basin and Range extension. The deformation that accompanied the Snake River Downwarp is reflected in the eastward dip of the beds throughout the area. The Basin and Range deformation is characterized primarily by north - south trending faults. Kittleman et al (1965) reports that the faults tend to be normal and dip steeply.

Displacement along the faults tends to be small, though a few are measured in the hundreds of meters.

Following the earlier portion of Basin and Range deformation, the beds referred to by Brown (1982) as the sediments of Captain Keeney Pass were deposited. Brown (1982) believes these rocks to be Pleistocene in age. Again the beds are primarily volcaniclastic in composition. The sediments of Captain Keeney Pass were deposited unconformably upon the Chalk Butte formation and differ in color, texture, and degree of consolidation from the underlying Chalk Butte Formation. The beds of Captain Keeney Pass are generally a light gray in color, while the Chalk Butte sediments are yellow brown. The grain size of the beds of Captain Keeney Pass are also finer, though the rock types are the same. The Chalk Butte sediments are also more competent and show a higher degree of lithification. The beds of Captain Keeney Pass were unconformably deposited on and were not disturbed by the earlier Basin and Range structures. This would suggest that this easrly period of deformation had been concluded by the Pleistocene. The beds of Captain Keeney Pass are, however, offset by faults that are believed to part of the Vale Fault Zone, believed by Lawrence (1976) to be a major right lateral strike slip fault zone. The Vale Fault Zone was probably active during the sometime between the Pleistocene to Recent. The structures associated with the Vale Zone also appear to offset the earlier Basin and Range structures.

Regional Structural Geology

The study area is located at the west end of the Snake River Downwarp, at the northern edge of the Basin and Range province. The structural position is reflected by the regional eastward dip of the beds in the Vale area. The Snake River Downwarp is a large structural trough which extends eastward from eastern Oregon across Idaho to the vicinity of Yellowstone Park. Cooper (1980) gave a Miocene to Pliocene age for the active period of deformation, during which the trough received thousands of meters of sediments.

The study area, and the areas to the west and south, are dominated by north trending normal faults that typify Basin and Range style structure. The regional structure, as defined by Bowen and Blackwell (1975), Lillie (1977), and Cooper (1980) shows horst and graben features. U.S. Department of Interior, Bureau of Land Management, Environmental Anaysis Report OR-030-4-1 (1975) suggests that there may be more faults within the area than previously mapped. The B.L.M. report stated that the faults are difficult to detect due to the nature of the poorly consolidated Pliocene cap rocks. Brown (1982) reports that beds of Captain Keeney Pass which cap the area are Pliestocene, not Pliocene, in age, based on mammalian fossils. The Pleistocene beds unconformably cap some of the earlier Basin and Range structures, while being offset by other later structures, indicating that deformation was still occurring during the Pleistocene.

Lawrence (1976) suggested the existence of a major right lateral

fault zone trending through the Vale KGRA. He has named this feature the Vale Fault Zone. Bowen and Blackwell (1975) identified the northern portion of this fault as the Willow Creek Fault. The Willow Creek fault, located northeast of Vale, is a westward dipping normal fault, which trends to the northwest. If the Willow Creek Fault also has a right lateral strike slip component, as reported by Lawrence, (1976), then the overall sense of movement is oblique. The Bully Creek fault, named by Bowen and Blackwell (1975), lies to the west of Vale is an eastward dipping normal fault. The Bully Creek and Willow Creek faults are the bounding structures of a large regional horst and graben combination. Further clarification as to the nature and sense of movement also supplied by Lillie (1977), who stated that regional scale geophysical evidence indicates oblique movement along the Vale Fault Zone. The Basin and Range structures of the Vale area display extension in the northeast-southwest orientation; superimposed upon this is a northwest trending, right lateral strike slip feature, the Vale fault zone.

CHAPTER III

GEOLOGY OF THE VALE AREA

Stratigraphy of the Vale Area

Chalk Butte Formation

Approximately 200 meters of continous section is exposed at Vale Butte. Brown (1982) reported the contact of the Grassy Mountain Basalt at a 200 meter depth in the Two States Oil and Gas well, located north of Rhinehart Buttes, in the Malhuer River floodplain, see Plate I. An estimate of total thickness for the study area, based on well data and exposed sections would exceed 500 meters. Accordingly about 1/2 of the section is exposed at Vale Butte. Bowen and Blackwell (1975) give a total thickness of the Chalk Butte Formation in the Cow Hollow area, about 15 km to the south as 750 to 1050 meters.

The rocks exposed consist predominantly of tuffaecous siltstone, with lesser amounts of volcanic sandstone and conglomerate. The relationships displayed by the sediments within the Chalk Butte formation are complex. The deposits are typically lenticular and laterally discontinous. The beds display cut and fill structures and forset-topset combinations are common. Beds interfinger and pinch out over relativly short distances. Beds are commonly truncated in conspicous angular unconformities.

Chalk Butte beds are grouped into sequences. A sequence, as used here, is a group or series of beds, which displays a form and order that is common throughout the study area. That form is a continuous coarsening upward grain size, progressing from fine silt to sand and somtimes up to boulder. In general a typical sequence consists of a thick siltstone bed, usually more than ten meters in thickness. The siltstones range from massive, with very little internal structure to finely laminated. The grain size coarsens upward, grading to sand size, or sometimes being unconformably overlain by sandstones. Within the sandstones the coarsening progression continues until grading to or truncated by a conglomerate. The sequence is then repeated with the renewed deposition of fine silts. Occasionally, the coarsest fraction is sand size, in which case the sandstones are unconformably overlain by fine silts. This progressively coarsening upward sequence is repeated four times in the continous section exposed at Vale Butte (see Plate 1).

Because of difficulties in establishing absolute correlation between exposures located in the study area, each of the locations will be examined seperately. Consequently, stratigraphic columns are shown seperately for each of the major exposures. The exposures are located in an unnamed gulch which trends northwest through sections 5,6, and 8, R45E, T19S; in an unnamed valley in the SW/4 sec. 4 and SE/4 sec 5, R45E, T19S; at Rhinehart Buttes; and Vale Butte. The columnar sections are shown in figure 2, and the locations are noted on the geolgic map, Plate I.

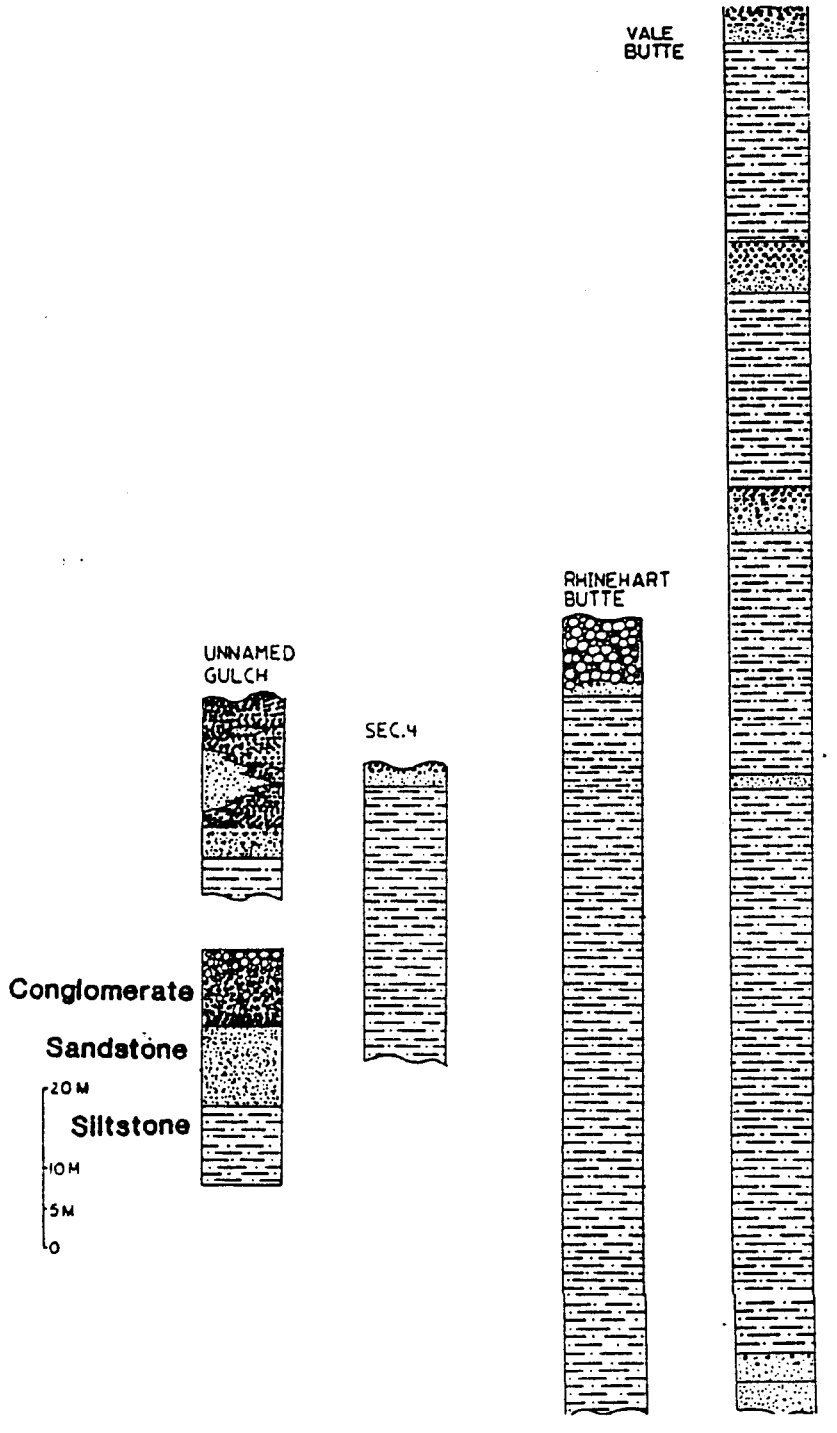

Figure 2. Columns showing the stratigraphy at four selected locations within the study area

In the westernmost unnamed gulch location, about five km SW of Rhinehart Buttes, is a sequence which displays variability. The dips of the beds vary between north and northeast, therefore, progressing to the southeast along the gulch the rocks exposed are continously lower in the section. At the mouth of the gulch, in the SE/4 sec. 6, T19S, R45E, a well stratified pebble conglomerate crops out. The total thickness is approximately 20 meters. The beds range in thickness from five cm to over one meter. Within the conglomerate are lenses of fine grained sandstone up to five meters thick. The pebbles are primarily well rounded basalt, with lesser amounts of quartz, and chert, in a coarse sandy matrix. Sedimentary structures include truncated beds, foreset beds, and cut and fill structures.

Directly beneath the conglomerate, exposed in the SW/4 sec. 5, is a massive-cliff forming sandstone. Approximately 35 meters of competent, medium grained, volcanic sandstone is capped by about 20 meters of the conglomerate beds exposed at the mouth if the gulch. In the NE/4 sec. 8, an underlying basal siltstone is exposed. The siltstone beds are about 30 meters thick. The entire sequence displays the typical coarsening upward character both within the beds and in the gross lithology of the sequence.

In the location in the SW/4 sec. 4, T19S, R45E, about 30 meters of section is exposed. The rocks of this location can be correlated to the sequence exposed in the unnamed gulch to the west. The cap rocks are sandstone and conglomerate beds. These beds are much thinner here, being only about two meters in total thickness. The contact between the underlying siltstone and the overlying coarse grained beds is

unconformable. At the base of the conglomerate beds is a layer of imbricated basalt cobbles in a coarse tuffaecous, sandy matrix. The bedding is parallel to the contact and the bed is about eight cm thick. Deposited on top is a series of small (2 cm thick) basalt pebble beds. The basalt pebble beds are tuffaecous, matrix supported, and the bedding is foreset. The matrix is also much finer grained than the basal bed. Overall grain size of the beds at this location is consistantly finer and the bedding is thinner than at the unnamed gulch location. The same sedimentary structures occur at this location, but their size is smaller.

There are many exposures in the Rhinehart Buttes area. To be able to relate the exposures and correlate them where possible the locations are described in relation to the structure. However, the area contains a large number of faults. The northwest trending fault along the crest of Rhinehart Buttes is the princple one. This fault is here informally named the Rhinehart Fault. Exposures in the Rhinehart Buttes area are catagorized as being either west or east of Rhinehart fault. At least five east-west trending faults cross the northern portion of Rhinehart Buttes, resulting in many exposures seperated by faults. Where exposures are of the same rock type, notably siltstone, correlations cannot be made with absolute certainty.

The lowest portion of the sequence exposed on the west flank Rhinehart Buttes is about 70 meters of the siltstone which forms the base of the western slopes of the northern Butte. The upper portion of this unit coarsens upward and grades upward into the overlying sandstone beds.

The sandstone beds range between one and two meters in thickness and are recemented with silica. The sandstones are fine grained, the silicification has obscured any primary depositional structures within the beds. These sandstone beds are truncated by conglomerate.

The conglomerate which forms the caprock of the west face of Rhinehart Buttes is variable. The exposures in the SW/4, SW/4 of section 28 are limonite stained, silicified boulder conglomerate (Brown, 1982). The bed is apparently massive, approximately ten meters thick. Again, as in the sandstones beneath them, the primary structures are obscured. The clasts are mostly basalt, about 80%, with about 20% white, alpha, quartz. The massive conglomerate at this location seperates laterally to the northwest into two distinct beds. The lower conglomerate is approximatelly one and a half meters thick and is matrix supported, friable, basalt, pebble, conglomerate. The beds are thin, about two cm thick, and consist of basalt pebbles, in a silty, fine grained, tuffaecous matrix. The outcrop is located about 200 meters from Rhinehart Fault and shows no evidence of silicification. The upper bed, at the same outcrop, is about 10 to 15 meters thick, and is a silicified basalt pebble conglomerate. The upper conglomerate is clast supported, with uniform bedding about 10 cm thick. Although it is silica flooded, it does not show limonite staining.

East of the Rhinehart Fault, in the valley between Rhinehart and Vale Buttes, a different sequence is exposed. The lowest rocks exposed in this section are sandstones. The sandstone is composed of two distinct members. The basal member is a well lithified, fine grained,

volcanic sandstone which is partially silicified. The degree of silicification is highest in the area of Rhinehart Butte and diminishes with distance away from Rhinehart Buttes. The bed varies in thickness, from less than one meter to three meters. This sandstone is thinnly bedded and the beds are approximately one cm in thickness. These sandstone beds are resistant, competent beds which form the prominent dip slope in the valley between Rhinehart and Vale Buttes.

Conformably overlying the basal sandstone beds is a friable, medium grained, matrix supported, tuffaeceous, volcanic sandstone. This sandstone displays some silicification, but the silicification is limited to areas immediately adjoining fault zones. Grain size within the sandstone coarsens upward, with occasional well rounded basalt pebbles occuring in the upper one third of the outcrop. The frequency of the pebbles increases upward, although volumeterically the pebbles never reach more than a very minor portion of the sandstone estimated at a maximum of five percent. Because of the lack of resistance to erosion of this bed the original total thickness is not exposed. Generally, in outcrop, this sandstone is approximately two meters thick, with the upper contact removed by erosion. Bedding within this sandstone is of variable thickness ranging from one cm to 20 cm. Climbing ripples were noted indicating a fluvial origin and suggesting that the paleocurrent direction was northward. Exposures are limited; and the bed is chiefly a slope former. This sandstone forms slopes on the east face of Rheinhart Buttes and flat irons in the valley between Rhinehart and Vale Butte. The flat irons are located in the SE/4 of sec. 28 and the NW/4 of sec. 33, T18S, R45E. The best exposures of the

bed occur in a resistant silicified portion in a stream cut on the line between secs. 33 and 34, T18S, R45E. The contact relationship with the overlying unit is uncertain. On the east flank of Rhinehart Butte, in sec. 28 the sandstone beds are apparently capped by siltstone. The nature of the contact between the sandstone and siltstone is not known. The only exposures of the overlying siltstone noted were in the silicified portion immediately adjacent to Rhinehart Fault. Because of the limited exposure no bedding, and/or depositional stuctures were observed. Where there were exposures the siltstones were noted as being silicified, limonite stained, and highly fractured. The fractures are filled with secondary, geothermally deposited calcite and quartz.

The northern portions of Rhinehart Buttes is crossed by at least five northwest trending normal faults. The exposures in this section are limited to steep faces of siltstone. The sandstone or conglomerate beds which were found in the southern portion of Rhinehart Buttes are not exposed. Most of the exposures of the siltstone are in areas of silicification very near the faults. The north face of Rhinehart Buttes is composed of a 55 meter thick section of siltstone exposed in a road cut on highway 20 at the base of the butte. The outcrop displays pervasive shearing. This shearing might be attributed to blasting during road construction, however this location is very near several fault locations, which might more likely be responsible for the structure. The siltstones are not silicified but silicification has occurred along some of the faults in the area. The siltstone is capped by 15 meters of thick, forset bedded sandstones. The sandstones are

fairly uniformly bedded, about 10 cm thick are fine grained and flooded with silica. The contact between the siltstone and sandstone was not found. Exposures are limited to seperated outcrops of either of the rock types.

Above the sandstone is a thick bed of siltstone. The siltstone forms the upper half of the north face of Rhinehart Butte. Outcrops are rare, limited to those which have been silicified and display limonite staining. The topographic expression, and intensity of the silicification suggests that fault contact is very likely.

The description of the north face of Vale Butte is very similar to that of Rhinehart Butte. The rocks display variable thickness in both bedding and total thickness. The coarse grained rocks at the north face of Vale Butte are conglomerates, not sandstones. The total thickness of these particular conglomerate beds varies from as little as three meters to over 15 meters. The individual beds range from ten cm to about one meter in thickness. The conglomerate is clast supported and has been flooded with silica. Limonite staining is present, but only mildly so and limited to the western portion of the beds. The staining decreases with distance eastward along Vale Butte. The rest of the north face of Vale Butte, up to the level of the middle conglomerate bed, see the stratigraphic column, figure 2, Vale Butte section, is composed of siltstone. The sandstone and conglomerate beds which occur in the rest of the Butte do not crop out on the north face. Either the beds have been faulted or are pinched out or perhaps are merely covered.

Vale Butte is, with the exception of the north face, composed of a

series of siltstone through sandstone/conglomerate sequences. A total of four sequences make up the Butte and are traceable through the west, south, and east side of the Butte. Vale Butte is the thickest (approximately 240 meters) unfaulted exposed stratigraphic section within the study area. The lowest exposures are sandstone. The sandstone is composed of two distinct sandstone types, lithologically very similar to those located on the eastern flank of Rhinehart Buttes. This outcrop is seperated from the Rhinehart Buttes sandstones by a fault.

Overlying the sandstones is a massive siltstone. The siltstone is about 60 meters thick. Unconformably capping the siltstone is a sandstone bed about one meter thick. The bedding is massive, and the composition is a coarse grained tuffaecous, sandstone. Within this sandstone are numerous vertically standing casts of trees. The trees include root casts extending into the underlying siltstone beds. The casts are limited to trunks and roots with no leaves or limbs preserved. None of the trees exceeds 10 cm in diameter, indicating that the buried forest was probably quite young. Apparently a forest was growing on the floodplain of the fluvial system and was subsequently buried after a few but indeterminate number of years. Three sequences composed of siltstones and conglomerates are deposited conformably above the sandstone. The sequence begins with 60 meters of slope forming siltstone. The siltstone is overlain by approximately six meters of resistant, limonite stained silicified conglomerate. The conglomerate beds are poorly stratified, composed of mostly basaltic pebbles, with less than 15% quartz pebbles. The beds are

clast supported and range in thickness from 10 cm to about one meter. The beds have been flooded with silica. These resistant conglomerates are cliff and bench formers. The conformable sequence continues with 25 meters of slope forming siltstone and is capped by about eight meters of silicified, limonite stained, clast supported, pebble conglomerate. The capping conglomerate is silicified, limonite stained, consisting of primarily basalt clasts in a coarse sandy matrix. As in the case of the previous conglomerate this rock is a resistant cliff and bench former. Above this is the fourth and topmost sequence. The top sequence is made up of about eight meters of siltstone and about six meters of silicified conglomerate which acts as a cap rock on the top of Vale Butte. The conglomerate is very similar to the other conglomerates which occur in this sequence.

The Rocks Of Captain Keeney Pass

Capping the Chalk Butte formation is the unit described by Brown (1982) as the sedimentary rocks of Captain Keeney Pass. These rocks are very poorly consolidated with limited exposures, and differ from the underlying Chalk Butte formation in color, texture, and degree of lithification. While the rocks of the Chalk Butte Formation are predominately light yellow brown in color the sediments of Captain Keeney Pass are light gray. The sediments of Captain Keeney Pass are not as well indurated as the underlying rocks. The sediments of Captain Keeney Pass are are also different in the expression of erosion. Maximum thickness of the sediments of Captain Keeney Pass is 100 meters on the hill in the center of sec. 3 R45E, T19S. Contacts

beneath and within this unit are obscured so no definite thicknesses of individual beds were determined. The variation in rock types are visible at this location, when viewed from a distance due to changes in vegetative cover. The rocks of Captain Keeney Pass, like the sequences within the Chalk Butte Formation generally coarsen upward. The unit consists of a lower siltstone member, which is tuffaecous and very fine grained, a medium grained volcanic sanstone member, and remnants of a capping bed of matrix supported basaltic pebble conglomerate. The composition of the beds was determined by examining float. Also within this unit is a thin bed of light gray air fall ash. Only small remnants of this ash bed remain, located in the upper portion of the sequence.

Structural Geology of the Vale Area

The study area is dominated by north to northwest trending topographic lineations. These lineations are formed by the valleys located just west of Rhinehart Buttes, on either side of Vale Butte, and the unnamed valley which trends northwest through sections 5,6 8, and 9. The buttes form a second set of lineations. Rhinehart Buttes and Vale Butte, along with the hills which extend southeast of Vale Butte contribute to this set.

Rhinehart Buttes are composed of a resistant silicified rocks. At the crest of north Rhinehart Butte, in the NW/4 of section 33 and in the SW/4 of section 28, is exposed the westward dipping Rhinehart Fault, (see Plate I). Rhinehart Fault, has a dip of 74° to 83°. Slickensides on the fault surface indicate the last movement was down

to the west. This movement classifies Rhinehart Fault as a normal fault. The fault trends N29°W and can be traced along the crest of the southern portion of north Rhinehart Butte. The fault trace extends part way down the valley seperating north and south Rhinehart Buttes and in the upper portion of the northern end of south Rhinehart Butte. There is an offset in the location of the fault trace on the opposite sides of the valley. The direction of the offset indicates that the fault located in the valley is down to the south, labelled I on the geologic map, Plate I.

Most of the linear ridges located within the study area were found to be cored with more resistant silicification zones. Consequently all areas of silicification were examined for possible structures. The areas of the highest amount of silicification were found to be the intersections of one or more faults (see Plate II, is a map showing silicified rocks). In the SW/4 of sec. 28 Rhinehart Fault is exposed along the narrow ridge crest, see geologic map, plate I, and is offset to the west by the two intersecting faults. In the area of the intersection is exposed rocks that have been highly fractured, fault gouge, and secondary deposition of quartz and calcite has occurred. Progressing away from the intersection, along each of the faults, the degree of silicification and secondary mineral deposition decreases. Northward along the line between secs. 28 and 29 is another fault intersection. Located about the middle of the line, just west of the radio towers is a large tower like outcrop of silicified siltstone. The tower is also marked by conspicous fault gouge, silicification and secondary deposition of quartz, calcite, and selenite. Again the

degree of silicifcation decreases away from the fault intersection.

Extending to the southeast from Rhinehart Buttes, in the south one half of section 28 is a linear ridge composed of silicified sandstone. The rocks on opposite sides of the silicified zone are of differing type. Northeast is a dip slope consisting of silicified sandstone. Southwest of the ridge is a level area underlain by siltstone, which truncates the sandstone. This suggests that they are offset by a fault, shown on Plate I as A. In the eastern 1/2 of section 33, the hill with elevation of 2614 is covered by a soft Pleistocene sedimentary unit. The Pleistocene sediments are truncated and in contact with older Chalk Butte sandstone in the northern portion of the ridge, see geologic map, Plate I, approximately in line with the interpreted fault. The northern portion this ridge continues to a small north trending valley in the NW/4, NE/4 of section 33. The narrowest portion of this valley has the shape of a backwards L, with exposures along both walls, which trend north-south and along the east-west trend which would be the horizontal portion of the L. Those rocks along the north face of the east trending section are fractured and dipping at considerable variance to the regional dip. The regional dip is to the northeast while the fractured rocks display a northwest dip. This is interpreted as a brittle fracturing type of drag folding. The drag folding and apparent offset of units indicates that movement along the fault would be down to the northeast.

The sandstone hill that forms the eastern wall of the valley is the same sandstone which forms the western wall at the SW/4 SE/4 of section 28. The small flatiron on the western side of the valley is

repeated when crossing the valley from west to east, suggesting a north trending fault occupies the valley. The movement necessary to produce the repetition of this unit is down to the west, labeled B on the geologic map.

Just north of the junction of the above mentioned southeast trending ridge and Rhinehart Butte, the east flank of the Butte consists of a dip slope of sandstone. The southern margin of that dip slope is a small valley. The sandstone bed continues uninterrupted across the valley at about the 2500 foot contour. To the west, the valley records progressively more offset all the way to the junction of the southeast trending ridge. This structure is a hinge fault; the offset is down to the south and increases to the west. Also at the junction of the hinge and the southeast faults, with Rhinehart Fault; Rhinehart Fault displays an offset to the west. The offset to the west of Rhinehart Fault fits the suggested sense of movement along the previously described faults.

The same kind of situation occurs at the east trending valley to the north of the dip slope, which is located near the center of section 28. Also the trend of the crest of Rhinehart Buttes is offset along the trend as the valley, and a small amount of alteration was noted along the crest of Rhinehart Butte on the same trend, at this location, noted as fault C on the geologic map. The sandstone dip slope is truncated at this valley and the northern valley wall consists of siltstone. The offset is down to the north, which would make the dip slope the top of a small horst.

In the SE/4 SW/4 NW/4 of section 28 is a small southeastward

trending knob. This knob shows silicification and limonite staining. Also noted was an apparent offset between the rocks on opposite sides of the small valley at the southern base of the knob. The apparent offset consists of the truncation of distinct beds. The beds occur on the ridge and southern wall of the southeast trending valley that marks the northern boundary of the ridge. Across the valley, to the north the slope consists of siltstone, and the marker bed was not located.

In the SE/4 NE/4 of section 33 is a northwest trending valley which parallels the foot of Vale Butte. This valley narrows to a small steep cut just to the south of the 2500 foot contour. The narrowing of the valley is due to a silicified zone of a sandstone bed. Just to the east, in the talus at the base of Vale Butte float contains slickensides. The main northwest trending fault, here informally referred to as the southern extension of the Willow Creek Fault, is located west of the base Vale Butte, identified as WC on the geologic map, Plate I. To the south, a series of unnamed hills forms a lineation along the east side of the trend of the Willow CreeK Fault. Fracturing and changes in dip on the hill located in the center of section 34, south of Vale Butte suggests drag folding, with the down thrown side to the west. The hill in the NW/4 of section 11, T19S, with an elevation of 3163 feet has an exposure of the Chalk Butte Formation which is outcropping through the overlying Pleistocene sediments. This exposure suggests that faulting occurred after deposition of the overlying unit and has offset the Pleistocene beds, allowing the removal of the upper beds. The unnammed hill which rises to the east the exposes about 90 meters of Pleistocene sediments.

A northwest trending fault, labelled as fault G on Plate I, apparently crosses through the saddle located on the northeast ridge of Vale Butte, near the center of section 27. The north slope of Vale Butte, west of the fault is composed of light yellow brown siltstone, siltstone float and locally weathered soils. Immediately east of the fault, the soils are a dark red brown, the float is composed of limonite stained silicified conglomerate. The juxtaposition of units suggests that the movement is down to the east. The beds which crop out west of this structure dip steeply to the east, and those on the east dip to the east, steeper than the regional dip. This evidence suggests drag folding, with a down to the east movement.

Upslope from the saddle, still on the northeastern ridge of Vale Butte, aerial photography reveals that the bench forming conglomerate beds of Vale Butte has been fractured by two small en echelon normal faults. The down to the east offset and fault traces show clearly in the photographs. Both of these structures are down to the east and the estimated offset is between five and ten meters.

At the southern end of Vale Butte there are two small hills. The northernmost is a small mesa like feature, which extends southward from Vale Butte. This hill is located in the SW/4 NW/4 of section 34. The units composing this hill are apparently the same units forming the southern extension of Vale Butte. The cap rock which forms both of these features is a silicified sandstone overlying an unaltered bed of siltstone. Therefore the fault separating them would be down to the south.

Near the center of section 34 is a small butte. This small butte

is south, across the northeast trending valley from Vale Butte and is composed of silicified sedimentary rocks. The topographic expression of the valley on the southern side of this butte, together with the alteration suggests a down to the north fault, trending to the southwest. The configuration of the two faults suggests that this fault block is a small graben.

South, the next hill, elevation 2887, exposes, in the valley at its western base an outcrop, which shows the same style of drag folding as found elsewhere. The beds show silicification and are brittly fractured. The crest of hill 2887 shows a small amount of silicification. The unique exposure shows that the Pliocene cap rocks have been altered by silicification. This suggests that the fossil hot springs (Bowen and Blackwell, 1975) were active after the deposition of the Pliocene beds.

In the SE/4 of section 2, T19S, R45E, is a small outcrop of limonite stained, slicified Chalk Butte siltstone. The outcrop is a free standing linear, dike like wall which outcrops through the Pliocene sediments. The strike of this structure is about N30° W. This orientation coincides with the other northwest trending structures within the area. On trend with this outcrop, several other Chalk Butte outcrops are noted, located on hill 2807, in the SW/4 of section 35, T18S, R45E, and the ridge immediately south, in section 2, T19S, R45E.

In the western part of the study area, several other proposed faults are exposed. In the large unnamed northwest trending valley in T19S, sections 5, 6, 8, and, 9 displays an offset in units which are downdropped to the west.

Near the center of the section boundary, between sections 8 and 5, is a small northward trending valley. Across this valley a small amount of offset can be observed. This valley runs to the north, truncating an outcrop of Chalk Butte Formation rocks, and farther north truncating Pliocene beds. The fault dips steeply to the east and is down to the east, though the offset is less than 10 meters.

The Geothermal System at Vale

The geothermal system at Vale produces four hot springs, shown on the geologic map, Plate I. The hot springs are located on the southern bank of the Malhuer River, on the flanks of Rhinehart Buttes. The southernmost two are low temperature, 22 and 27 °C. The northern two, located between the bridges of highway 20, are high temperature. The temperatures measured at these springs is 97 and 98 °C. The analysis of the waters from these two springs, based on confidential data from Renewable Energy Incorperated, indicates that the flow is composed of about 90% river water and less than 10% geothermal water. The springs are fed by an aquifer in the recent alluvium in the floodplain located at a depth of about 20 meters. The temperature of the water in the aquifer increases toward the southeast, as measured in the wells which tap the aquifer (Brown, 1982). The temperature increases from about 97 °C at the hot springs to a high of about 115 °C in a well at the foot of Rhinehart Butte, located southeast of the hot springs. The temperatures of the water in the aquifer decrease both to the north and south of the hot springs. The pattern displayed by the temperatures within the aquifer suggests a point source for the outlet of the

geothermal system feeding the high temperature waters into the aquifer.

Heat flow measurements in the Vale KGRA ranged from almost two to almost five times the worldwide continental average (Bowen and Blackwell, 1975). Bowen and Blackwell (1975) reported measuring heat flow values that ranged from 2.8 HFU to 6.4 HFU. Heat Flow Units (HFU) are measured in microcalories per square centimeter per second. The worldwide continental average is 1.4 HFU. Black (pers. comm., 1984) stated that to achieve that high a heat flow value convective heat transfer through a liquid medium is necessary. The source of the fluid or reservoir has been suggested by Bowen and Blackwell (1975) to be either the Owyhee Basalt or the Grassy Mountain Basalt both of which are suggested to excellent reservoir rocks. Field mapping has shown that Rhinehart fault was probably the main controlling structure for the fossil geothermal system at Vale (Bowen and Blackwell, 1975). The present hot springs are located near the trace of Rhinehart Fault. The aquifer that feeds the hot springs shows an increase in temperature east of the trace of Rhinehart Fault. Consequently Rhinehart Fault may not be the controlling structure at source of the geothermal fluids for the aquifer itself.

Silicification in the Vale Area

The rocks of the Vale area, notably the Chalk Butte Formation display widespread silicification. The areal extent of silicification seems to be controlled by the permeability of the country rock (Benson, pers. comm., 1981). The distance from the faults which controlled the flow of the silica bearing geothermal waters that resulted in

silicifation is noted generally decreases as grain size of the country rock decreases.

Rhinehart Buttes is an erosionally resistant, silicified fossil hot spring (Bowen and Blackwell, 1975). The main controlling structure of this fossil geothermal system seems to be Rhinehart Fault. The areas of the most intense silicification, which combines limonite staining and secondary mineralization, all occur along the traces of Rhinehart Fault. With an increase in distance away from Rhinehart Fault, first secondary mineralization, then limonite staining and lastly silicification decreases and then disappears. The silicification may extend for up to kilometers away from the fault in what were the more permeable beds. The clast supported conglomerates have been noted to be silicified at and beyond Vale Butte. This distance is greater than one km east of Rhinehart fault. The section about 200 meters to the west of the Rhinehart Fault shows a silicified clast supported conglomerate overlying an unsilicified conglomerate which supported by a fine grained tuffaecous matrix. Coarse grained sandstones display lateral silicification in the range of hundreds of meters. The coarse grained silicified sandstones are found to have a uniform grain size. Those sandstones which are composed of two or more distinct grain sizes, especially those which are analogous to matrix supported rocks show a limited areal extent of silicification. Siltstones, which are noted by Bowen and Blackwell (1975) as being relatively impermeable show silicification within only a few tens of meters around Rhinehart Fault.

CHAPTER IV

GEOPHYSICS

Introduction

The region surrounding Vale KGRA has been the subject of numerous investigations; Bowen and Peterson (1970), Bowen (1972), Bowen and Blackwell (1975), Couch et al (1975), Hull (1975), Couch and Baker (1977), Lillie (1977), Applegate and Donaldson (1979) and Boler (1979). Because of the alignment of thermal features along structural lineations the Vale geothermal system is suggested to be of the Basin and Range type (Bowen and Blackwell, 1975). A critical feature of this type of system is the location of the controlling structures, usually faults, along which the geothermal fluids migrate.

Magnetic and gravity surveys were conducted under the supervision of Dr. Tsvi Meidev, during 1981. Well logs and previous work, principly by Couch et al. (1975) Lillie (1977), Boler (1979), and Applegate and Donaldson (1979), suggested that the necessary geologic parameters to achieve good results with magnetic and gravity surveys existed in the study area. The most important of these parameters was the existence of a basalt unit at a depth of less than one km.

Lillie (1977) reported that the sense of movement along the faults in the Vale area is oblique to normal. Normal faulting would juxtapose basalt and lower density sediments generating a density contrast. The

horizontal density contrast should result in a gravity anomaly. Basalt has a high value of magnetic susceptibility in comparison to sedimentary rocks. The same structures which good gravity anomalies should result in the generation of a significant magnetic anomaly. However, the critical feature would be the depth to the basalt flows. This parameter is important because of the relationship between depth and the wavelength of a magnetic anomaly. The planned magnetic survey lines were to be approximately three km in length. So the source depth must be less than one km to be able to record the complete waveform of a magnetic anomaly.

Berg and Thiruvathukal (1967) reported the results of a state wide gravity survey and published the state map of the Complete Bouguer Anomaly (CBA) and the Free Air Anomaly (FAA) values. Thiruvathukal and others (1970) discussed the results of the state survey, particularly with respect to the thickness of the crust and the anomaly patterns. Later workers, Bowen (1972), Bowen and Blackwell (1973, 1975), Couch et al (1975), and Hull (1975) delineated the major structures in the Vale area. Lillie (1977) and Boler (1979) produced comprehensive magnetic and gravity surveys of the Vale one degree quadrangle. Boler (1979) analyzed the regional scale magnetic anomalies particularly with respect to the depth of magnetic basement and crustal relationships. The study area is located on a regional magnetic high which is caused by a deep seated, about five kilometers, crustal uplift (Boler, 1979). Lillie (1977) refined the picture of the crustal structure in the area

and also provided both seismic velocities and densities of the proposed crustal sections.

Survey and Data Reduction Procedures

Magnetics

The magnetic survey was conducted in March, 1981, under the direction of Mr. Roert O. Walston, then the project manager for Renewable Energy Inc. A grid pattern was established which consisted of six lines and was centered on the Renewable Energy Inc. lease, shown in figure 3. Three of the lines B,C, and D lines were oriented N70° E. The other three lines, E, F, and G were oriented N20° W. The lines were oriented in an attempt to cross the main structural lineations at right angles, as shown in figure 4. A base station was established. Secondary bases, at the terminis of each of the lines and at the line crossover junctions were established and tied to the base station. While the secondary bases were being established, the base station was reoccupied at hourly intervals to check for drift. After establishing of the main and secondary base stations, the magnetic readings were corrected for drift and the corrected readings recorded. The data are shown in appendix B.

The magnetic surveying was done on foot at a height of 2.25 meters using a Gisco proton precession magnetometer. Station separation, within the lease boundaries was 30 meters (100 ft.). Outside the periphery of the lease, the separation was expanded to 76 meters (250 ft.). On those lines which extended more than one km beyond the lease

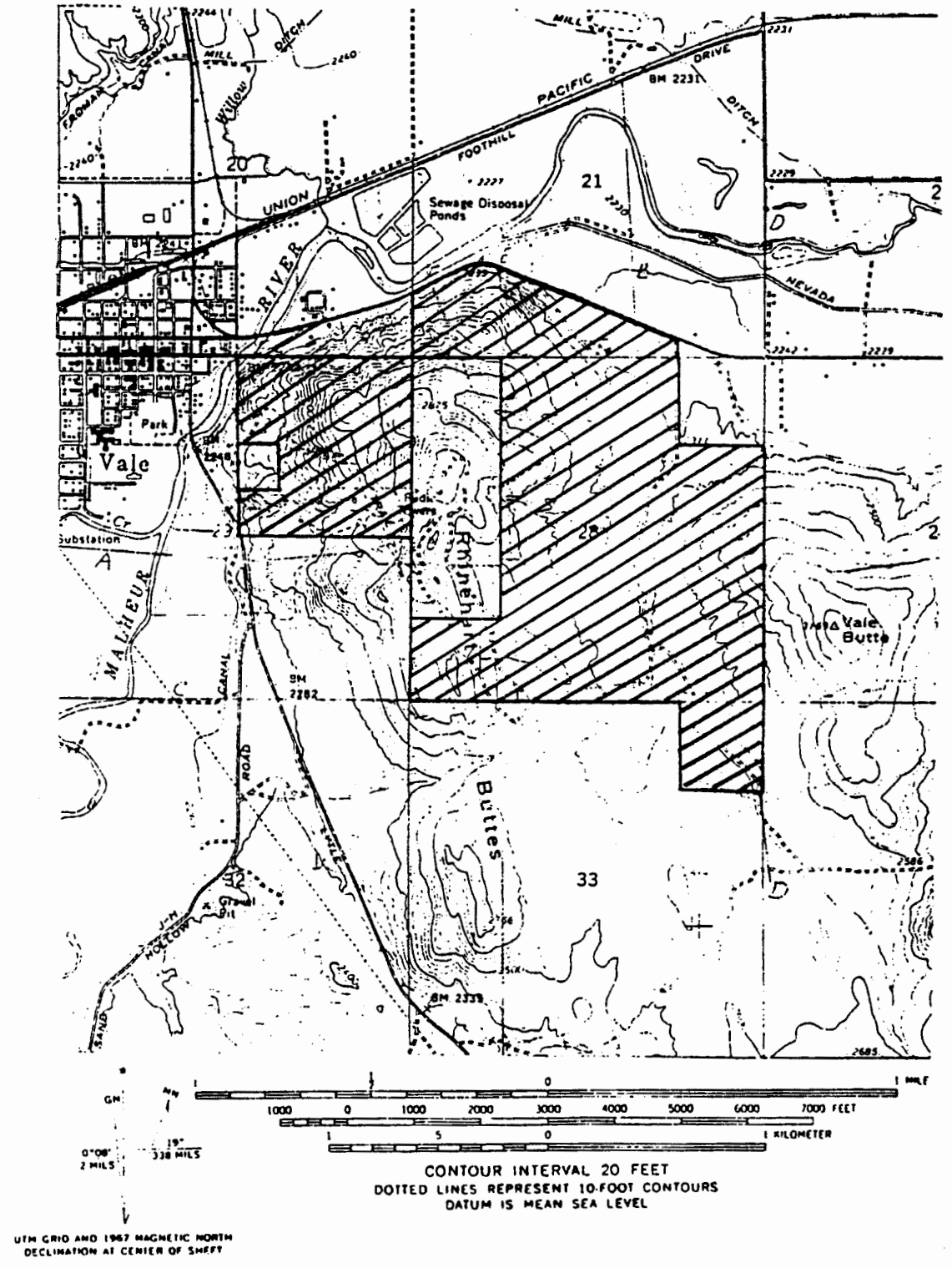

Figure 3. The Renewable Energy Incorporated lease area

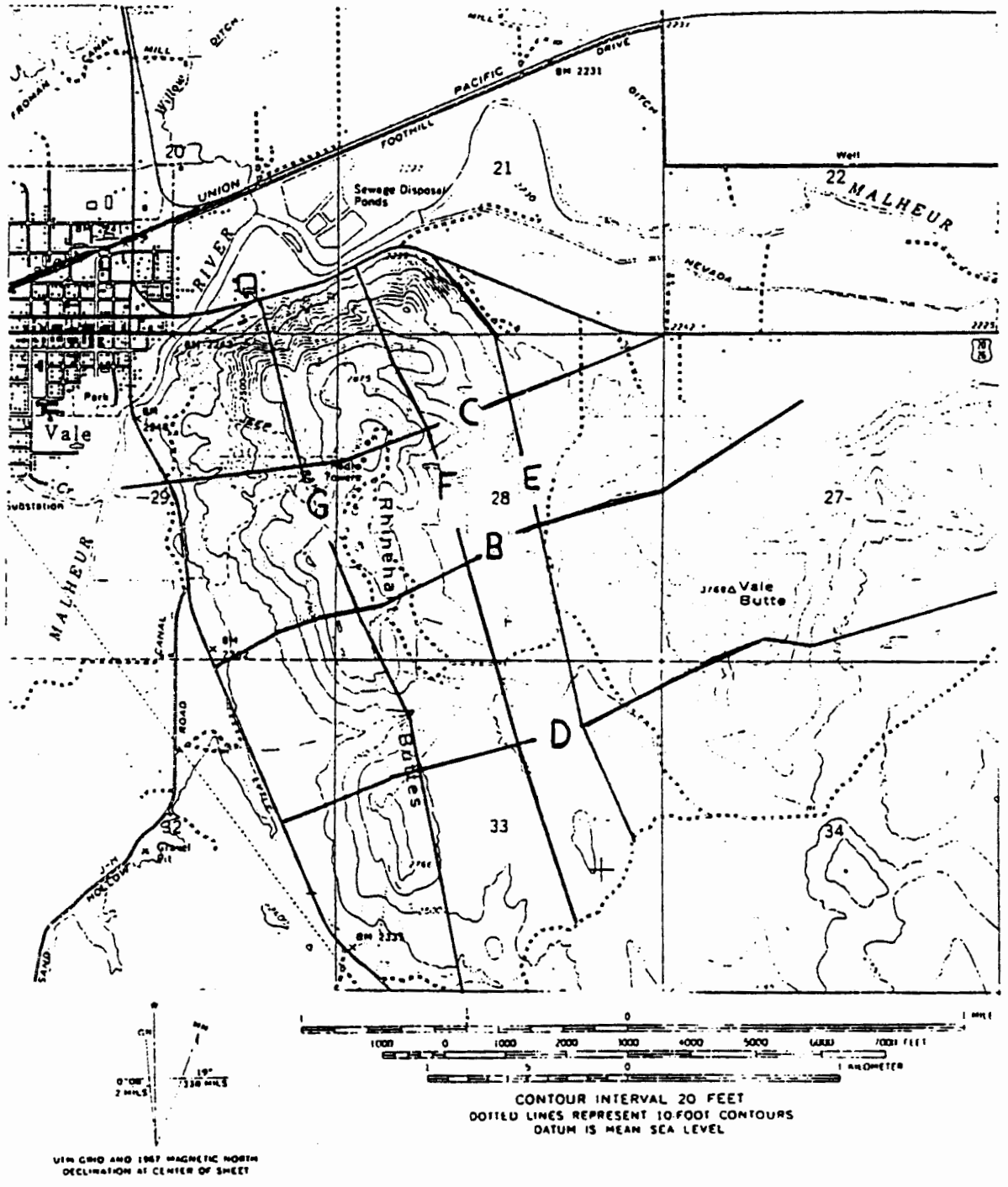

Figure 4. Location and orientation of the magnetic survey grid

boundaries, the station separation was again expanded to 152 meters (500 ft.).

The lines and stations were established by pace and compass. At each station three readings of the magnetic field were taken to insure continuity and every fifth station within the lease area was flagged and staked with appropriate information. Outside the lease area markers were placed every 76 meters.

Upon completion of the survey, the data were corrected for drift, and profiles for each line plotted. All information was then forwarded to both the main office and to Dr. Meidev for interpretation. The data were then contoured by Dr. Meidev and the interpretations returned to the field crew.

Gravity

The gravity survey was conducted in April and May, 1981. A similar grid pattern survey was laid out; but the orientation was changed to east-west and north-south, as shown in figure 5. The lines were labeled A,C, and F lines in the E-W direction, with A line through the base station. B, D, and E lines ran N-S with B line running through the base station. In addition, three lines, L, M, and R were on the periphery of the survey grid and were coincident with the other line terminal stations. The gravity base station, which was coincident with the magnetic base station, was tied to the Smithsonian gravity base station at Ontario airport.

Station separation was 76 meters (250 ft.) within the lease area. The separation was expanded to 152 meters (500 ft.) in the sections

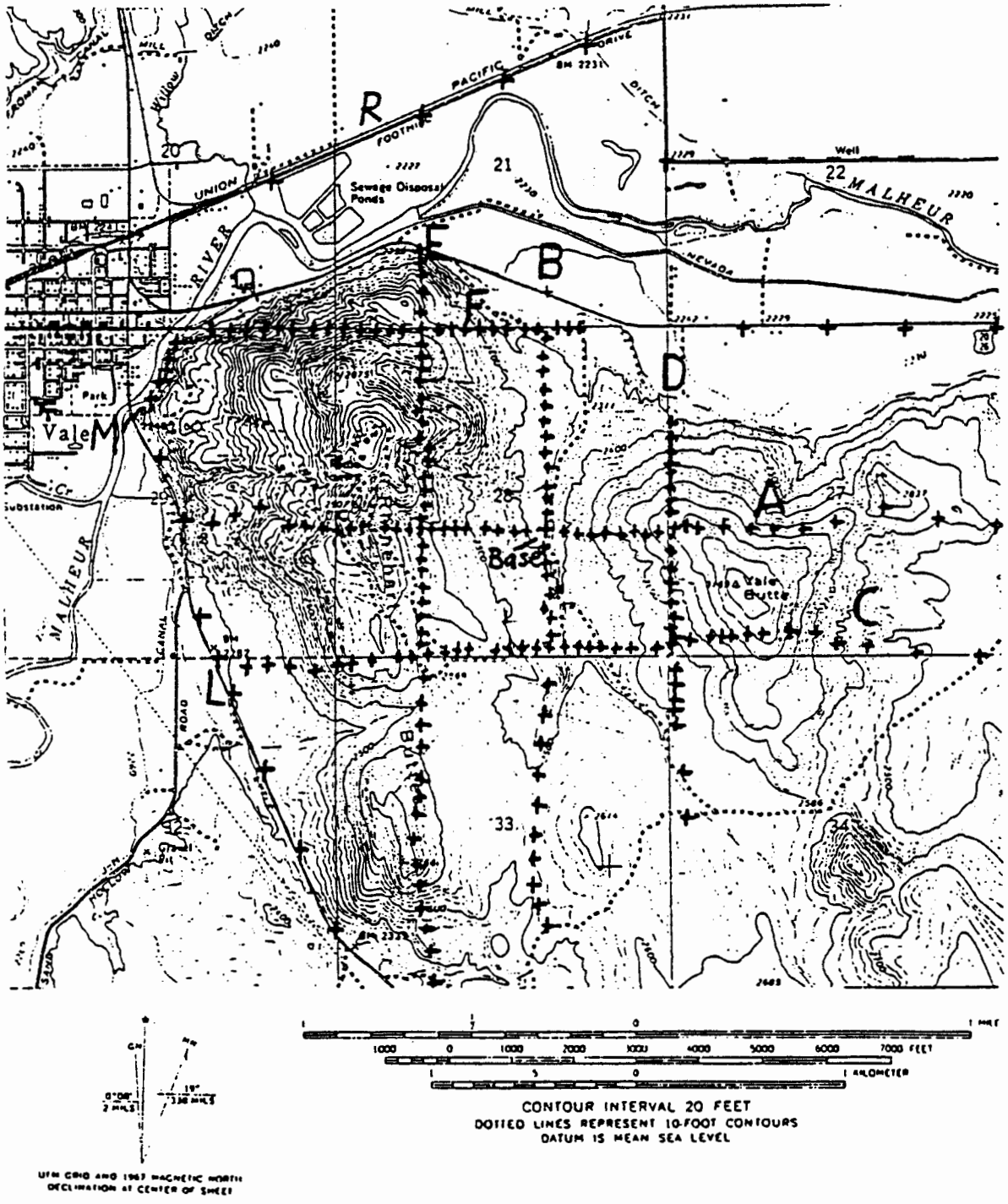

Figure 5. Location and orientation of the gravity survey grid

immediatly adjacent to the lease boundaries, and expanded further to 304 meters (1000 ft.) on those sections of the lines which were more than an estimated one km beyond the lease boundary. All peripheral lines had a station seperation of 402 meters.

The readings were taken with a LaCost-Romberg gravimeter. All stations were established by pace and compass. Immediatly after the gravity reading was taken, the station was flagged and staked, again with all pertinate information. When recording the gravimeter reading also noted was the time and an estimated elevation change in a 30 meter radius; the radius of B ring on the Hammer method of estimating terrain corrections, Hammer (1939). A base station was reoccupied hourly to check for drift.

The surveying was done by Mr. Robert Walston using a laser theodolite E.D.M. The stations were surveyed in immediately after the gravity readings were taken, as part of the gravity reading procedure. There were two bench marks within the lease area, on Vale and Rhinehart Buttes. Most of the gravity stations were visible from these locations. However, it was necessary to establish five secondary instrument stations.

Mr. Robert Walston did the survey reductions and computed the distance to the 44th parallel for each station. All readings were corrected for drift, and earth tide, Goguel (1954). Latitude corrections were then applied to place all stations on a relative latitude of 44 degrees. Terrain corrections were estimated manually using the Hammer method. The terrain corrections were then modified for use with reduction densities of 2.0, 2.1, 2.2, 2.4, gm./cm^3. The

terrain correction values were modified because, in light of the published geology of the area, the standard reduction density of 2.67 $gm./cm^3$ was expected to be too high. The free air correction factor was also computed. The observed gravity was then calculated using the absolute gravity value from Ontario airport.

The computer program GRAVPLOT Jones (1977) was used to complete the reduction of the gravity data. The GRAVPLOT program when supplied with the station number, station elevation, latitude, terrain correction, and observed gravity calculated the theoretical gravity, free air correction, free air anomaly, and the simple and complete bouguer anomalies, (see appendix A). The program was then modified to calculate the same results using reduction densities of 2.0, 2.1, 2.2, and 2.4 $gm./cm^3$. A value of 2.1 $gm./cm^3$ was selected for use in the upper layer, which also matched the value in Lillie (1977) for the uppermost unit in his cross section, shown in figure 6.

The Portland State University Honeywell computer was used to do the modeling. The program, FREEAIRFIT, which had been previously adapted (Jones (1977), was used to model the Free Air Anomaly. The modeling program, however, considers only a two dimensional cross section. The third dimension is considered infinite and parallel to the strike of the model line. Contributory errors due to terrain not considered in the two dimensional approximation will not be accounted for at this point. In the modeling program the subsurface geology is represented as polygonally shaped blocks of varying density. The effect of which is calculated at a series of locations on the surface of the model.

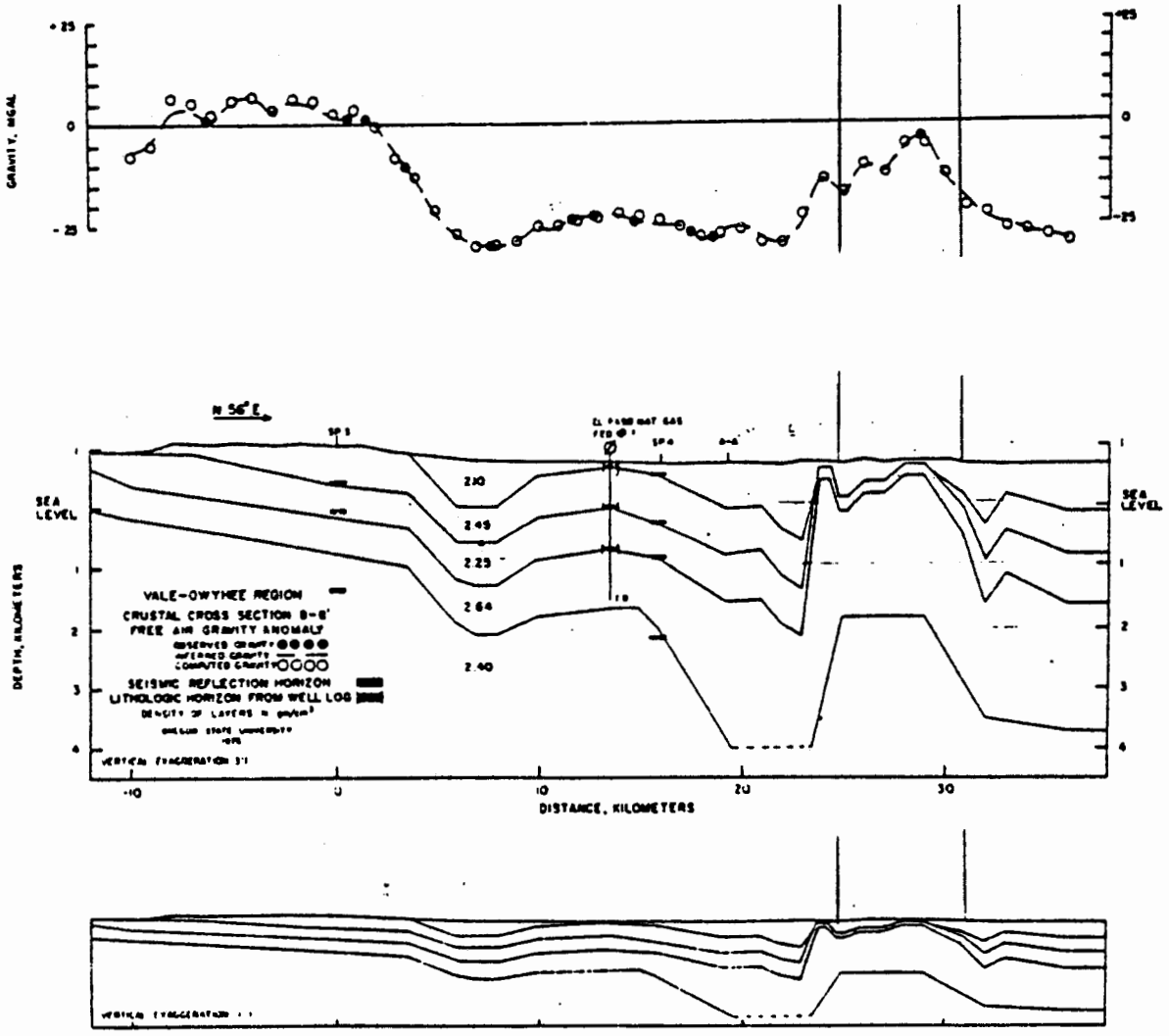

Figure 6. Regional Cross Section along section B-B'. The study area is highlighted in black at the right. Densities shown were used in the modeling program, from Lillie (1977)

Regional models were constructed which extended 95 to 100 km from the ends of the survey lines. Two master regional models were constructed, one oriented N-S and the other extending in the E-W direction. The regional models were constructed to eliminate edge effects caused by the termination of the model and to account for the gravitational effects of terrain which was not covered by the survey and to duplicate the regional gradients of the surrounding area. The regional Free Air Anomaly map is shown in in figure 7, while the contoured Free Air Anomaly map of the Vale area is shown in figure 8.

Gravity Modeling

Results and Discussion

The initial gravity models were run using a single block. This was done in an attempt to contrast the shape of the anomaly with the topography. The object was to determine which sections of the anomaly would be explained solely by change in elevation. Changes in gravity values are caused by either changes in density or elevation.

The results of the initial model were compared with the profile of the observed anomaly. If the values generated by a section of the model were too high then it would indicate an area whose density value was too high and suggest boundaries of that block, see figures 9 and 10 for examples. The computed value could be reduced by installing a down dropped block. A down dropped block would incease thickness of the upper layer which has a density 2.1 gm./cm^3. By increasing the thickness of the volcaniclastic layer the effective density of the column in question would be lessened. This then should indicate

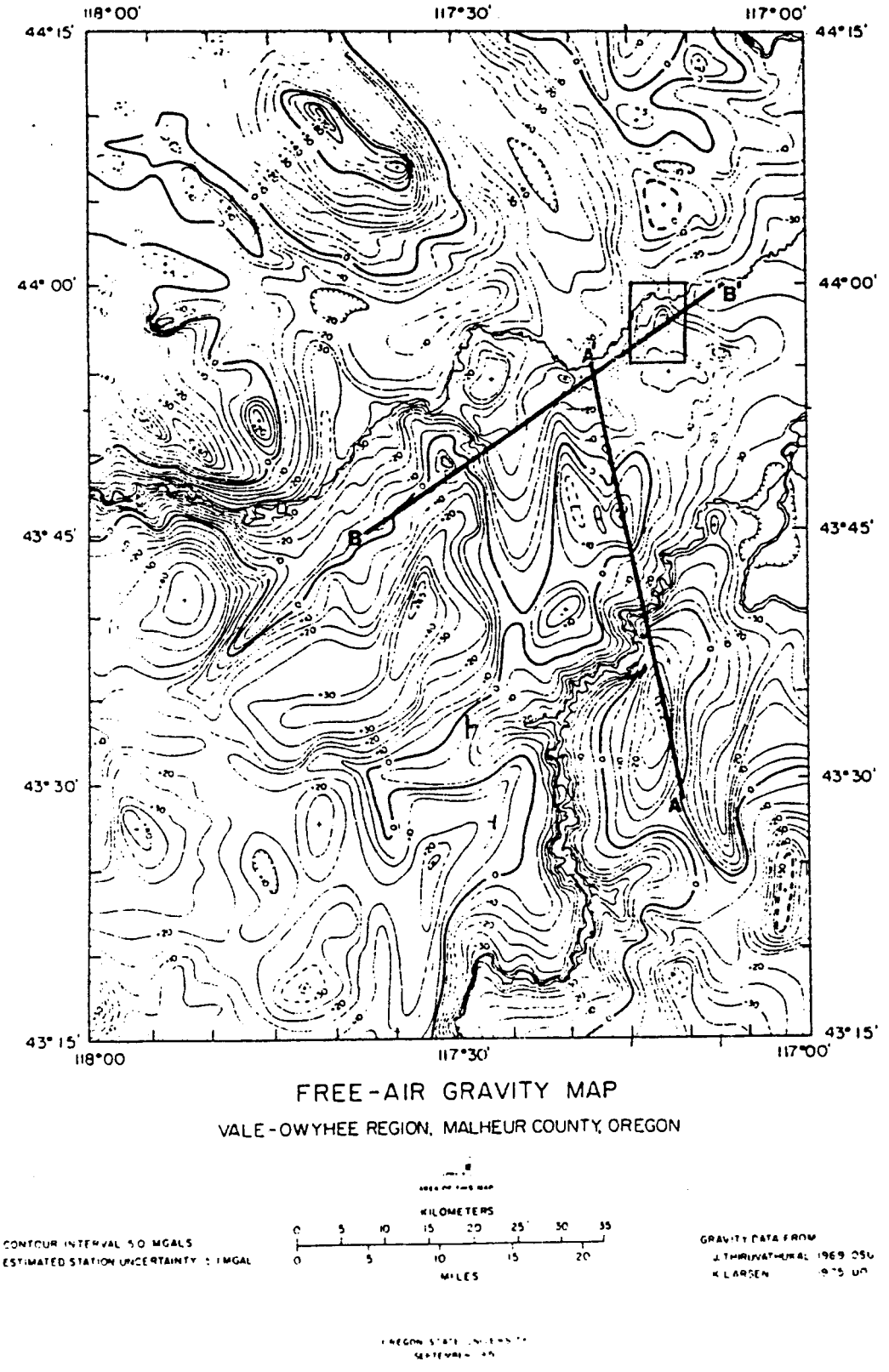

Figure 7. Regional Free Air Anomaly Map. The study area is outlined in black in the upper right, from Lillie (1977)

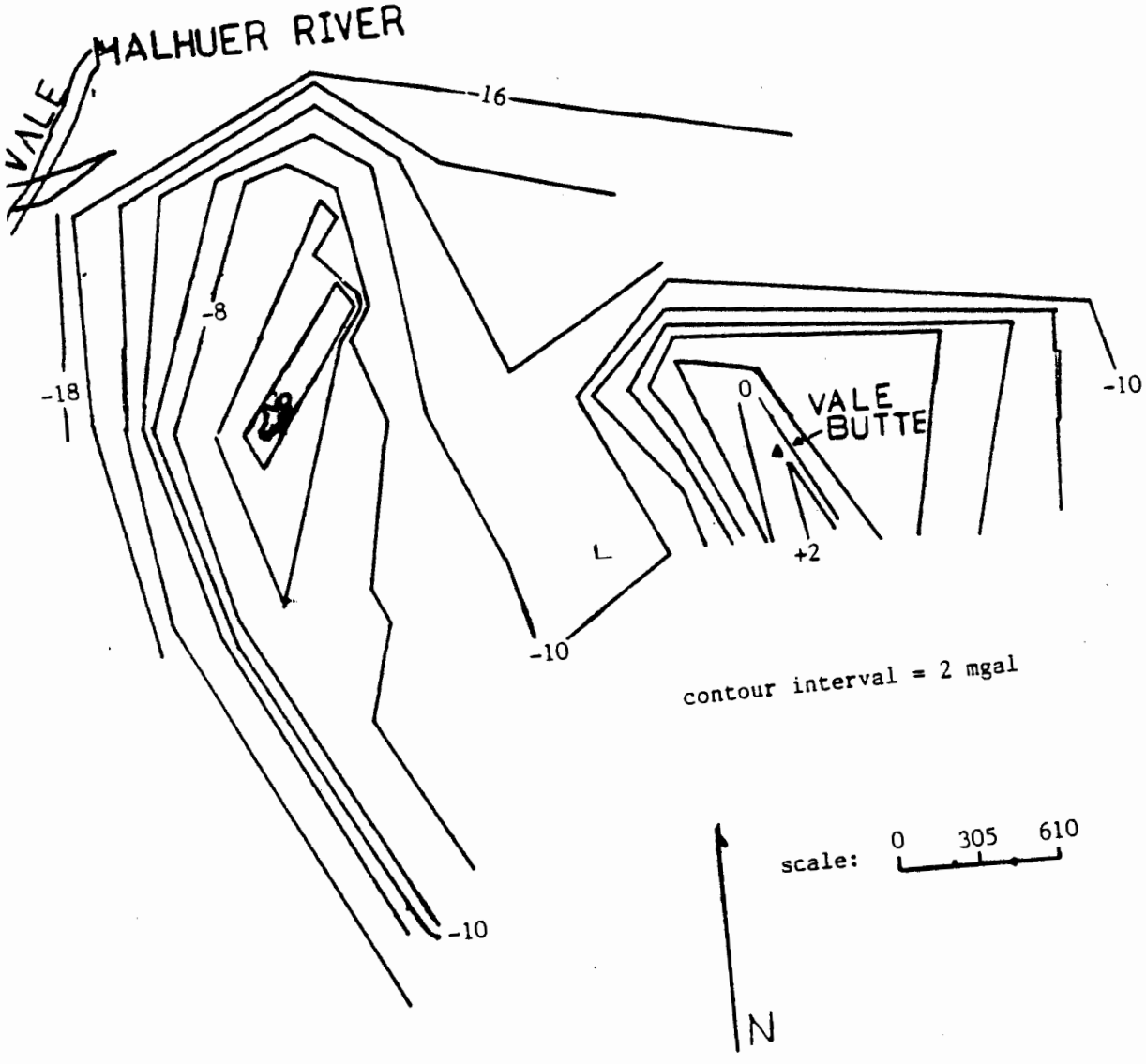

Figure 8. Contoured Free Air Anomaly Map of the Vale Area. The town of Vale is located at the upper left corner.

direction of movement while the magnitude would be determined by the depth of the block boundary. In some cases this offset should indicate depth to a depositional contact. This instance is valid in areas where landslides and recent alluvium is being modeled.

Changes in the model that would require an increase in density could be explained two ways. Either a structural block could have been uplifted, increasing the average density of the block by thinning the low density layer at the surface, or there was an in situ increase in the density of the block. The in situ increase in density might occur in areas that were mapped as silicified zones. In areas of silicification the country rock is flooded and recemented with silica, given a density of 2.7 g/cm^3 in Telford et al (1976). This filled the available pore space, resulting in an increase in density of the rock.

The survey area was bordered on the western through the northern sides by the Malhuer River flood plain. These areas layer of low density, unconsolidated, recent alluvium is deposited upon the older layers. The alluvium of the flood plain was assigned a density of 2.0 gm/cm^3, an average value for recent alluvium from Teleford et al (1976).

The following modeling procedure was and used on each of the survey lines. The initial model contained only one layer of density $2.35g/cm^3$. Changes that were made to that model were done in the simplest format possible and then changes of increasing complexity were made only as required. The simplest changes were using rectilinear blocks, with vertical and horizontal block boundaries. If the fit was sufficient then no other changes were made. If more complex shapes were

required then shapes were evaluated in 15° increments from the horizontal or vertical, and the best fit solution was then adopted. At this point of the modeling it was not attempted to relate the model to the geology. In some areas, field evidence suggested that a more sophisticated shape should be used, but if the fit using the rectangular blocks were good, then no changes were added. Although the rectilinear blocks may fit the gravity data, the actual surfaces are usually dipping a few degrees from horizontal and vertical. On larger blocks, with long dipping surfaces it was necessary to account for the dipping surfaces.

A line

The initial modeling was done on A line, see figure 9 because the structures crossed by this line were thought to be located most precisely. The line was oriented in an east-west direction and included the gravity base station, which was shared with the B line. The line is composed of 44 stations, labeled AE 1 through AE 20, AW 1 through AW 23 and the base, the data is displayed in appendix. A. A" line also intersects both D and E lines at stations AE-9 and AW-9 respectively. Elevations ranged from a low of 683.51 meters at AW 23, in the town of Vale, to a high of 900.26 meters at AE 11 on the north side of Vale Butte. The total length of A line was 5.4351 km. The Free Air Anomaly (FAA) values for A line ranged from a low of -23.472 mgals at station AW-23 to a high value of -0.578 mgals at AE-12. The terrain corrections used ranged between 0.016 and 2.600 mgals.

The survey line ran from AW 23 eastward across the alluvial plane of the Malhuer River across Rhinehart Buttes, the west flank of which is covered by a large landslide deposit. The eastern portion of A line continues across Vale Butte with the line terminated in the valley east of the Butte.

The result of the initial one layer model is shown in figure 9.. Changes are needed except at the center of the line. The center of the line was chosen as acceptable because the greatest number of stations closely matched the values of the observed gravity. There were thus less changes to model and to allow easier comparison with B line. The changes to the model will be described from west to east.

The values calculated for the model were 2.33 mgals to 2.35 mgals too high in the area of the Malhuer River alluvial plain. The flood plain sediments were modeled using a value of 2.0 gm./cm^3. A density contrast of 0.35 gm/cm^3 is generated, and the required depth found to be a range of 200 meters to 218 meters, as shown in figure 10. The length of the block is 3.0236 km. If the density of the sediments is less, than the thickness of the alluvium will decrease correspondingly.

The next change to be instituted was at the location of the landslide deposit on the west slope of Rhinehart Buttes. The landslide deposit is composed of large blocks of silicified rock in a matrix of country rock debris. The deposit itself is very poorly consolidated. A density of 2.1 gm/cm^3 was assigned. The apparent lack of lithification suggests that a density of less than 2.1 gm/cm^3, the density of the country rock, should be used. However, the presence of extremely large, dense, blocks of the altered rock could offset the

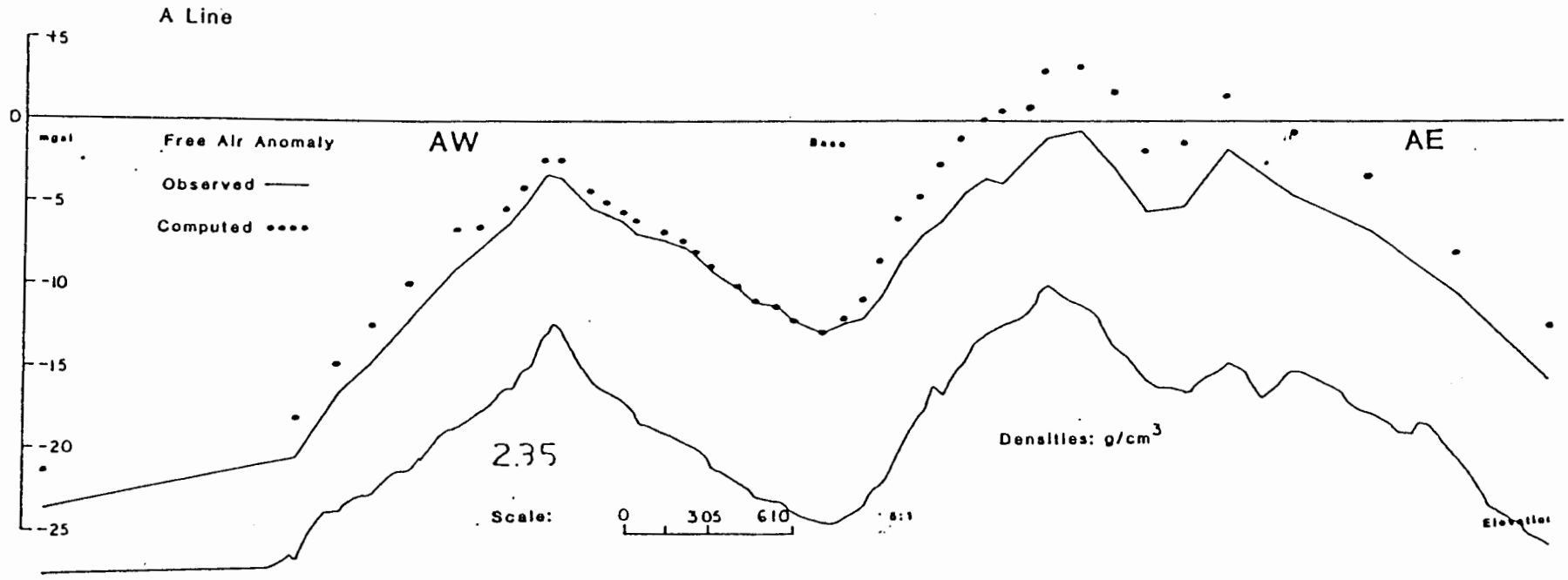

Figure 9. Gravity line A, showing initial model composed of one block

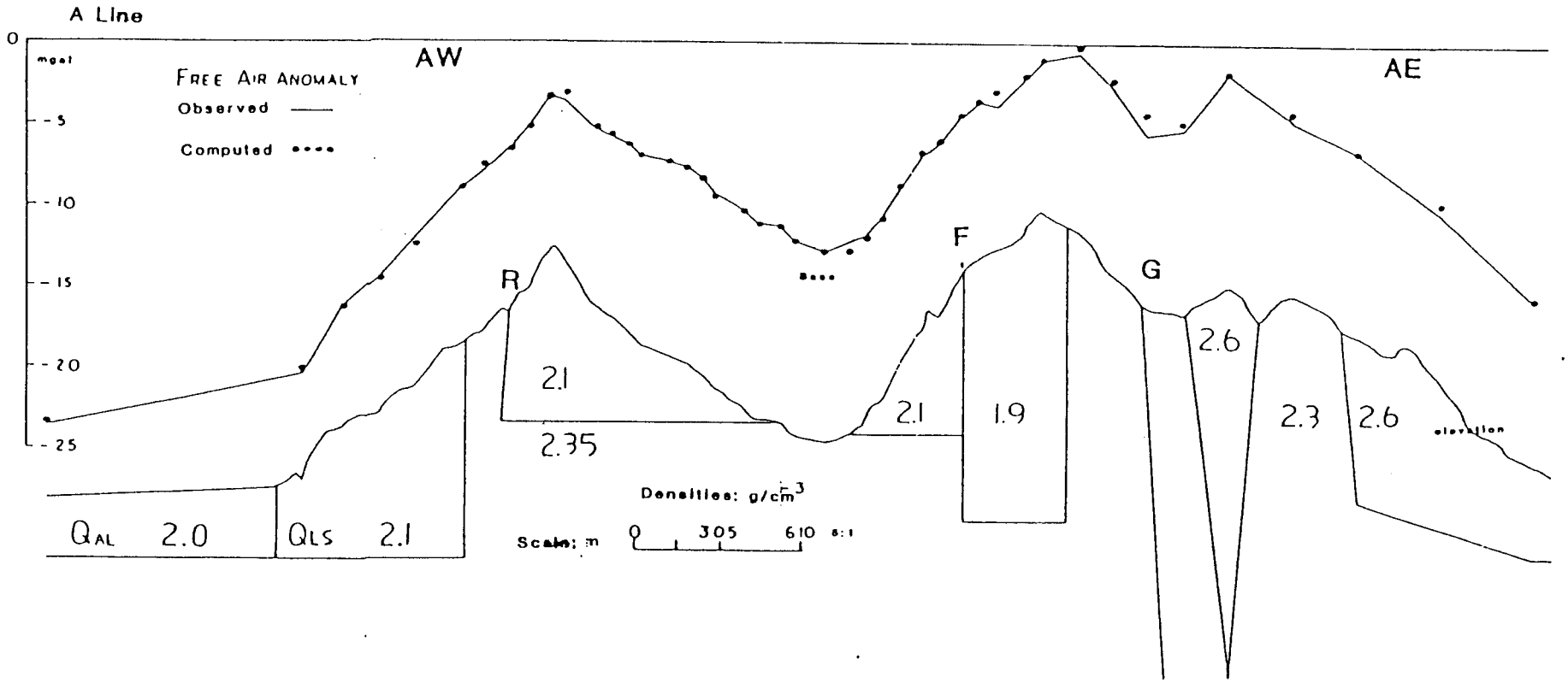

Figure 10. Gravity line A, showing finished model

apparent decrease in density of the deposit. The locations of the contacts or margins of the landslide had been mapped geologically, so the block boundaries were based on this information.

When compared to the observed anomaly on the west of Rhinehart Buttes the initial model indicated too high a value. The differance ranged from 1.60 mgals, on the western edge of the block, to 2.27 gals, near the eastern margin. The thickness of the block was solved by trial and error with the best fit obtained with the base of the landslide block at an elevation of 482.9 meters. The landslide block has a thickness which ranges from 200 meters to 313.3 meters and a length of 664.9 meters. There still are some one point anomalies that have not been corrected. It is felt that these are probably the result of older topography which was buried by the landslide. As the base of this deposit was modeled as a straight, smooth surface any buried topography, which may be a buried density contrast, would manifest itself as an anomally in the calculated effect of the model.

The values to the east of the landslide block were still slightly too high, approximately 0.5 mgal, and increased rapidly from the location of Rhinehart fault, to a maximum of 1.18 mgals at AW 13 on the crest of Rhinehart Butte. The values then decrease until matching the observed at station AW 2. The first to model this block used was a block with a horizonal lower boundary, beginning at station AW 2 and continuing westward. The elevation was the same as AW 2, 730.42 meters. The western boundary was the crest of Rhinehart Butte. The initial model did not fit the observed anomaly. A series of changes were instituted until a fit was achieved. The simplest solution was a

steeply dipping, 75 degrees, western block boundary. This boundary coincided with the mapped location of Rhinehart Fault. The final configuration is a roughly triangular shaped block with the west face dipping 75 degrees and a thickness of 85.4 meters which increases to 134.2 meters at the crest of Rhinehart Buttes and then tapers to zero meters in height. The length is 1044.3 meters.

The fit of the model was good from station AW 2, located on the east side of Rhinehart Butte through the base. The section of AE line, from the base station to the crest of Vale Butte was examined next. The model was again too high. The values ranged from matching the observed at base to a high of being 4.03 mgals over at AE11. The differance in the values seemed to increase with the change in elevation. A similar situation was encountered in modeling the previous block

The same procedure was used as in the previous block used. The values calculated for the model ranged from being too low, 0.34 mgals at AE 1, to being 4.03 mgals too high at AE 11. The first model placed the contact at station AE 2 and the lower block boundary was horizontal at that elevation. The result was that the model was still too high and the contact established at a block corner between stations AE 1 and AE 2. The lower block boundary was horizontal at an elevation of 731.7 meters that resulted in a block whose dimensions were a height of 113.6 meters with a length of 408.7 meters. Station AE 1 remained too low. A series of vertical and later dipping dike like bodies, density 2.7 gm./cm. were installed to bring up the values at that location. The values for AE 1 were brought up to match the observed, however the adjoining stations were then too high. There remains a

small difference in elevation between the two blocks of the upper unit which lie in close proximity to each other. This could be the result of the regional dip, which is to the northeast. Alternatively it could also be the result of a structure which lies between the two blocks. This structure could be masked by a section where strike-slip movement has eliminated a density contrast. This last explanation, however, seems unlikely in view of the fairly large amounts of vertical offset generated in adjoining sections of the fault systems. The fit between the model and the observed was acceptable only for stations AE 2 through AE 5. The fit of the portion of the line between AE 6 and and AE 11 was still too high. The differance was 0.6 mgals at AE 7 and 1.12 mgals at AE 11.

To generate the needed density contrast and still maintain the estimated throw of the block a density of 1.9 gm/cm^3 was used. The lower boundary was established at an elevation of 631.7 meters. The magnetic modelling, however, suggested a deeper seated structure at that location. If a value of 2.1 gm/cm^3 were substituted, the block would have to be thickened. The lower boundary at that density is calculated to be at an elevation of 519.7 meters, which agrees with the results of the magnetic modeling. The section would then have a length of 359.9 meters and a maximum height of 380.6 meters.

The section of A line, from AE 14 through AE 20 was also too high. The values calculated for the one layer model indicated, at least at AE 17 to be 3.53 mgals too high. After several unsuccessful attempts using small surficial blocks, a larger, deep seated block as suggested by Lillie (1977) as shown in figure 6, was used. To decrease the

values the appropriate amount a density of 2.3 gm/cm^3 was used. The block was extended to a depth of 2,300 meters. The fit was at some locations satifactory, while at others it was less so. Stations AE 17, AE 19, and AE 20 were by comparison still far too low. Station AE 17 was 4.56 mgals too low while the other two were less.

The area of station AE 17 was mapped as a silicified zone. To achieve the needed amount of increase in density to raise the calculated value for the station a high density wedge shaped block was used. A wedge, with the apex beneath the station would effectively increase the mass while still acting as a point source. A density of 2.6 gm/cm^3 was assigned on the basis that the rock consisted of, for modeling purposes, pure silica.

Various depth and width combinations were tried and the best fit was a wedge 254.0 meters across and 342.4 meters deep. The wedge was centered under station AE 17 and none of the boundaries extended as far as the neighboring stations. The inverted triangular shape is not be a common geological occurrence, however.

The last two stations of A line AE 19 and AE 20 were modeled in the same way as the previous block. The amount of correction required was determined and the shape necessary to achieve the best fit was achieved by trail and error method. Because of the large block of dense, 2.6 gm/cm^3, material required and the nature of the structure of the silicification zones, which display a tendency to be linear features, it is believed that the zone under stations AE 19 and AE 20 is probably quite narrow and sub parllel to the survey line. The final configuration of the block was approximately wedge shaped having

maximum dimensions of 200 meters in thickness and 1084.6 meters in length.

B Line

B line was the second line to be modeled. The line ran north-south in the valley between Vale and Rhinehart Buttes. B line, as shown in figure 11, consisted of 34 stations including the base, which was shared with A line. Like A line it was divided into two segments, BN and BS, at the base station. BN ran north of base and consisted of 14 stations. BS ran to the south and consisted of 19 stations. The elevation profile was lowest in the north and generally increased in elevation to the south. The elevations ranged from a low of 680.92 meters at BN13 to a high of 770.87 meters at BS 15. The FAA values ranged from a low value of -17.677 mgals at station BN-10 to a high of -9.049 at BS-15. The terrain correction values for B line ranged between 0.061 to 0.549 mgals.

The same modeling procedures were used on B line as were used on A line. An initial model consisting of one block was used first. The one block model, shown in figure 11, revealed an excess of mass on the alluvial plain, and several locations which could be considered to display either an excess of mass or alternatively, adjoining areas which were mass deficient. Both alternatives were considered.

The modelling proceeded from north to south. As was done with A line the block representing the unconsolidated alluvium was the first step. A value of 2.0 gm/cm^3 was used to represent the alluvium. The comparison indicated a difference of three mgal between the measured

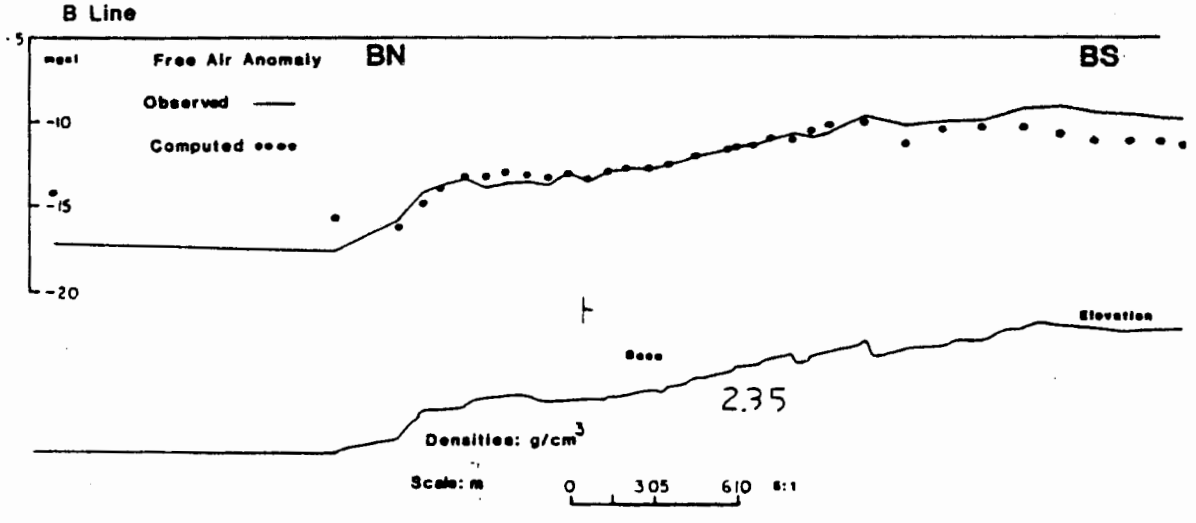

Figure 11. Gravity line B, showing initial model, composed of one block

and the observed. A block was modeled with a depth to the bottom of the block of 258 meters.

Because of the evidence of silicified zones close to B line it was decided to incease the density of those areas to raise the value of the computed gravity, shown in figure 12. Twenty meters south of station BN 12 a vertical dike like body of silicified rock, density 2.6 g/cm^3 was installed. This block was 20 meters wide and was 442 meters deep. The addition of this block brought the value calculated for the model up to match the observed values, but would necessitate the placement of a low density body adjacent to it to the south.

As was done with A line, a block was described which would reduced the values to match the observed. This block, density 2.1 gm/cm^3 was also bounded by vertical contacts with a width of 396 meters and a depth of 123 meters. This block was in the area of stations BN 4 through BN 9. The fit was good for the rest of the line through station BS 11.

At the location of station BS 11, the values of the one block model indicated another mass deficiency. The calculated value was 2.11 mgals too low. The addition of a block, density 2.7 gm/cm^3, which was vertical and was 220 meters wide and 500 meters deep emplaced the correct amount of mass.

B line was then done using the technique of reducing the mass in those places where the calculated values were too high, as shown in figure 13. The block inserted was 2.0057 km. long and had a thickness of 48.3 meters. The block of simulated alluvium reduced the calculated values the required 0.56 mgals.

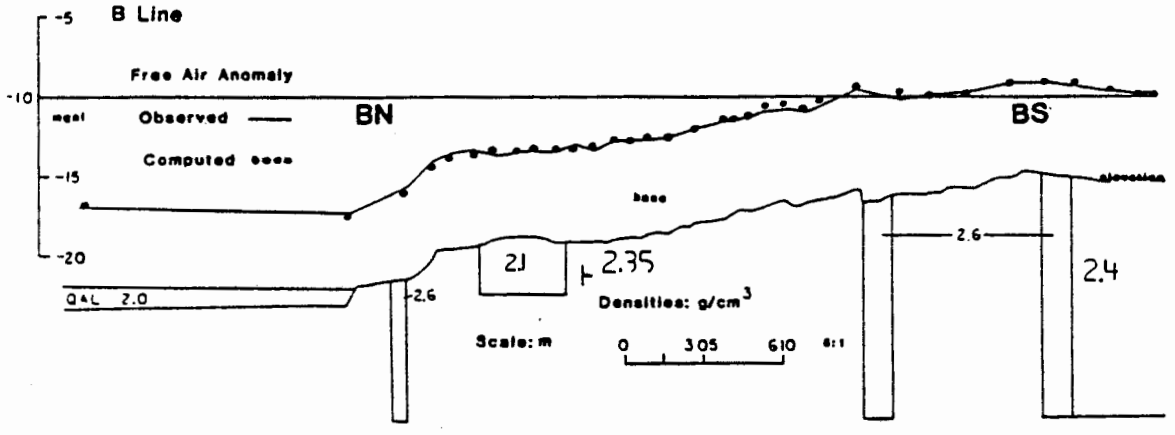

Figure 12. Gravity line B, showing the finished model of the mass deficient interpretation

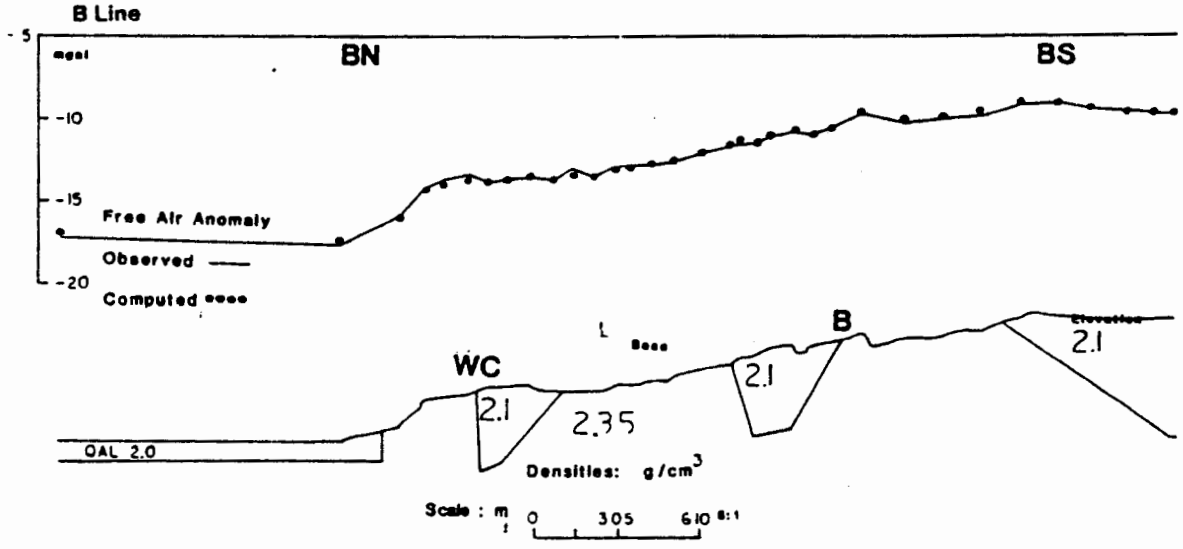

Figure 13. Gravity line B, showing the finished model, showing the preferred excess mass interpretation

The next location to be adjusted was a high that ran from BN 4 through BN 8. This location deviated from the observed by a maximum of 40 mgals. The block was as a wedge shaped configuration, with a density of 2.1 gm/cm^3. The thickness ranged from zero at the edges increasing to a maximum of 120 meters somewhat north of the center of the block. The overall length is 306.7 meters.

The next area was located between stations BS 4 and BS 10. This area was a maximum of 2.0 mgals high. Using the same method as the other locations resulted in a block 60 meters thick, having both the north and south contacts dipping inward to meet a gently northward dipping lower boundary. The maximum depth was at an elevation of 749.0 meters. The resulting length of the block was 414.8 meters. The final area on B line that required adjustment was the southern end, consisted of the last six stations, BS 14 through 19. This section indicated a maximum variation at station BS 19. The variation was 1.05 mgals too high. A southward dipping wedge was inserted, having a maximum thickness at the location of BS 19. The thickness is 90 meters, at an elevation of 679.2 meters.

The format established on A and B lines was used for the rest. All the lines all contained segments which were located on the Malhuer River floodplain, which extended around both the western and northern sides of the survey area. In all these segments a value of 2.0 gm/cm^3 was assigned. On the rest of the lines an upper layer of volcaniclastics with a density of 2.1 gm/cm^3 was used, where needed. The remaining four lines will be described in terms of the finished

model rather than the corrective steps to achieve the fit to the observed gravity.

Interpretation

A line

The configuration of the finished model is shown in figure 10. The sections in the western parts of the model have already been discussed earlier. It may be noted due to a number of reasons that the area of recently alluvium is certainly shallower than depicted in the model. Some of the reasons may be that the alluvium has a density less than the assigned value, or there may be a layer of density 2.1 g/cm^3 overlying the lower layer. This occurrance would have certainly made the layer of recent alluvium in the model much thinner. In the area around Rhinehart fault, marked R on figure 10, suggests a steeply westward dipping reverse fault. The interpretation suggested is that Rhinehart Fault is a westward dipping normal fault, with the increase in density on the western side of the model provided by silicification. Field evidence suggests that this interpretation may be valid. The area west of the fault is composed of silicified country rock, while the area to the east displays very little silicification. The section between Rhinehart Fault and the landslide deposit is a third composite unit. The average density of which happens to be 2.35 gm/cm^3. It consists of a mixture of volcaniclastic sediments and dense silicified country rock.

The section of A line located just east of the base may be interpreted as a section of the volcaniclastic sediments which has not only been truncated by a fault, marked as F on figure 10, but also offset by a second fault, along a different trend. Alternatively, the area modeled, in light of field data is a complex intersection of faults, consequently because of the possibility of a highly fractured area the effective density may be as low as 1.9 gm/cm^3.

To the east, the next section to be interpreted is the downward wedge. From field mapping, the area around station AE 16 is composed of silicified conglomerate beds, with a large areal extent above a siltstone unit. The siltstone units have low permeability and consequently the alteration zones are very narrow. The block could represent a narrow feeder zone of silicified silstone which is capped by conglomerate with silicification of a much larger horizontal extent. The actual configuration may be likened to a T. But, for the model a downward pointing wedge has matched the coputed values with those of the observed.

East of the wedge location is the regional scale boundary fault, shown as fault G on the figure. Brown, 1982, reports that at the location in question is a normal fault which is downthrown to the west. The down to the west is the opposite interpretation of Lillie, 1977, see figure 6, or field evidence, in this report. If the structure were down to the west, perhaps the offset would be sufficiently large enough to raise the Grassy Mountain Basalt to generate a density contrast and increase the density of the block in question.

B Line

The northern portion of B Line is modeled as relatively thin layer of alluvium. Although there are a number of wells in the immediate vicinity, the logs were not helpful. Either the wells did not penetrate beyond the alluvium or those that did the depth of the horizon was not noted. In figure 13 the initial block modeled, to the south of the alluvium is a wedge of upper layer volcaniclastics. This wedge shaped block was interpreted as being bounded by fault planes, marked as faults WC and E on figure 13. The low angle of the dip of the block boundaries is probably due to the intersection of B line and the fault planes at an oblique angle. The closer the angle of intersection between the survey line and a boundary plane is to 90^{o}, the steeper dip, and the closer the boundary plane approximates the actual dip of the fault plane. Another possible interpretation is that the block is actually a landslide deposit, and it could have a density somewhat lower than the value used in the model. In that case the deposit would be slightly thinner than the block shown in the model.

The next block to the south is another graben. The downdropped block is bounded by the faults marked as A and B on Plate I and figure 13. These two structures also occurred on C Line and the magnetic models as well as being identified in the field mapping portion.

The southernmost portion of B Line is another apparently downdropped block of the upper layer. However, the interpretation of this block is ambigous, with several possilble, equally valid explanations. The first and most obvious is that the block boundary

represents another oblique intersection of a fault plane. However in this particular area B line crosses a small area of recent alluvium, and poorly consildated Pliocene sediments. If these deposits are less dense than the 2.1 gm/cm^3 value assign the thickness of the block will be correspondingly thinner. A third possible explanation is that the block represents a combination of both of these events.

C line

C line is an east-west line located about 300 meters south of A line. Elevations range from a low of 684.79 meters, in the west to a high of 927.51 meters at Vale Butte. It is composed of 46 stations; C-0 which is coincident with BS-9 and CE section with 22 stations and the remaining 23 in CW section.

The initial models of the western edge of C line indicated a simple flat bottomed fill of recent alluvium would not match the observed gravity. Only four data points were located on the area of recent alluvium. The structural interpretation developed by Lillie (1977) was used. The model suggested that the floodplain was underlain by a segment composed of small scale horst and graben stucture. This solution satisfied the requirements of the model. The depth requirement for the recent sediments was calculated for each individual point and then integrated into the model as a whole. Older topography, which was buried by the Malhuer River sediments may account for the configuration of the terrain beneath the sediments. The block of recent sediments, alluvium and coluvium, extends westward to the base of Rhinehart Buttes. From that location extending to the east, is a layer of low

density material, that has been faulted by a series of normal faults. Field work suggests that the area is crossed by a number of normal faults. These faults are small scale horst and graben extensional type faulting.

The model of C line, shown in figure 14, consists of one block of low density material, in the western portion. To the east it contains three blocks of volcaniclastics, and the eastern segment is one block of high density material set into the lower layer. The country rock, density 2.35 gm/cm^3, extends from beneath the floodplain to the east, rising to meet a low density block of volcaniclastics at the location at which the recent sediments end. This would suggest that a normal fault, downdropped to the east occurs at this location, This fault is identified as H on figure 14 and Plate I. If the thickness of the recent sediments were to be more than the assigned value then to match the observed gravity at that location an increase in density of the underlying rock would be necessary to compensate for reduction in overall density for the column at that location.

From the margin of the recent sediments eastward 450 meters to the east flank of Rhinehart Butte is a block of volcaniclastic sediments which is downdropped relative to the block adjacent to the east. The location of the eastern block boundary does not agree with the field mapping location of the Rhinehart Fault, which is exposed in that location. The block boundary in the model, labelled R in figure 14 is located about 100 meters east of the Rhinehart Fault. This may be due to the presence of a narrow zone of silicification that occurs along the Rhinehart Fault trace at this location. The offset, suggested by

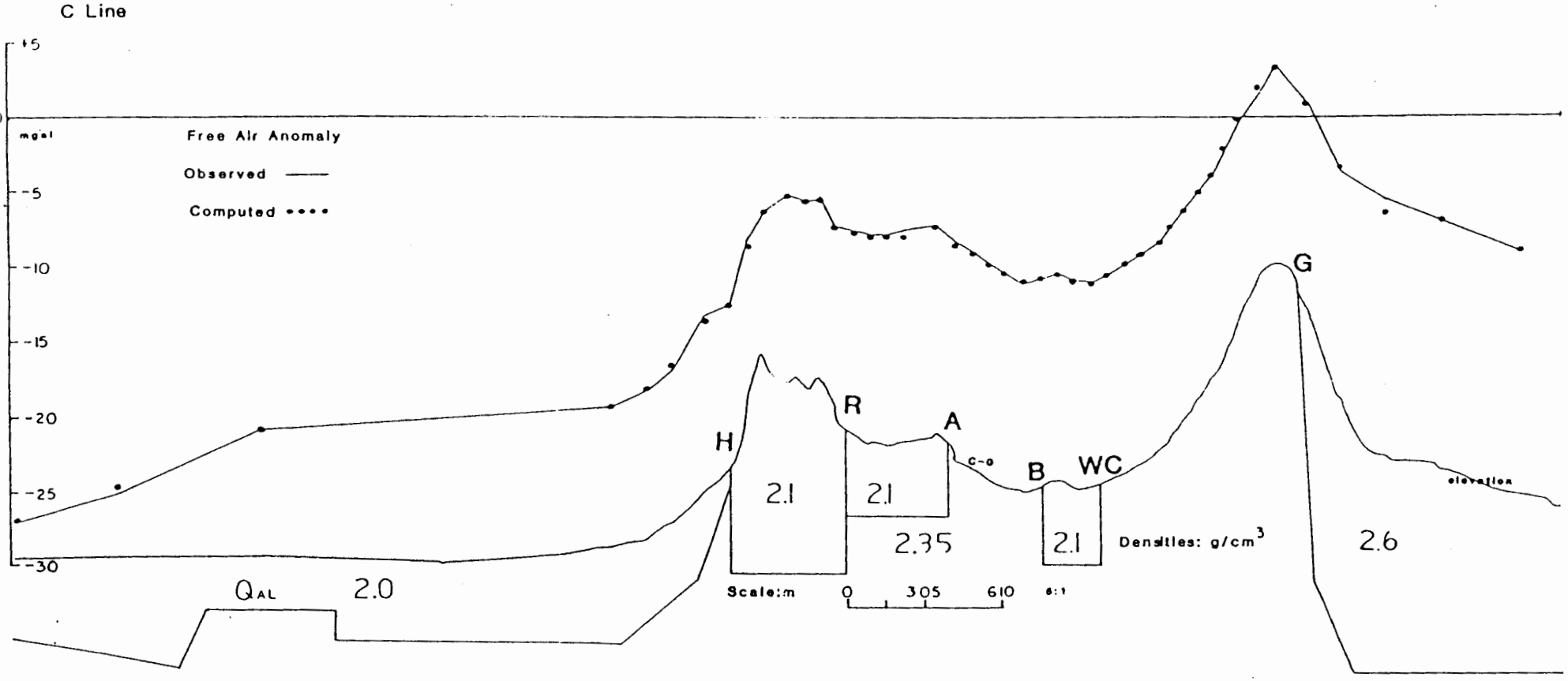

Figure 14. Gravity line C, showing the finished model

the model is about 50 meters, along a vertical boundary. The upper block east of the Rhinehart Fault continues to the east about 390 meters. The block boundary is again vertically downdropped approximately 60 meters relative to the block to the east. The fault at this location is labelled as A. The next block to the east extends about 360 meters. This block is composed of the lower combined layer of density 2.35 gm/cm^3. This block is bounded on both the east and west by blocks of the 2.1 gm/cm^3 volcaniclastic upper layer. C line to this point appears to be described as two en echelon normal faults that are down to west, followed by a horst block which is bounded on the east by a normal fault which is down to the east, shown in figure 15. The offset measured on the model is about 60 meters. Field mapping compliments the modelling as to the location of the this boundary, which appears to be a fault. However, the offset may be less than the 60 meters predicted by the model. The next eastward block is a block of volcaniclastics about 420 meters in length. It is bounded on the west by the previously described horst block and on the east by a vertical boundary. The vertical contact is believed to be another normal fault which is down to west, identified as B. This would describe a small graben, complimenting the horst which lies to the west. This normal fault has been refered to as the southern extension of the Willow Creek Fault by Brown (1982) and trends to the northwest and lies just west of Vale Butte, marked WC. The Willow Creek Fault is westward dipping normal fault, which in the model displays an offset at this location, of approximately 55 meters. To the east of the main Vale fault is a long block of 810 meters which includes all of Vale

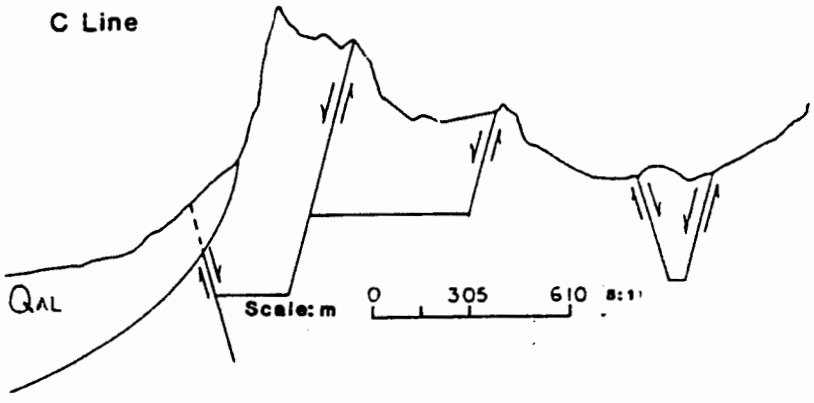

Figure 15. The interpretation of the model of C gravity line

Butte. The block is terminated as an eastward dipping contact located on the eastern margin of Vale Butte. From this structure westward the model suggests an upper layer of low density volcaniclastic material which extends across the lease-study area. This layer of volcaniclastic material has been faulted and offset since deposition during the Pliocene. The layer becomes progressively thinner from the west until it is faulted out at the small horst block. At that point the structure changes from en echelon down to the west normal faults to horst and graben type structure.

The last block on C line is composed of high density, 2.6 gm/cm^3, material. The interpretation of this large mass is that there may be a dike like silicification zone extending subparallel to C line. The area coincides roughly with the eastern section of A line.

D Line

The D line is a north south line which runs parallel to the A line. It is located about 300 meters east of A line and follows the section line between sections 27 and 28 along the west flank of Vale Butte. The model of the D line, shown in figure 16, consists of one block of low density material in the north, with one block of volcaniclastics in the center of the line and the south end has one block of slightly higher density material. To the north the area is recent sediments which are deposited on the lower layer of the model. From the contact at the south end of the floodplain lower layer is exposed. From the crest of Vale Butte to a point 300 meters south is a small block of the upper volcaniclastic unit. It is bounded on the

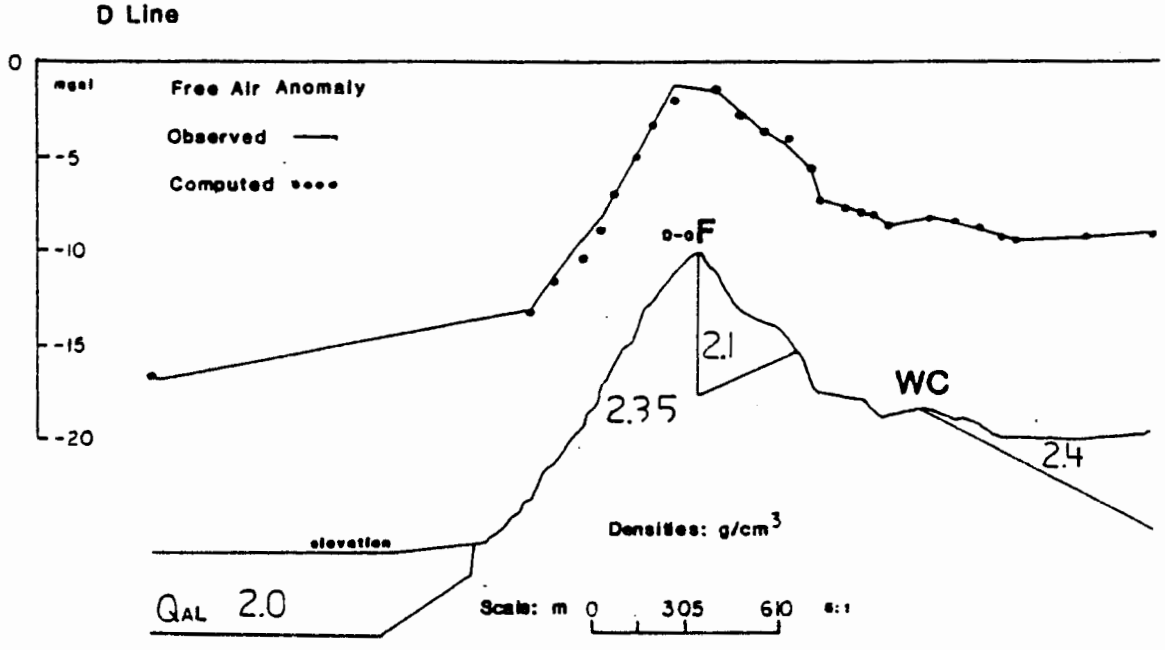

Figure 16. Gravity line D showing the finished model

north by a vertical contact, shown as fault F on figure 16. The boundary on the south is a gently dipping contact. The interpretation suggests a steeply dipping fault which trends roughly east-west occurs at the the northern boundary of this block. The southern boundary may be a fault which crosses the survey line at an oblique angle. This combination would meet at an angular intersection east of D line. The geometry describes a section of a graben formed by two non parallel normal faults. The only other structure denoted by the model of D line is the southern 720 meters is a block whose lower boundary dips to the south and extends beyond the area suveyed. The density of this block was calculated to be 2.4 gm/cm^3. This density value does not agree with the other values used in the model so the interpretation of this block is more difficult. Because of the dip of contact, the model suggests that it may be fault which is crossed at an oblique angle. The geometry of the contact suggests that the contact is a down to the south normal fault. The location and sense of movement are appropriate to the Willow Creek Fault, which would actually be down to the west. The density, however is higher than either the upper or lower layer. It may be an area of silicification combined with the upper layer. small hills around the nothern end of the contact show evidence of silicification. The density selected for silicification zones was 2.7 gm/cm^3, if a small area composed of silicified rocks were combined with a larger area composed of the upper layer the result would be to raise the density of the block in question.

E Line

The E line is a north-south line located about 300 meters west of A line. It runs along the east flank of north Rhinehart Butte and crosses the peak of south Rhinehart Butte. Rhinehart Fault approaches E line in the southern part of Rhinehart Buttes and then gradually trends northwestward away from the survey line. E line crosses A, C, and F lines in areas of the models of those lines which are described by having an upper layer of the 2.1 gm/cm^3 volcaniclastic unit.

In the north, E line is composed of recent sediments overlying the lower layer of 2.35 gm/cm^3. The model of E line, shown in figure 17, consists of a low density block to the north. Immediately south is a small block of high density material. The rest of the line consists of six blocks of volcaniclastics, which are set into the lower layer. At the southern contact of the Malhuer River floodplain the model suggests a one point anomaly which requires a wedge of 2.6 gm/cm^3 material. This could be either a narrow silicified zone, or possibly a bad or missed reading. The high density block is about 90 meters in width while extending to a depth of 50 meters.

To the south of this block is a portion of the lower layer which extends to the surface. This may be an erosional remnant which used to extend to the north, before being eroded by the Malhuer River, or there may a fault located in association with the high density silicification zone. If this latter case is true the location and offset may be masked by the silicification. The rest of the E line consists of a layer of the upper unit volcaniclastics, which have been offset in a

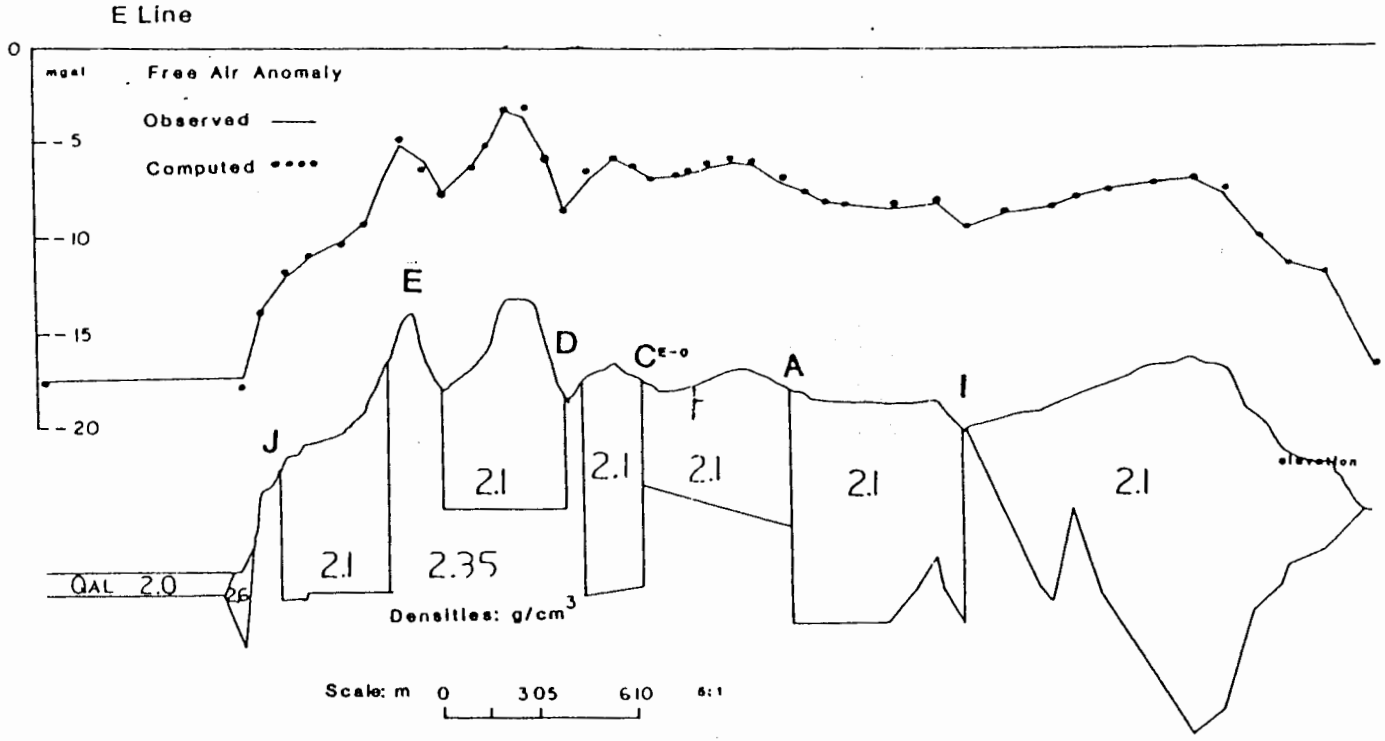

Figure 17, Gravity line E, showing the finished model

horst and graben configuration, with narrow zones of the lower unit extending between some of the blocks.

To the south of the northern block of the lower layer is a block of the low density upper layer which is bounded on the north by a vertical contact, noted as fault J on figure 17. This block is about 360 meters wide and the northern contact suggests an offset of 70 meters. Field evidence suggests that in this location probably is a north dipping normal fault could be present, fault E on the figure 17. The rest of the block is a zone 180 meters wide of the lower layer. The density of 2.35 gm/cm^3 is perhaps not a window of the lower layer but a combined unit composed of a narrow high density silicification zone. At all locations modeled by the planes of the lower unit are conspicous zones marked by silicified country rocks. Such an interpretation would allow continuity of the upper layer across the length of the model and allow the offsets between blocks of the upper layer to be held down to a more reasonable distance. In the field at the these locations the fault is not visible because of the silicification and the offset is contained within one of the thick siltstone beds that characterize the formation. Wherever silicification has occurred within one of these siltstone beds it is characterized by a very narrow width along a fault trace.

The southern boundary of the silicified zone is marked by a vertical contact with the upper layer. This block is bounded both north and south by the silicified zones and suggests that it is horst block which is raised in relation to the blocks on either side of it. This is interpreted as being bounded by a north dipping normal fault to

the north and a southward dipping one to the south, labelled as faults D and E in figure 17. The northern offset would be about 52 meters while to the south the offset would be 53 meters. The block has a width of about 390 meters. The silicification zone to south of this block is about 30 meters wide and probably is a southward dipping normal fault, as shown in the interpretation, figure 18.

To the south of this alteration zone is a narrow, 180 meters block of the upper unit which is downdropped to a graben position relative to the neighboring blocks. The bottom of the block dips gently to the north. The regional dip is to the northeast, so the northward component of the dip agrees with the field mapping. The offset of this block is modeled as 53 meters on the northern contact and 60 meters along the southern contact. The contact of the block is again vertical, but as with the other contacts a steeply dipping normal fault would seem appropriate. These blocks are all generally small and the offsets are also quite small so the amount of variance induced by steeply dipping contact is negligible when compared to a vertical plane over a small distance. The next block to the south is interpreted as a horst block. The bottom contact of this horst block dips to the south. The offset is again 60 meters in the north but increases to 170 meters on the southern contact. This southern contact is believed to be the same contact which bounds the western end of the small horst block in the middle of C line, marked as A. The field evidence suggests a southeastward trending fault which runs between Rhinehart Fault and Wllow Creek Fault. This unnamed fault is a down to the west fault, so the sense of movement and location agree very well with the field

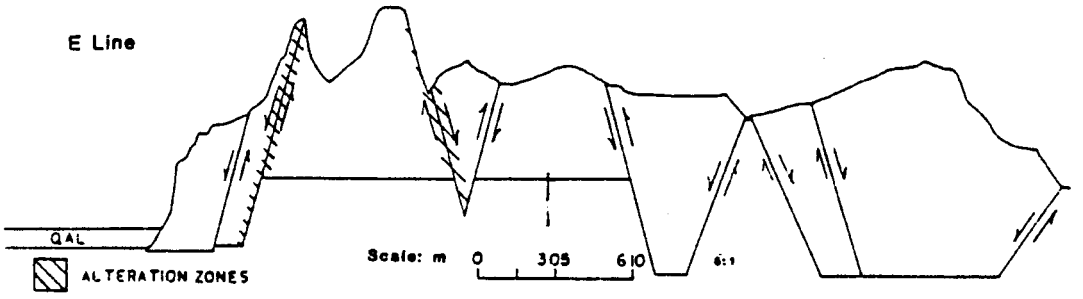

Figure 18. The interpretation of the model of E gravity line

evidence. The southward dip of the block bottom is at odds with the local and regional dip. One interpretation may be that at depth along the northern contact there may exist an silicified zone. This would have the effect of increasing the density within a small area and would be compensated for by raising the contact of the bottom of the upper layer.

The last block that composes north Rhinehart Butte is about 540 meters in length, and is a graben. The contact on the north and south are modeled as vertical. The block bottom is flat, with the exception of a one point anomaly. The anomalous value was considerably higher than the surrounding readings. The depth placement of that particular point was solved individually. The rest of E line southward contained several of these anomalous readings and the depth to each one had to be resolved individually. To the south is another silicified zone followed by a single block 1260 meters in length. The gravity model shows a very complex series of one point anomalies which contribute to make the bottom contact irregular and sawtoothed. The area consists of, at the surface, highly silicified country rock. The combination of normal faults and the large extent of silicification within this area have combined to present an irregular pattern of density contrasts. Field mapping and aerial photography study suggest that the valley between north and south Rhinehart Buttes is fault controlled. The Gravity model suggests that the valley is a complex intersection of possibly as many as four normal faults, this area is noted as I on figure 17. It would seem that south Rhinehart Butte has two en echelon normal faults, down to the south, which are closely spaced immediately

south of the valley seperating the Buttes. The southern end of south Rhinehart Buttes also shows a variable geometry along the climbing basal contact. This may be a single fault plane which displays areas of variable silicification at depth, see Plate I.

F Line

The F line is an east-west line that follows the section line between sections 21 and 28, and is about 300 meters north of A line and crosses the northern end of Rhinehart Buttes. The model of the line, shown in figure 19, presents a similar type of picture as E line. The structure is that of the upper low density layer which has been subjected to en echelon westward dipping normal faulting. The portion of the line which crosses Rhinehart Buttes is made up of three blocks of volcaniclastics, and one block inserted into the lower layer east of Rhinehart Buttes. The westernmost block is about 780 meters in length and composes the entire western half of the Butte. Into this block are inserted two narrow bodies of high density which may represent silicification zones. The contacts along F line are all westward dipping at 75^{o}. This solution agrees with the field measurements of 74^{o} and 83^{o}. The offsets are 95 meters and 90 meters along the faults. An offset in a prominent bed at this location can be seen in the field. The offset is less than ten meters, down to the east. The blocks east of the western block are 330 meters and 270 meters in length and occur in locations which agree with the model of E line. The eastern fault noted as fault J. The block immediately east of of the Buttes is a block of the lower layer, bounded on the west by a vertical contact.

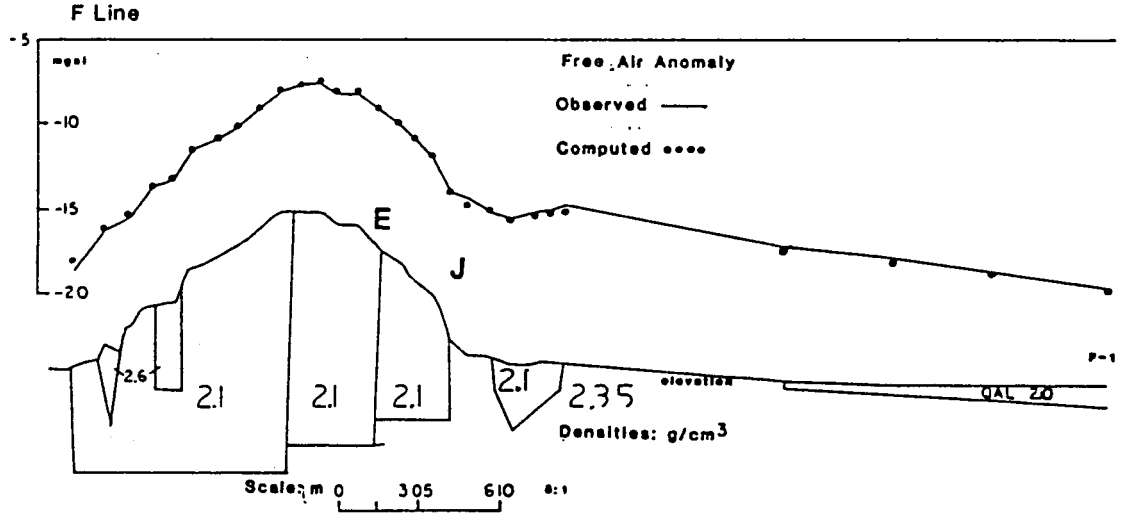

Figure 19. Gravity line F, showing the finished model

This structure may be a small horst block. To the east of the horst block is a wedge shaped block of the upper layer, set into the lower layer. This structure may be a small graben bounded by normal faults trending at an angle to each other and intersecting near F line. The two faults are noted as faults WC and E on figure 17, and Plate I. The eastern, down to the west fault has a location which corresponds highly to expected location of the Willow Creek Fault.

The composite picture shows a structure possibly a down to east normal fault which lies just west of Rhinehart Buttes. Immediately to the east, near the crest of Rhinehart Buttes is the down to west Rhinehart Fault which would delineate the western portion of Rhinehart Buttes as a small graben. The area east of the fault consistantly appears as a downdropped block of the upper layer which has been deformed by a series of norteast ot east trending normal faults. This section displays typical Basin and Range horst and graben structure, particularly in the north-south section. To the east from both the east-west and north-south directions the structure continues as horst and graben type structure. Vale Butte, after crossing the down to west Vale Butte Fault, seems to be one large block, with the exception of the northern shoulder. The northern end of Vale Butte shows a complex intersection of apparently normal faults. The field mapping of this area lends weight to this hypothesis, but does not supply enough to completely constrain the exact location of these structures.

Magnetic Modeling and Interpretation

There are several unknowns which make the magnetic modeling a qualitative procedure, the susceptibility (k), which is dependant upon the magnetite content of the rock, and the remnant magnetization of the rock. Magnetic anomalies are caused by the differing magnetization of the rocks which is caused by differing amounts of amount of magnetite contained in the rocks and the remnant magnetization which is small and can be extremely variable. The anomaly in most cases is assumed to be generally caused wholly by induced magnetization (Telford et al, 1976). A proton procession magnetometer measures the total magnetic field of a station. The measurement is along the earth's field vector. F, the earth's field, is much larger than the local disturbance, T, because of this, the resultant vector is almost the same magnitude and direction as F. In the Vale area the strength of the earth's magnetic field is about 55,000 gammas (0.55 gauss) and the inclination is 72^0 to the north. The declination of 72^0 can approximate a total field vector that is vertical (Van Blaricom, 1980).

The size and shape of a magnetic anomaly are due primarily to the depth and magnetic susceptilbility of the source. In general, the wavelength of the anomaly is a function of the depth to the source. The longer the wavelength the deeper the source. The depth value is a maximum value for the depth to the source. The source may be, and usually is shallower than 1/2 the wavelength.

The magnetic modeling contains three basic assumptions. The first is that the shape modeled will be a simple shape, such as a slab, or a

sphere. Second is that there will be a uniform value for magnetization of the object being modeled. Thirdly, that there is a contrast between the magnetic susceptitibility values inside the object being modeled and the surrounding medium. Along with the assumptions made during the modelling there are several sources of error. Errors can be caused by magnetic noise, from power lines, radio towers, cars, and fencing. Magnetic storms can also cause error.

The reduced profiles of the six survey lines were first examined and compared to Boler's (1979) magnetic data, shown in figure 20. The purpose was to establish the location and magnitude of any regional magnetic anomalies. Because of the length of each of the survey lines, four to six kilometers, the relationship between the location and position of the survey lines and the regional anomalies had to be considered. The study area, see figure 21, is located on a large, southwestward rising, regional anomaly. The northeastern portion of the survey area recorded the lowest values, about 55,500 gammas. The values generally increased toward the southwest with a maximum value of 55,900 gammas occuring west of Rhinehart Buttes. Because of the regional anomaly the zero value for the modeling was established as 55,650 gammas. The contoured data revealed the relationship between the regional pattern and the local anomalies. The study area occupies the junction of two major trends, one which trends about N60^{o}W and the other about N60^{o}E. The northwest trending line is an parallel to Lawerence's (1976) Vale Fault Zone, while the other may be related to an older Basin and Range trend. Lines C and G contained no clearly identifiable anomalies, other than the regional. Lines B,E, and F

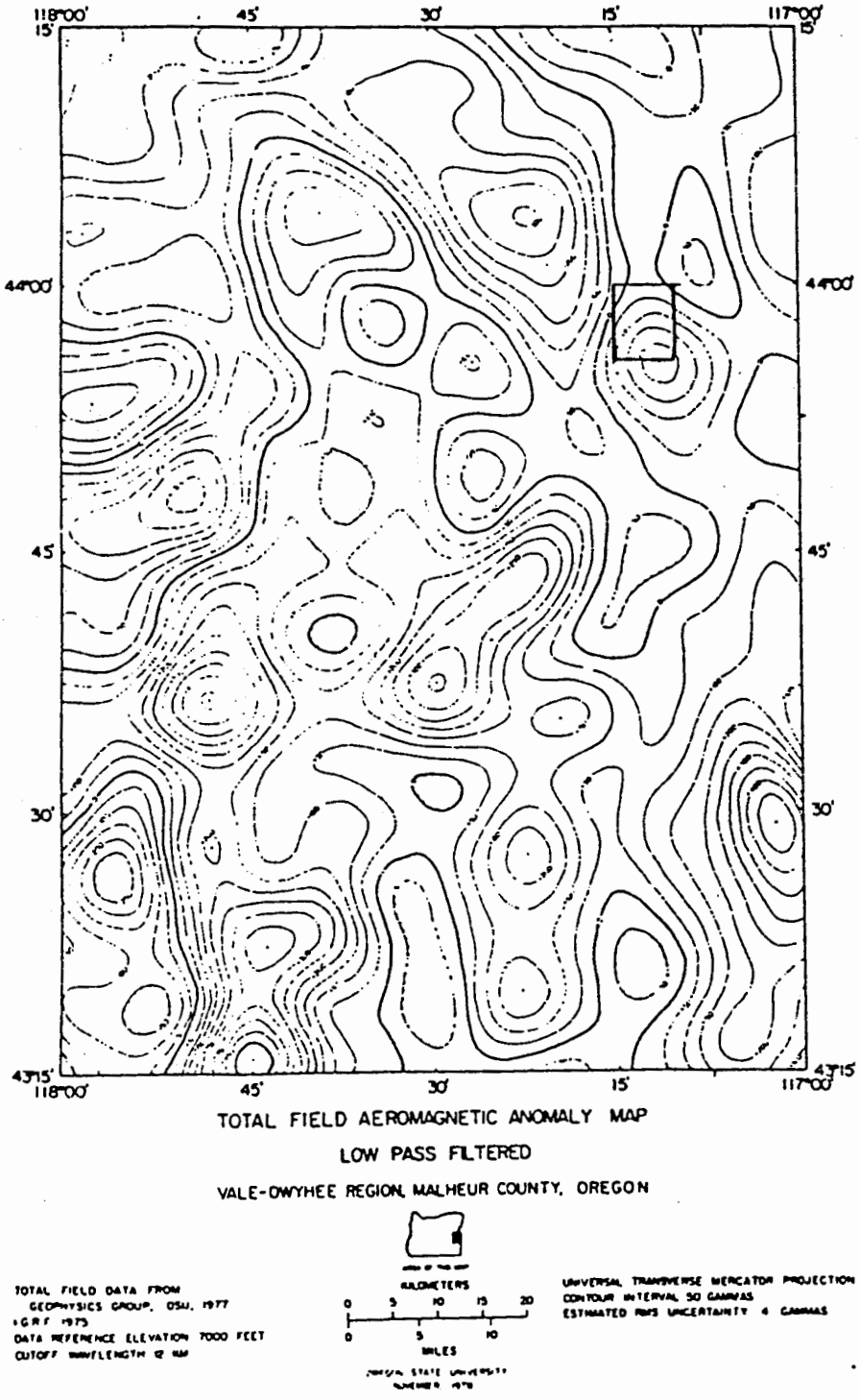

Low pass filtered aeromagnetic anomaly map of the Vale-Owyhee area.

Figure 20. Regional Magnetic Anomaly Map. The study area is outlined in black, from Boler (1979)

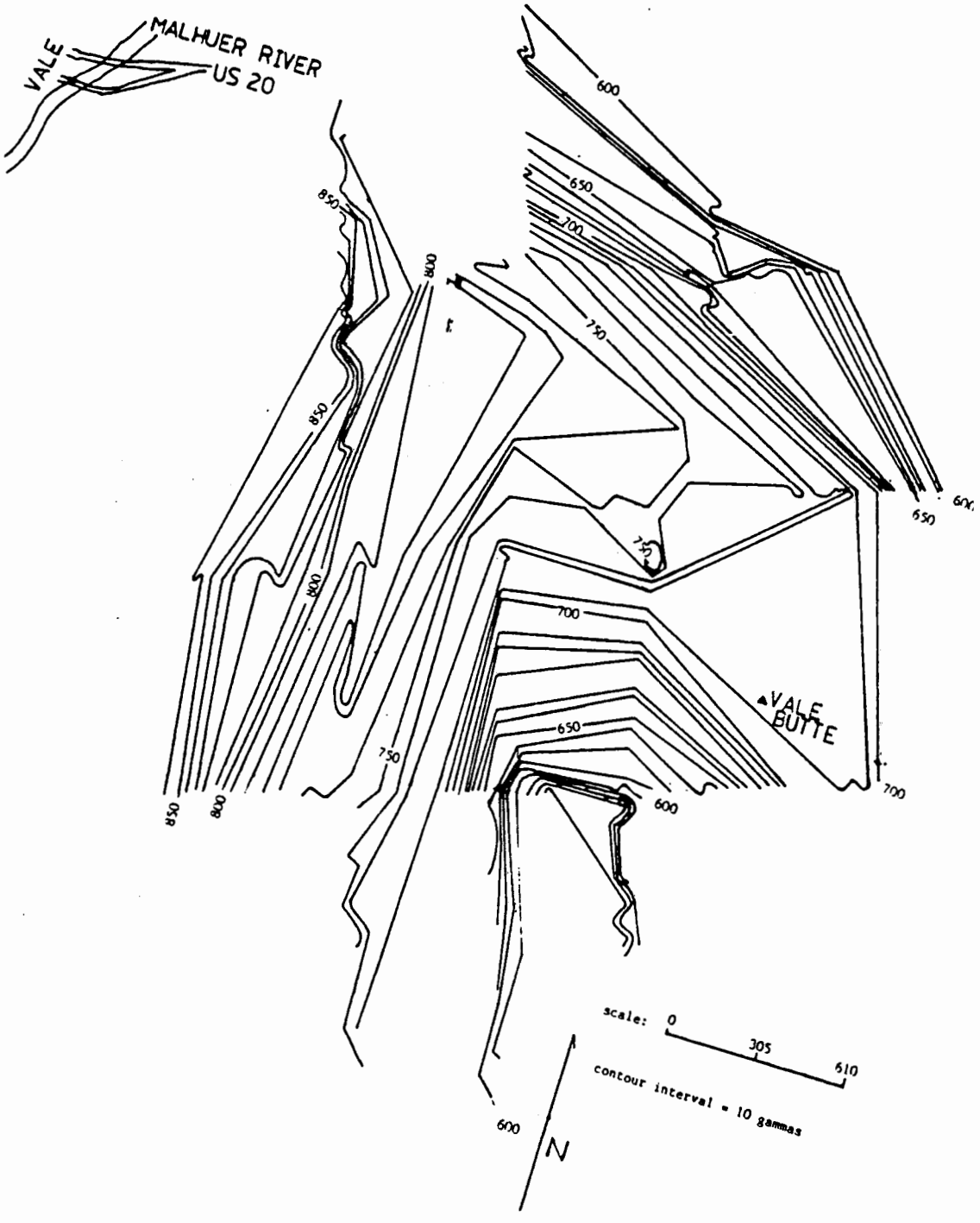

Figure 21. Contoured Magnetic Anomaly Map of the Vale Area. The town of Vale is located at the upper left.

contained one recognizable anomaly of the appropriate wavelength each. Survey line D contained at least four local anomalies.

The initial step of the modeling process was to classify the type of the anomaly to be modeled. An anomaly could be result from a number of different sources. Example curves were prepared for the waveforms of anomalies generated by following features: alteration zones, a subsurface magnetic body, a thin magnetic sheet, and a faulted magnetic slab, these type curves are shown in figures 22 and 23. The alteration caused magnetic anomaly was ruled out because the waveform shape was different than the observed anomalies, the location of the observed anomalies were not coincident with known locations for the silicified zones and magnetic susceptability of the observed silicified rocks was not in the magnitude range necessary to produce the anomaly. The other sources were each examined in this method, and evaluated for the possible use as a model. The only source which fulfilled the criteria for matching the observed anomalies was to model the faulted magnetic slab, where the magnetic susceptibility was in the range exemplified by basalt.

The modeling procedure was similar to that used in the gravity modeling. The simplest model was prepared first, and checked for fit, and if necessary models of increasing complexity were prepared as needed. The first stage was to examine each line to roughly determine the parameters needed for the model. The next step was to generate an initial simple model for comparison to the observed values. As needed the model would adjusted to obtain the best fit to the observed data.

The initial model which was used to determine the cause of the

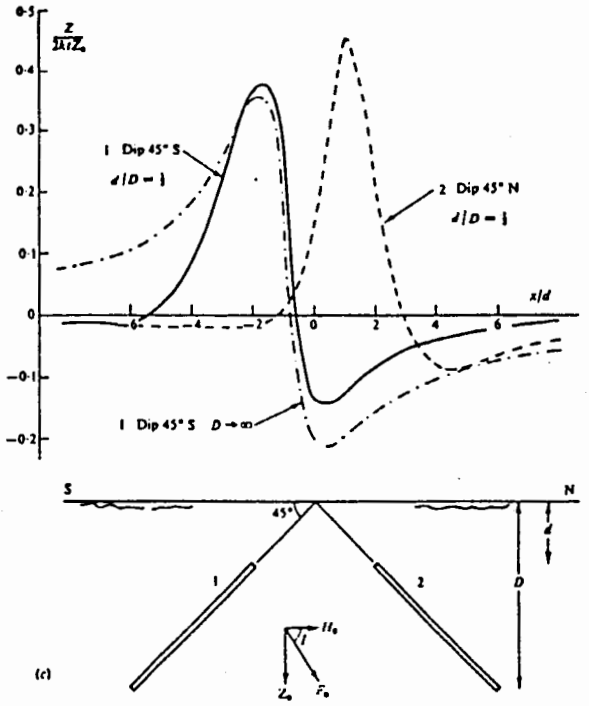

Fig. 3.26 Thin sheet, Z curves, $I = 60°$. (*a*) Sheet striking NW–SE, dipping 45°NE; (*b*) sheet striking N–S, dipping 45°E, 90°; (*c*) sheet striking E–W, dipping 45°S, 45°N.

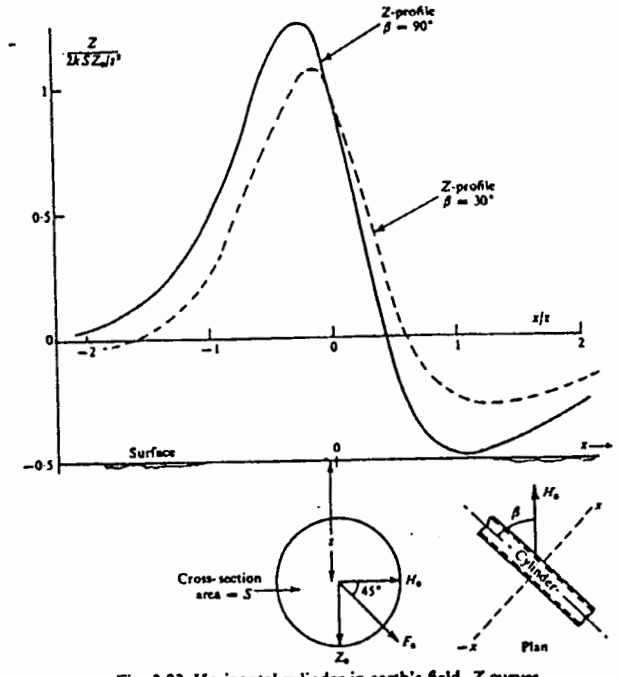

Fig. 3.23 Horizontal cylinder in earth's field, Z curves.

Figure 22. Typical magnetic anomaly wave form and sources, from Telford et al (1976)

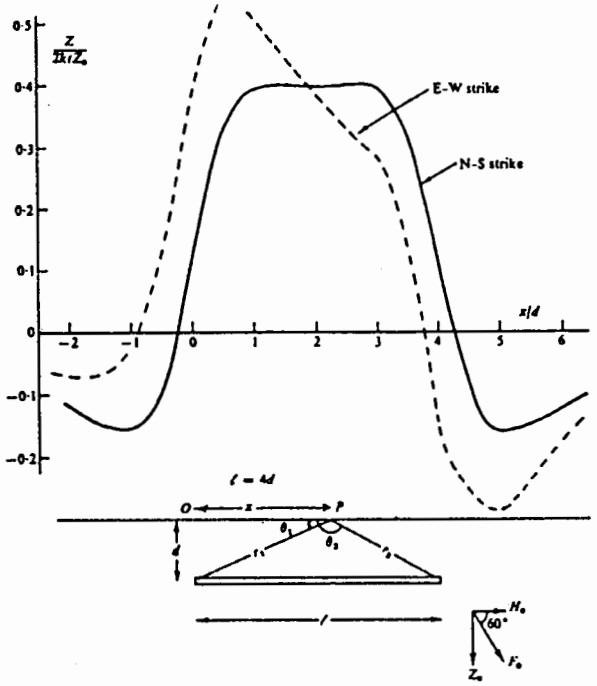

Fig. 3.27 Horizontal sheet striking N–S or E–W, Z profiles.

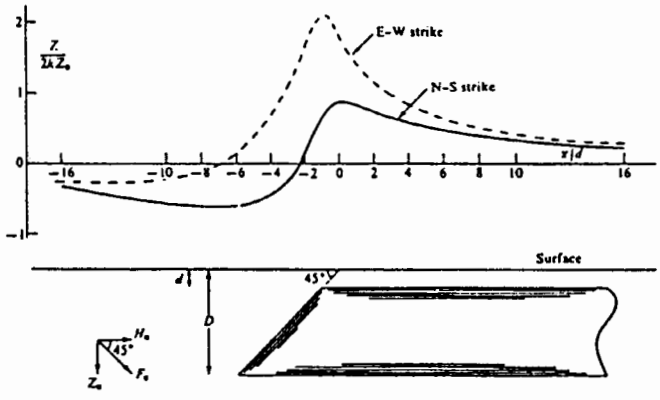

Fig. 3.30 Semi-infinite horizontal slab, edge striking N–S or E–W.

Figure 23. Typical magnetic anomaly waveform and sources, from Telford et al (1976)

anomalies was a thick, horizontal buried slab of basalt, which was offset by vertical faults (Telford et al, 1976). The model was used as a basis for the rest of the modeling. Where necessary, the model was changed to utilize different burial depths, varying dips on the fault planes and faulted dipping beds. Various combinations of these models would be necessary to compare to the observed. The fault plane solutions were worked out for fault dips of 90,75, 60, and 45°. Additionally, the magnetic susceptability of the units modeled wre estimated from Telford et al (1976).

B Line

The initial model was prepared for B line, shown in figure 24, which trends N70°E and includes the magnetic base station. B line crosses gravity lines A and B at the base station. The magnetic profile of B line displays a distinct local anomaly with a wavelength of about 1150 meters, superimposed upon the regional trend. The anomaly is centered over the northwest shoulder of Vale Butte. The depth to the feature causing the anomaly is vital in this location. Brown (1982) states that basalt of the Grassy Mountain type is found at a depth of about 200 meters in the Malhuer River floodplain, north of Rhinehart Buttes. The best fit solution indicates that the depth is in the 400 meter range. However, because of the reasons referred to in the opening paragraphs of this section, the 400 meter depth is considered a maximum value. The model predicts that the anomaly is generated by a fault with an offset of about 100 meters. Again the value of the offset should be considered a maximum value with the actual value

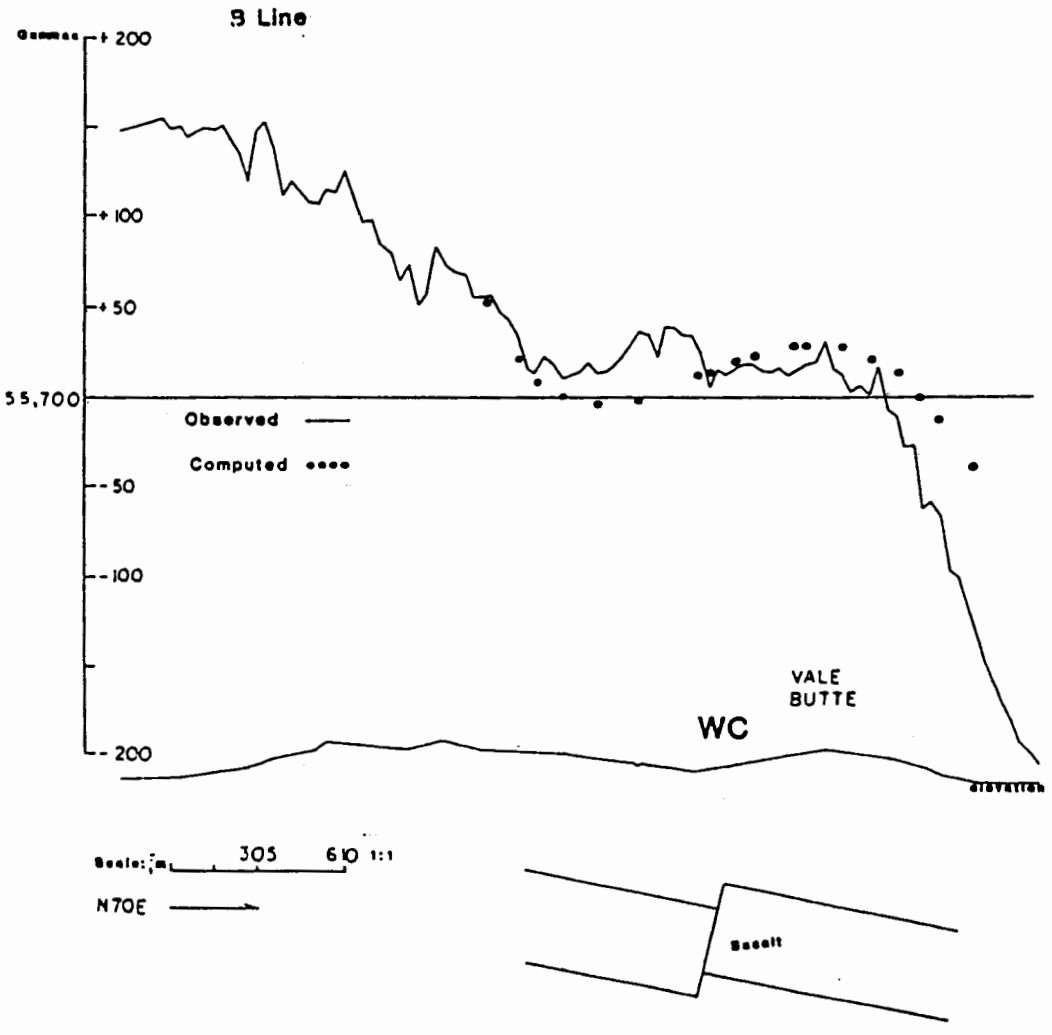

Figure 24. The model of the magnetic anomaly located on magnetic line B

probably less. These maximum depth values fit within the constraints supplied by the well log data (Brown, 1982).

The best fit solution called for a thick eastward dipping slab of basalt which has been offset 100 meters by a normal fault which dips westward at an angle of 75°. The fact that the model predicts a slab that dips to the east at 15° and field mapping gives the dip of the beds in that location as ranging from 8 to 18° to the northeast represents a reasonable correlation.

D Line

The D line trends parallel to B line at N70° E. The line is the most southerly of the survey lines, and crosses C gravity line at the crest of Vale Butte. The profile of the magnetic values for D line show six distinct local anomalies. Three of the anomalies occur east of Vale Butte in an area where coverage by verifying gravity and magnetic survey lines is limited. Although the anomalies were modeled, shown in figure 25, verifying data from other sources is lacking. The portion of the line running between Vale and Rhinehart Buttes is fully supported by both other magnetic and gravity lines.

The modeling procedures outlined earlier were used to estimate the depth and sources of the anomalies. The sources of the anomalies are normal faults. All have suggested offset of about 100 meters, and the variations in the computed depth to the structure generally concurs with the local estimated dip of the units.

The easternmost fault is a normal fault, which dips to the west at 75°. A number of faults occur in the area, however identification of

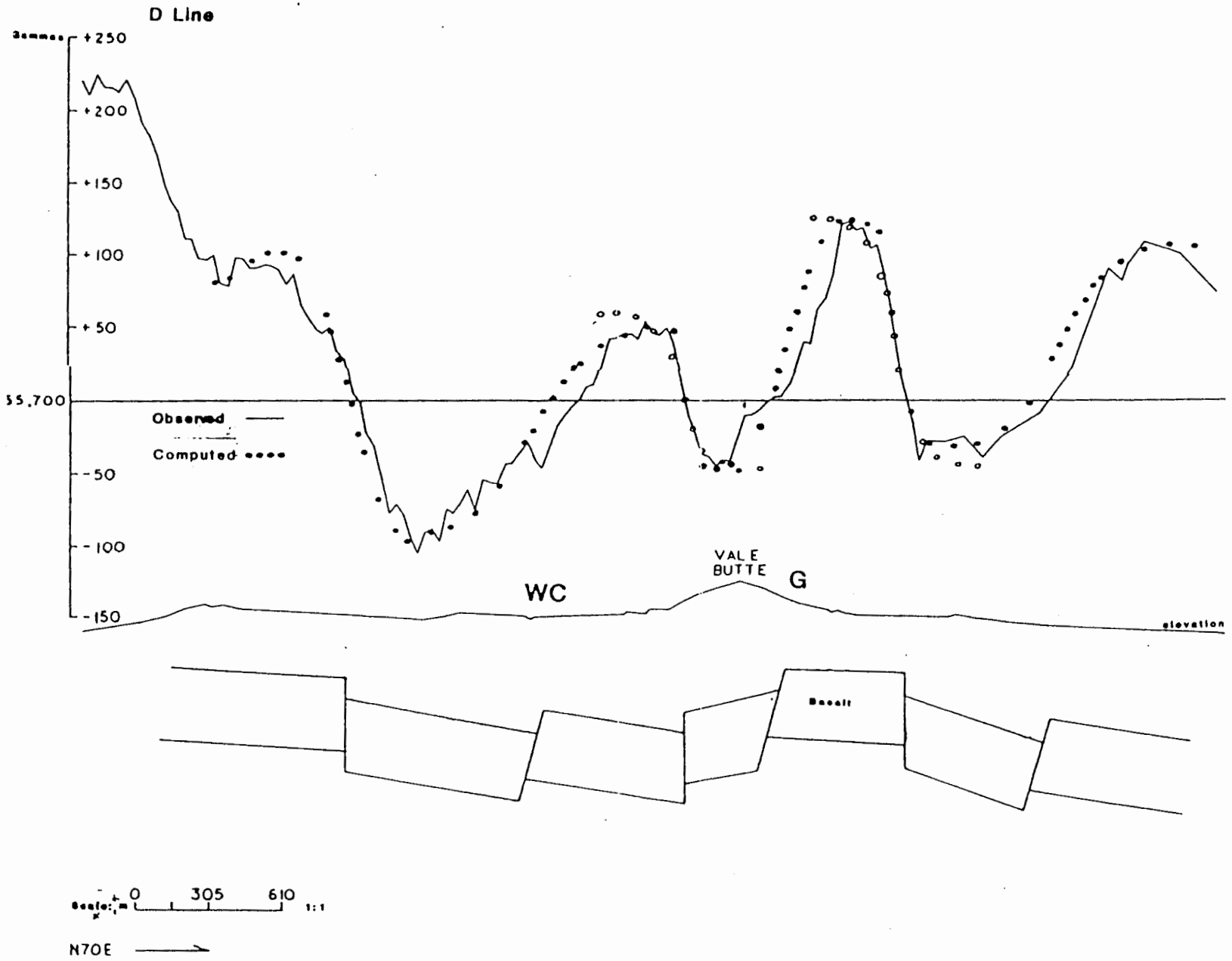

Figure 25. The model of the magnetic anomalies located on magnetic line D

that particular structure has not been accomplished. Note on Plate I there are several faults in the immediate vicinity which can fit the model. The depth to source is 300 meters and is down to the west. This fault may be either the east-west trending fault or the northeast trending fault, which are both located in close proximity to this portion of the D line. The same applies to the next fault to the west. As this particular area is crossed by several faults of differing trends, each fault has possiblities of being the fault that is the source of the anomaly. The depth to source is 240 meters, and the fault is vertical. The fault located on the eastern flank of Vale Butte does not agree with data from the gravity model of C line which occupies the same general area. A gravity line, to the north of the location of the magnetic anomaly suggests an eastward dipping normal fault, see figure 10, fault G. Because of the nature of the structure of the area these two structures may in fact both be present and be two distinct and unrelated features.

The third fault to be modelled on D line occurs near the western base of Vale Butte. The model depicts a down to the east normal fault. The model predicts the presence of a vertical normal fault at a depth of about 480 meters. This particular fault has not been identified in either the gravity modeling portion, or by field mapping. The next fault to the west, noted as WC is the Willow Creek Fault. The magnetic model has a source depth of 500 meters. The depth estimate is believed to be too deep, but this estimste is a maximum value, and the physical presence of the structure is believed to be somewhat shallower. The location of this fault, agrees well with that predicted by the gravity

models for a westward dipping normal fault. The amount of offset agrees with that predicted by the model of A gravity line for the same feature. The offset required by the model of C gravity line is somewhat less. Field mapping has added evidence of offset in that area.

The final and westernmost anomaly modeled on D line occurs on the eastern flank of south Rhinehart Buttes. The model predicts an eastward dipping normal fault with an offset of about 100 meters. This fault, together with the Willow Creek Fault are the boundaries to a small graben, occuping the valley between the Buttes. This graben, is present only in the southern portion of the survey area and is terminated by cross faulting near C gravity line. Again this structure agrees with both the gravity modeling and field evidence as to location and sense of movement. Because of the consistant evaluation of the offset at 100 meters, and the approximation style of the magnetic modeling the value of the offset is suggested as maximum value. The most important aspect of the magnetic modeling is the fact that those faults which extend down to the Grassy Mountain Basalt generally agree in both location and sense of movement with those faults that have been modeled as part of the gravity study and field mapping.

E and F Lines

Both E and F lines trend N20° W, and are shown in figures 26 and 27. E line is the easternmost of the magnetic lines and crosses through the magnetic and gravity base station. F line is parallel to E line and is located about 500 meters west of the E line. The solutions

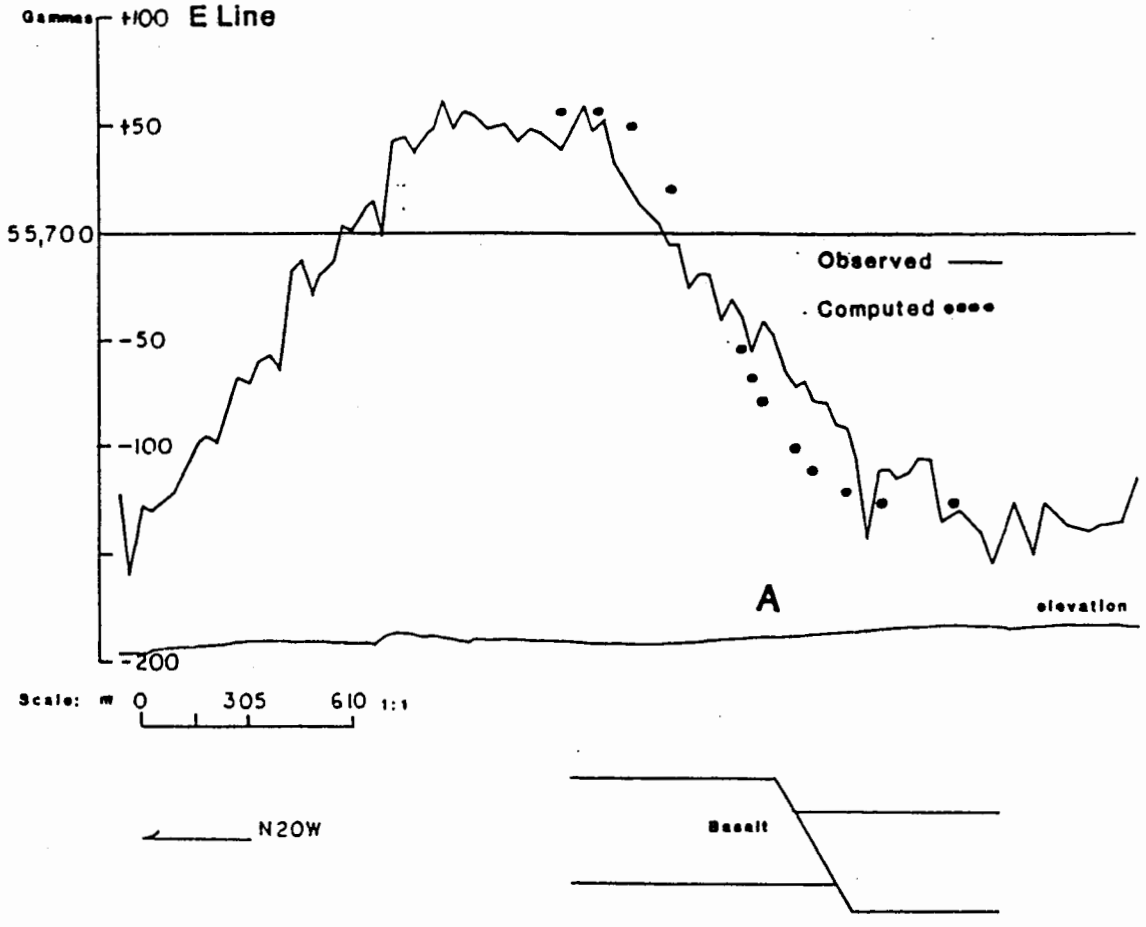

Figure 26. The model of the magnetic anomaly located on magnetic line E

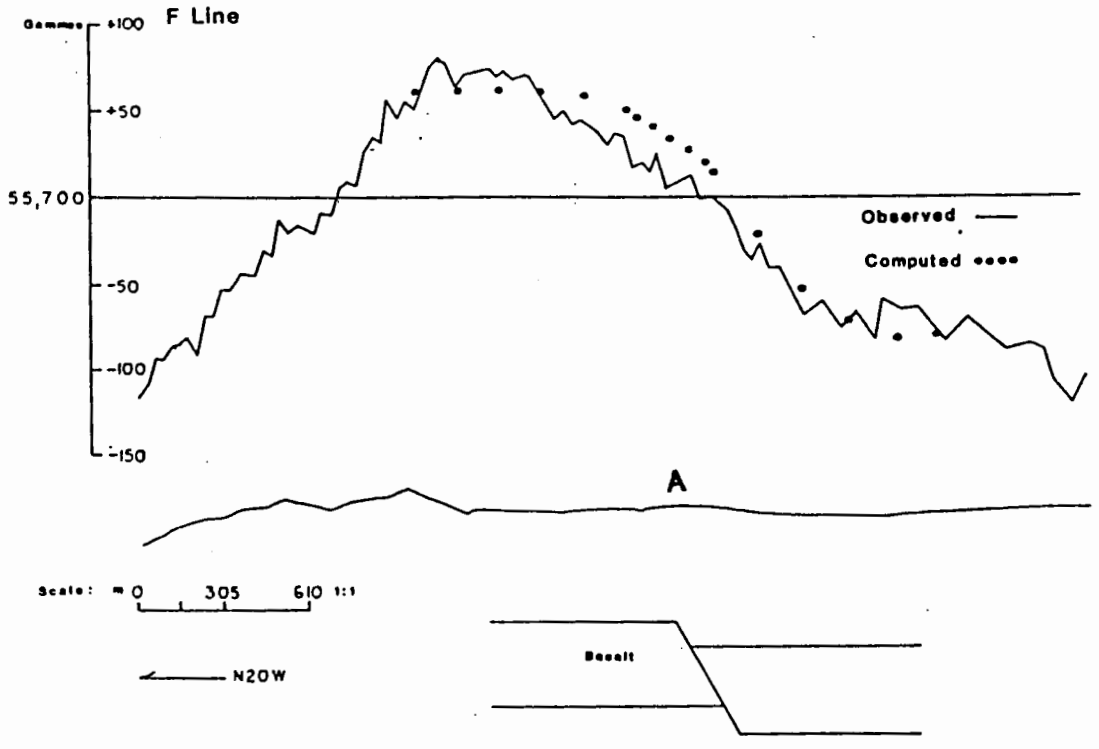

Figure 27. The model of the magnetic anomaly located on magnetic line F

and structures for the models for both are very similar and are probably caused by the same structure. The locations and apparent dip suggest that the structure, a southward dipping normal fault are the westernmost anomaly causing fault which is described in D line. The apparent dip, which the model suggests as 60^{o} is probably a steeply dipping fault plane which is crossed at an oblique angle by both survey lines. The model has a source depth of 400 meters and an offset of 100 meters. The source is the fault labelled A in the figures and Plate I.

CHAPTER V

CONCLUSION

Located beyond the western margin of the study area is a large, normal fault which dips steeply to the west. This fault is unnamed and has been identified only through the use of geophysical techniques. There is no fault trace visible at the surface. This unnamed fault has been located and verified by both Lillie (1977), and although it lies outside the study area is seen in this study. The estimated displacement along this fault which may be part of, or possibly, an extension of the Bully Creek Fault is 850 meters. The fault is a boundary between a regional horst and graben. The graben lies to the west of the study area, which is centered on the horst. The blocks have been informally named the Vale horst and graben. The Vale Horst underlies the study area.

The western portion of the study area consists of a set of smaller horst and graben structures, which are on the western edge of the Vale horst block. These smaller structures are also located by geophysical studies under the alluvial plain west of Rhinehart Buttes. There are no visible fault traces at the surface. The size, horizontal separation and estimated offsets along these structures is smaller than the Vale horst and graben and these smaller structures have been classified in this study as belonging to the Vale horst structure. On the western edge of the study area is a small horst, see Plate I. The

horst block is about 500 meters wide. Geophysical modeling suggests that displacement is about 300 meters upward, relative to the eastward adjacent portion of the Vale horst. The orientation of bounding faults of this block were not determined because only one geophysical line transversed the structure; however Lillie (1977) suggested that the orientation is to the northwest, approximately parallel to other structures within the area.

The eastern boundary of the small horst is an eastward dipping normal fault. This eastern boundary is located about 1000 meters to the west of Lytle Boulevard and beneath the meanders of the Malhuer River in sec 32 shown on Plate I. This structure was located in the modeling of the C gravity line.

Located at the western base of Rhinehart Buttes is an eastward dipping normal fault. The gravity model suggests that the fault is down to the east. The displacement of this fault is about 90 meters. This fault, labeled H on Plate I is covered by colluvium and is not visible on the surface.

The crest of Rhinehart Buttes is marked by a fault which dips 83° to the west and the west side is downthrown. The western portion of Rhinehart Buttes is a graben. The model of the C gravity line (see figure 10) suggests a maximum throw of about 50 meters. The valley to the east of Rhinehart Buttes contains several faults. The principal fault trends N60° W and is located at the western base of Vale Butte. The west face of Vale Butte is an eroded fault scarp. Willow Creek Fault is a west dipping normal fault. The gravity models of B and C lines, the magnetic model of the D line and possible stratigraphic

correlations suggest a maximum displacement of about 100 meters along the fault. This is the fault denoted as WC on Plate I. gravity and magnetic modeling do not detect strike slip movement. Strike slip movement is detectable only if the movement resulted in a density contrast, for gravity, or resulted in the offset in a vertical sense of the basalts at depth, for magnetics. There is a clear change of structural orientation across the Willow Creek fault. To the west the small cross faults strike about N30°W while those to the east have a consistent strike of about N30°E. The north-south offset in the topography between Vale and Rhinehart Buttes, also suggests right lateral motion. Several faults, traceable over a considerable distance and are in the appropriate location, are considered as the southern extension. On all of these structures the fault trace is lost both to north beneath the alluvium of the Malhuer River and to the south, beneath the Pliocene to Pleistocene sedimentary rocks.

The other major structure within the valley between Rhinehart and Vale Buttes is another normal fault which fault trends about N40W and dips to the west and is labeled A on Plate I and figures 14 and 17. Fault A has been detected in the models of gravity lines C and E and magnetic lines E and F, as well as by field mapping. This fault runs from Rhinehart Buttes to the east side of the valley where it intersects the Vale Butte Fault. Fault A was part of the conduit system for the fossil hot springs and shows silicification along part of the length. That part of the fault which displays silicification is the linear ridge in the SW/4 of sec 28 (see Plate I). The ridge is an example of inverted topography where the silicified rocks are more

resistant than the country rock. Displacement along fault A is a maximum of about 30 meters and the Rhinehart fault is displaced to the west along the trend of fault A indicating that it was active after the formation of Rhinehart fault. Fault A may have been active as recent as the Pleistocene because at one location the sediments of Captain Keeney Pass are truncated by this structure. The Pleistocene rocks may have been deposited over the fault or up against the fault scarp and erosion exhumed the trucation (see plate I).

In the horst block, bounded by the Rhinehart Fault on the west and the Willow Creek Fault on the east, are a number of north to west trending normal faults. These faults, when viewed on a north-south section, shown in Plate III, show a series of small horst and graben structures which extend the length of Rhinehart Buttes. Some of these fault seem to reach their maximum offset at or near the Rhinehart Fault and the offset diminishes to the east. Some of these small hinge faults appear to end before reaching the Willow Creek Fault while others apparently intersect the fault (see Plate I). These small faults must have occurred after the activation of Rhinehart Fault as it is offset by these smaller structures. These small faults show silicification in places, see Plate II, so may have been active during the existence of the hot spring system which caused the silicification along Rhinehart Fault.

The northwest trending fault east of Vale Butte is another of the regional structures. Lillie (1977) suggests a normal fault, or possibly a strike slip fault with oblique movement, traverses the area east of Vale Butte. While Lillie (1977) suggests a down to the east

movement the supportive evidence in this report is ambigous. Field evidence in the northern part of the section indicates a down to the east movement, while in the southern portion the sense of motion is down to the west. The gravity models of the A and C lines based on Lillie's (1977) model do concur, and field evidence, apparent drag folding and apparent offset of conglomerate beds on the northeast shoulder of Vale Butte agree, see map, Plate I. Brown (1982) suggests a down to the west movement. Supporting Brown's (1982) contention are: the magnetic modeling (see figure 25), drag folding in the sandstones that form the dip slope east of the southern part of Vale Butte and the apparent offset of the beds of Captain Keeney Pass in the southern portion of the study area, see geologic map, Plate I, support Brown's (1982) contention. The fault is probably a scissors type fault which is down to the east in the north and down to the west in the south, with the hinge located just to the south of Vale Butte.

Along the northern side of both Vale and Rhinehart Buttes the pattern seems to be one of en echelon normal faulting. The dip of the fault planes is generally northward, with the north side downthrown. The northern section of Rhinehart Buttes may be composed of either a series of slump blocks or a series of small en echelon fault blocks. The gravity studies in this study show a distinct series of blocks with en echelon progressive down to the north along the northern side of the Butte. Brown (1982) has mapped this area as landslide debris. The model predicts a series of block of the same density as the country rock. Field mapping also shows conflicting evidence. In some areas the bedding and fabric of the country rock is shattered and distorted

while in another outcrop the same features appear normal. This could be the result of post deformational slumping along the fault planes or could be the result of blasting during highway construction.

The structural history seems to indicate that the Rhinehart Fault was active earliest. This was probably during the early Pliocene at the latest. These systems can probably tied to Basin and Range deformation. Sometime later a second episode of deformation resulted in the stuctures which have a more western component in their trend. These displaced the earlier structures, notably the Rhinehart Fault. These faults indicate extension, via horst and graben faulting, to the northwest-southeast. These faults may be associated with right lateral movement of the Vale Fault Zone. The direction of extension is in the appropriate direction and it is possible that much of the strike slip component of the movement took place as both right lateral and ball bearing type extension of the entire Vale Fault Zone. Also possible is that the right lateral movement of the Vale Zone and Willow Creek Fault was a seperate episode of deformation.

The results of this study support the conclusions of previous authors, notably Lillie (1977) and Bowen and Blackwell (1975). The study area is composed of regional horst and graben features, of which the Vale Horst occupies most of the study area. The Vale Horst is composed of a large number of small, fault bounded blocks as suggested by the gravity and magnetic modeling. The majority of the structures suggested by the geophysical studies have been confirmed by the presence of supporting field evidence such as drag folding, offset of units or repetition of units. The overall sense of movement is

probably oblique. However, the evidence supporting the contention of a right lateral component of the movement is marginal, limited to topographic expression.

The results of the gravity survey suggest that the study area is centered on a large horst. The boundaries of the horst lie about two kilometers west of Rhinehart Buttes and to the east of Vale Butte. The horst is capped by a low density, 2.1 gm/cm^3, volcaniclastic unit which has been offset a series of small, short throw, local faults. These small faults are normal faults. The base of the upper unit shows distinct offset, and the density contrast is generated by the faulting of the upper unit against the more dense lower unit. At areas identified by field as silicified zones the gravity modeling suggests dense, 2.7 gm/cm^3, bodies which parallel the known faults at those locations. Field evidence shows the silicified zones are located along the faults, which acted as plumbing for a fossil geothermal system. Rhinehart Buttes are erosionally resistant silicified remnants of a fossil hot spring system (Bowen and Blackwell, 1975). Rhinehart fault apparently was a conduit for the fossil hot springs. The most intense silicification and secondary mineralization occurs along the fault trace. The degree and distribution of the silicification seems to be controled by the location of the fault plane and the permeability of country rock intersected by the fault (Benson, 1981 pers. comm.). In units of low permeability, the silicified zone is narrow and centered on the fault plane while in units of higher relative permeability the zone is much wider. Rhinehart fault is offset by other, later faults. Those areas which display the highest degree of silicification are

localized in areas where Rhinehart fault interescts other faults. Gravity modeling predicts that the silicified zones are generally dense dike like bodies in a matrix of lighter, 2.1 gm/cm^3, volcaniclastic material of the upper layer.

The magnetic models correlated well with the gravity models. The magnetic models predicted that the Grassy Mountain Basalt, which underlies the upper layer examined in the gravity modeling, is offset at several corresponding locations by normal faults. The main, larger faults extend downward into and possibly through the Grassy Mountain formation. The locations of the larger faults are coincident with those predicted by the gravity modeling.

The heat flow measurements, Bowen and Blackwell, (1975), support the hypothesis of greater than average heat flow. The world wide average for continental areas is 1.4 Heat Flow Units (HFU), measured in microcalories per cm^2 per second, while in the Vale KGRA heat flow measurements range from a low of 2.3 to a high of 6.4 HFU, (Bowen and Blackwell, 1975). This condition requires that a fluid medium must be available to circulate and transfer the heat (Black, 1984, pers. comm). Conductive heat transfer is not effective enough to maintain the high rate found in the Vale KGRA. The hot springs located both to the north and west of Rhinehart Buttes are evidence that fluid medium is present. However, the amount of geothermal fluid acting as a heat source at the hot springs is limited. The Grassy Mountain Basalts underly the volcaniclastic rocks that are exposed on the surface. The fractured nature of basalt flows could make excellent reservoir rocks for the geothermal water. The drilling operations so far have not encountered

any appreciable fluid flow at depth. None of these wells however were drilled near the intersection of the faults believed to be controlling the upward fluid migration.

The structural controls of the the hot springs at Vale were examined. The area of present primary interest is located at the north end of Rhinehart Buttes. The linear, directional pattern of temperature increase within the acquifer that feeds the hot springs combined with the structural configuration suggest that the controlling structure is probably associated with those structures at the northern end of Rhinehart Buttes. Of particular interest is the Rhinehart Fault. The orientation of the Rhinehart Fault trace coincides with the location of the group of hot springs that occur along the Malhuer River. The drilling operations conducted in April, 1982 were unsuccessful at encountering the uprising thermal waters. However, Rhinehart Fault was intercepted at a depth of about 360 meters. The drilling was suspended upon loss of circulation due the large void spaces encountered at Rhinehart Fault. The void spaces are an indication that the altered, brittle, and highly fractured rocks along the fault have the porosity necessary to allow the upward fluid migration. The directional temperature increases noted within the shallow warm water acquifer show a trend of S29° E. The north end of Rhinehart Buttes appears to be structurally composed of a series of en echelon down to the north normal faults. The east-west trending ridge which composes the north end of Rhinehart Buttes is cored by a northeast trending, northward dipping fault. This ridge shows evidence of silicification and brecciation at several places along its length.

The location of this fault is S15° E in relation to the hot springs. The direction of temperature increase within the shallow acquifer trends toward a part of this fault (Brown, 1982). This fault is probably the crucial factor in controlling the injection of thermal waters into the shallow acquifer. Rhinehart fault, which probably was at one time, the primary structure appears, as a result of the 1982 drilling to be secondary, but may be a primary control at depth (Gannett, 1986, pers. comm.).

BIBLIOGRAPHY

Applegate, D.E. and L.L. Donaldson. 1979. Seismic section in Ontario Oregon: Geothermal Resources Council Bulletin, v. 3, p. 15 -17.

Baldwin, E.M., 1964, Geology of Oregon: Eugene, Oregon, University of Oregon Cooperative Bookstore, 165 p.

Baldwin, H.L., and Hill, D.P., 1960, Gravity survey in part of the Snake River Plain, Idaho -- A preliminary report: U.S. Geological Survey, open file report (200) R290, No. 511.

Berg, J.W. and Thiruvathukal, J.V., 1965, Gravity base station network, Oregon: Journal of Geophysical Research, v. 70, p. 3325 - 3330.

----, 1967a, Free air gravity anomaly map of Oregon: Oregon Department of Geology and Mineral Industries, GMS 4a, scale 1:500,000.

----, 1967b, Complete Bouguer gravity anomaly map of Oregon, Department of Geology and Mineral Industries, GMS 4b, Scale 1:500,000.

Boler, F.M., 1979, Aeromagnetic measurements, magnetic source depths, and Curie point isotherm in the Vale - Owyhee Oregon geothermal area: unpublished thesis, M.S., Oregon State University, Corvallis, Oregon.

Bowen, R.G., 1972, Geothermal gradient studies in Oregon: The Ore Bin, v. 34, no. 4, p. 68 - 71.

Bowen, R.G., and Blackwell, D.D., 1973, Progress report on geothermal measurements in Oregon: The Ore Bin, v. 35, no. 1, p. 6 - 7.

---- 1975, The Cow Hollow geothermal anomaly, Malhuer County, Oregon: The Ore Bin, v. 37, no. 7, p. 109 - 121.

Bowen, R.G., and Peterson, N.V., 1970, Thermal springs and wells in Oregon: Oregon Department of Geology and Mineral Industry, miscellaneous paper number 14.

Brown, D.E., 1982, Map showing geology and geothermal resources of the Vale East 7 1/2' Quadrangle, Oregon: Oregon Department of Geology and Mineral Industries, GMS 21, scale 1: 24,000.

Bryan, K., 1929, Geology of reservoir and dam sites with a report on the Owyhee Irregation Project, Oregon: U.S. Geological Survey, water supply paper 597-A:89 p.

Cooper, J.A. 1980. Oregon geothermal overview study. Oregon Graduate Center, Beaverton Oregon.

Cope, E.D., 1883, On the fishes of the Recent and Pliocene lakes of the western part of the Great Basin, and of the Idaho Pliocene Lake: Acadamey of the Natural Sciences of Phiadelphia Proceedings:134-166.

Corcoran, R.E., Doak, R.A., Porter, P.W., Pritchett,F.I., and Privrasky, N.C., 1962, Geology of the Mitchell Butte Quadrangle, Oregon: GMS 2, scale 1:125,000.

Couch, R.S., French, W.S., Gemperle,M., and Johnson,A.G., 1975, Geophysical measurements in the Vale, Oregon Geothermal resource area: The Ore Bin, v. 37, no. 8, p. 125 -129.

Couch, R. and Baker, B., 1977, Geophysical investigations of the Vale-Owyhee Geothermal Region, Malhuer County, Oregon: Technical Report No. 2, U.S. Geological Survey, Geothermal Research Program.

Evernden, J.F., and James, G.T., 1964, Potassium-argon dates and the Tertiary floras of North America: American Journal of Science, v. 262, p. 945 - 974.

Goguel, J., 1954, A universal table for the prediction of the lunar-solar correction in gravimetry: Geophysical Prospecting, v. 2, p.1 - 32

Hammer, S., 1939, Terrain corrections for gravimeter stations: Geophysics, v. 4, no. 3, p.184 - 194.

Hull, D., 1975, Geothermal studies in the Vale Area, Malhuer County, Oregon: The Ore Bin, v. 37, no. 6, p. 104 - 106.

Johnson, A.M., 1961, Stratigraphy and lithology of the Deer Butte Formation, Malhuer County, Oregon: unpublished thesis, M.S., University of Oregon, Eugene Oregon, 144 p.

Jones, T.D., 1977, Analysis of a gravity traverse south of Portland, Oregon: unpublished thesis, B.S., Portland State University, Portland, Oregon.

Kirkham, V.R.D., 1931a, Pevision of the Payette and Idaho Formations: Journal of Geology, v. 39, p. 193 - 239.

Kittleman, L.R., Green, A.R., Hagood, A.R., Johnson, A.M., McMurray, J.M., Russell, R.G., and Weeden, D.A., 1965, Cenozoic stratigraphy of the Owyhee region, Malhuer County, Oregon: Eugene, Oregon, University of Oregon Museum of Natural History Bulletin 1, 45 p.

Kittleman, L.R., Green, A.R., Haddock, G.H., Hagood, A.R., Johnson, A.M., Mc Murray, J.M., Russell, R.G., and Weeden, D.A., 1967, Geologic map of the Owyhee region, Malhuer County, Oregon: University of Oregon Museum of Natural History Bulletin, 8, scale 1:125,000.

Lawrence, R.D., 1976, Strike-slip faulting terminates the Basin and Range Province in Oregon: Geological Society of America Bulletin, v. 87, no. 6, p. 846 - 850.

Larson, K., and Couch, R., 1975, Preliminary gravity maps of the Vale area, Malhuer County,Oregon: The Ore Bin, v. 37, no. 7, p. 138 -142.

Lillie, R.J., Subsurface geologic structure of Vale, Oregon KGRA: thesis, M.S., Oregon State University, Corvallis, Oregon.

Lindgren, W., 1898, The mining districts of the Idaho basin and the Boise Ridge, Idaho: U.S. Geological Survey, 18th Annual Report, part 3, p. 617 -744.

Malde, H.E., and Powers, H.A., 1962, Upper Cenozoic stratigraphy of weatern Snake River plain, Idaho: Geological Society of America Bulletin, v. 73, p. 1197 - 1220.

Mariner, R.H., Rapp, J.B., Willey, L.M., and Presser, T.S., 1974, The chemical compostion and estimated minimum thermal reservoir temperatures of selected hot springs in Oregon: U.S. Geological Survey, Open - File Report, 27 p.

Newton, V.C. Jr., and Corcoran, R.E., 1963, Petroleum geology of the western Snake River basin, Oregon-Idaho: Oregon Department of geology and Mineral Industries Oil and Gas Investigations 1, 67 p.

Renick, B.C., 1930, The petrology and geology og a portion of Malhuer County, Oregon: Journal of Geology, v. 38, p. 481 - 520

Storm, B.A., 1975, Stratigraphy and petrology of the Grassy Mountain Formation, Malhuer County, Oregon: unpublished thesis, M.S., University of Oregon, Eugene, Oregon, 63 p.

Telford, W.M., Geldart, L.P., Sheriff, R.S., and Keys, D.A., 1976, Applied geophysics: Cambridge, Cambridge University Press

Thiruvathukal, J.V, Berg, J.W., and Heinrichs, D.F., 1970, Regional gravity of Oregon: Geological Society of America Bulletin, v. 81, no. 3, p. 725 - 738.

Van Blaricon, R., Ed., 1980, Practical geophysics for the exploration geologist: Spokane, Northwest Mining Association.

APPENDIX A

STATION NUMBER	ELEVATION (METERS)	LATITUDE	LONGITUDE	OBSERVED GRAVITY (MGALS)	THEORETICAL GRAVITY (MGALS)	TERRAIN CORRECTION (MGALS)	FREE AIR ANOMALY (MGALS)	SIMPLE BOUGER ANOMALY (MGALS)	COMPLETE BOUGER ANOMALY (MGALS)
Base	724.45	43° 58'23.45"	117° 12'41.34"	980302.691	980539.072	0.646	-12.819	-76.587	-75.861
AE-1	726.46	43° 58'23.34"	117° 12'40.21"	980302.666	980539.072	0.671	-12.223	-76.080	-75.418
AE-2	737.89	43° 58'23.35"	117° 12'37.13"	980299.433	980539.072	0.730	-11.929	-76.799	-76.061
AE-3	754.41	43° 58'23.13"	117° 12'34.40"	980295.579	980539.072	0.691	-10.685	-77.007	-76.306
AE-4	780.53	43° 58'23.41"	117° 12'31.57"	980289.403	980539.072	1.322	-8.800	-77.419	-76.097
AE-5	807.32	43° 58'23.52"	117° 12'27.77"	980282.982	980539.072	1.404	-6.955	-77.927	-76.524
AE-6	817.75	43° 58'23.70"	117° 12'24.91"	980280.574	980539.072	1.041	-6.194	-78.085	-77.044
AE-7	845.33	43° 58'23.00"	117° 12'22.42"	980273.562	980539.072	1.800	-4.644	-78.959	-77.159
AE-8	860.66	43° 58'23.62"	117° 12'19.57"	980269.895	980539.072	2.040	-3.577	-79.243	-77.203
AE-9	869.84	43° 58'23.78"	117° 12'16.71"	980266.689	980539.072	1.931	-3.954	-80.424	-78.494
AE-10	883.92	43° 58'23.77"	117° 12'14.25"	980264.358	980539.072	2.075	-1.940	-79.648	-77.573
AE-11	900.26	43° 58'23.49"	117° 12'11.57"	980260.255	980539.072	2.600	-1.001	80.145	-77.545
AE-12	883.43	43° 58'23.45"	117° 12'05.23"	980265.870	980539.072	2.876	-0.578	-78.243	-76.658
AE-13	850.09	43° 58'23.40"	117° 11'59.64"	980273.961	980539.072	1.846	-2.777	-77.511	-75.665
AE-14	827.32	43° 58'23.14"	117° 11'54.29"	980278.135	980539.072	1.704	-5.650	-78.362	-76.658
AE-15	820.61	43° 58'23.56"	117° 11'48.19"	980280.458	980539.072	1.602	-5.376	-77.519	-75.917
AE-16	842.35	43° 58'24.41"	117° 11'41.54"	980277.303	980539.072	1.755	-4.024	-75.870	-74.122
AE-17	837.19	43° 58'26.56"	117° 11'30.43"	980276.058	980539.072	1.317	-4.659	-78.259	-76.943
AE-18	806.10	43° 58'24.67"	117° 11'18.37"	980283.697	980539.072	0.813	-6.614	-77.481	-76.668
AE-19	774.10	43° 58'23.43"	117° 11'03.47"	980289.878	980539.072	0.653	-10.309	-78.363	-77.711
AE-20	711.46	43° 58'22.79"	117° 10'47.71"	980303.912	980539.072	0.228	-15.665	-78.152	-77.924
AW-1	730.42	43° 58'23.54"	117° 12'47.62"	980301.557	980539.072	0.765	-12.109	-76.323	-75.558
AW-2	740.24	43° 12'23.63"	117° 12'50.79"	980299.372	980539.072	0.558	-11.765	-76.342	-75.784
AW-3	742.16	43° 58'23.73"	117° 12'54.09"	980299.041	980539.072	0.452	-11.004	-76.249	-75.797

STATION NUMBER	ELEVATION (METERS)	LATITUDE	LONGITUDE	OBSERVED GRAVITY (MGALS)	THEORETICAL GRAVITY (MGALS)	TERRAIN CORRECTION (MGALS)	FREE AIR ANOMALY (MGALS)	SIMPLE BOUGER ANOMALY (MGALS)	COMPLETE BOUGER ANOMALY (MGALS)
AW-3	742.16	43°58'23.73"	117°12'54.09"	980299.041	980539.072	0.452	-11.004	-76.249	-75.797
AW-4	751.36	43°58'23.99"	117°12'57.23"	980297.113	980539.072	0.442	-10.991	-76.146	-75.704
AW-5	763.46	43°58'24.12"	117°13'00.50"	980294.359	980539.072	0.596	-9.111	-76.230	-75.643
AW-6	775.81	43°58'24.14"	117°13'03.19"	980291.450	980539.072	0.439	-8.211	-76.414	-75.984
AW-7	784.37	43°58'24.30"	117°13'05.56"	980289.328	980539.072	0.425	-7.690	-76.646	-76.221
AW-8	790.22	43°58'24.36"	117°13'08.48"	980287.934	980539.072	0.433	-7.208	-76.749	-76.296
AW-9	797.08	43°58'24.41"	117°13'10.97"	980286.249	980539.072	0.734	-6.846	-76.920	-76.186
AW-10	808.63	43°58'24.38"	117°13'13.19"	980283.281	980539.072	0.470	-6.242	-77.339	-76.869
AW-11	817.29	43°58'24.39"	117°13'15.30"	980281.052	980539.072	0.497	-5.887	-77.650	-76.960
AW-12	827.68	43°58'24.41"	117°13'17.90"	980278.246	980539.072	0.835	-5.406	-78.170	-77.335
AW-13	865.21	43°58'24.71"	117°13'23.18"	980268.574	980539.072	1.847	-3.499	-79.567	-77.718
AW-14	694.52	43°58'25.75"	117°14'02.30"	980304.428	980539.072	0.431	-20.318	-81.576	-80.745
AW-15	733.29	43°58'25.51"	117°13'56.31"	980296.338	980539.072	1.046	-16.444	-80.910	-79.864
AW-16	745.48	43°58'26.51"	117°13'51.02"	980294.509	980539.072	0.674	-14.511	-80.048	-79.424
AW-17	764.04	43°58'27.68"	117°13'45.17"	980291.330	980539.072	0.440	-11.961	-79.131	-78.691
AW-18	796.20	43°58'24.79"	117°13'38.94"	980284.472	980539.072	0.881	-8.896	-78.892	-78.011
AW-19	805.74	43°58'24.56"	117°13'35.95"	980282.656	980539.072	0.777	-7.768	-78.603	-77.831
AW-20	862.74	43°58'24.14"	117°13'26.26"	980269.656	980539.072	1.348	-3.179	-79.025	-77.676
AW-21	837.35	43°58'23.99"	117°13'29.24"	980275.696	980539.072	1.040	-4.974	-78.588	-77.548
AW-22	819.91	43°58'24.29"	117°13'32.60"	980279.553	980539.072	0.864	-6.497	-78.578	-77.715
AW-23	683.51	43°58'27.10"	117°14'43.85"	980304.670	980539.072	0.016	-23.472	-83.562	-83.546

STATION NUMBER	ELEVATION (METERS)	LATITUDE	LONGITUDE	OBSERVED GRAVITY (MGALS)	THEORETICAL GRAVITY (MGALS)	TERRAIN CORRECTION (MGALS)	FREE AIR ANOMALY (MGALS)	SIMPLE BOUGUER ANOMALY (MGALS)	COMPLETE BOUGER ANOMALY (MGALS)
BS-1	727.53	43° 58' 18.46"	117° 12' 38.02"	980301.901	980539.072	0.549	-12.659	-76.618	-76.069
BS-2	733.78	43° 58' 18.15"	117° 12' 39.00"	980300.509	980539.072	0.452	-13.123	-76.631	-76.179
BS-3	737.59	43° 58' 15.09"	117° 12' 41.54"	980299.720	980539.072	0.423	-11.736	-76.539	-76.157
BS-4	740.60	43° 58' 13.99"	117° 12' 43.06"	980298.921	980539.072	0.394	-11.604	-76.712	-76.318
BS-5	742.34	43° 58' 11.95"	117° 12' 44.66"	980298.510	980539.072	0.345	-11.478	-76.740	-76.395
BS-6	748.95	43° 58' 09.95"	117° 12' 43.55"	980296.903	980539.072	0.296	-11.044	-76.887	-76.592
BS-7	750.91	43° 58' 07.71"	117° 12' 43.47"	980296.594	980539.072	0.177	-10.751	-76.766	-76.589
BS-8	747.77	43° 58' 05.56"	117° 12' 43.79"	980297.335	980539.072	0.251	-10.979	-76.718	-76.467
BS-9	751.27	43° 58' 03.38"	117° 12' 44.05"	980296.632	980539.072	0.261	-10.610	-76.657	-76.396
BS-10	761.02	43° 57' 59.02"	117° 12' 45.90"	980294.575	980539.072	0.211	-9.640	-76.552	-76.341
BS-11	754.75	43° 57' 54.78"	117° 12' 45.17"	980296.009	980539.072	0.161	-10.151	-76.503	-76.342
BS-12	757.12	43° 57' 50.53"	117° 12' 45.90"	980295.442	980539.072	0.142	-9.985	-76.546	-76.404
BS-13	760.63	43° 57' 45.88"	117° 12' 46.62"	980294.426	980539.072	0.123	-9.919	-76.798	-76.656
BS-14	770.08	43° 57' 41.21"	117° 12' 47.25"	980292.251	980539.072	0.080	-9.170	-76.078	-76.790
BS-15	770.87	43° 57' 36.38"	117° 12' 47.81"	980292.133	980539.072	0.053	-9.049	-76.819	-76.766
BS-16	768.71	43° 57' 32.59"	117° 12' 47.91"	980292.451	980539.072	0.061	-9.401	-76.901	-76.920
BS-17	766.97	43° 57' 28.12"	117° 12' 47.80"	980292.866	980539.072	0.068	-9.522	-76.949	-76.881
BS-18	767.33	43° 57' 23.69"	117° 12' 46.57"	980292.529	980539.072	0.079	-9.747	-77.205	-77.126
BS-19	769.22	43° 57' 19.89"	117° 12' 45.30"	980291.942	980539.072	0.090	-9.750	-77.375	-77.285
BN-1	722.16	43° 58' 25.95"	117° 12' 43.05"	980303.396	980539.072	0.508	-12.819	-76.307	-75.799
BN-2	720.30	43° 58' 28.37"	117° 12' 43.93"	980303.746	980539.072	0.526	-12.921	-76.280	-75.754
BN-3	717.86	43° 58' 30.72"	117° 12' 44.01"	980304.059	980539.072	0.543	-13.402	-76.592	-76.049
BN-4	718.02	43° 58' 33.19"	117° 12' 44.09"	980304.444	980539.072	0.485	-13.050	-76.174	-75.689
BN-5	718.35	43° 58' 35.59"	117° 12' 44.15"	980303.651	980539.072	0.426	-13.740	-76.893	-76.467

STATION NUMBER	ELEVATION (METERS)	LATITUDE	LONGITUDE	OBSERVED GRAVITY (MGALS)	THEORETICAL GRAVITY (MGALS)	TERRAIN CORRECTION (MGALS)	FREE AIR ANOMALY (MGALS)	SIMPLE BOUGER ANOMALY (MGALS)	COMPLETE BOUGER ANOMALY (MGALS)
BN-A	721.52	43° 58'38.05"	117° 12'44.20"	980302.835	980539.072	0.465	-13.570	-77.009	-76.545
BN-7	721.07	43° 58'40.56"	117° 12'44.27"	980302.839	980539.072	0.503	-13.715	-77.164	-76.663
BN-8	720.36	43° 58'42.99"	117° 12'44.36"	980302.828	980539.072	0.464	-13.942	-77.272	-76.808
BN-9	714.88	43° 58'45.77"	117° 12'44.46"	980305.006	980539.072	0.425	-13.465	-76.310	-75.886
BN-10	711.59	43° 58'48.43"	117° 12'44.30"	980305.696	980539.072	0.429	-13.783	-76.341	-75.912
BN-11	707.96	43° 58'50.86"	117° 12'44.14"	980306.468	980539.072	0.433	-14.130	-76.369	-75.936
BN-12	691.13	43° 58'53.25"	117° 12'43.78"	980310.014	980539.072	0.476	-15.777	-76.536	-76.060
BN-13	680.92	43° 59'00.56"	117° 12'43.03"	980311.265	980539.072	0.434	-17.677	-77.539	-77.105

STATION NUMBER	ELEVATION (METERS)	LATITUDE	LONGITUDE	OBSERVED GRAVITY (MGALS)	THEORETICAL GRAVITY (MGALS)	TERRAIN CORRECTION (MGALS)	FREE AIR ANOMALY (MGALS)	SIMPLE BOUGUER ANOMALY (MGALS)	COMPLETE BOUGUER ANOMALY (MGALS)
CE-1	742.22	43°58'05.38"	117°12'40.79"	980290.297	980539.072	0.352	-11.729	-76.980	-76.628
CE-2	746.85	43°58'05.28"	117°12'38.18"	980297.717	980539.072	0.302	-11.379	-77.037	-76.736
CE-3	751.09	43°58'05.15"	117°12'35.45"	980296.123	980539.072	0.257	-11.166	-77.197	-76.940
CE-4	747.34	43°58'05.11"	117°12'32.59"	980296.906	980539.072	0.344	-11.540	-77.241	-76.896
CE-5	747.83	43°58'05.08"	117°12'29.82"	980296.707	980539.072	0.432	-11.588	-77.332	-76.900
CE-6	753.86	43°58'04.96"	117°12'26.59"	980295.326	980539.072	0.511	-11.107	-77.301	-76.870
CE-7	760.90	43°58'04.88"	117°12'23.60"	980293.816	980539.072	0.590	-10.444	-77.338	-76.748
CE-8	760.27	43°58'05.21"	117°12'20.73"	980292.204	980539.072	0.699	-9.799	-77.335	-76.637
CE-9	778.92	43°58'05.66"	117°12'18.18"	980289.800	980539.072	0.807	-8.901	-77.378	-76.571
CE-10	792.30	43°58'06.01"	117°12'15.60"	980286.821	980539.072	0.817	-7.751	-77.404	-76.587
CE-11	805.53	43°58'06.23"	117°12'13.52"	980283.820	980539.072	0.827	-6.662	-77.478	-76.651
CE-12	820.83	43°58'06.50"	117°12'10.96"	980280.347	980539.072	0.980	-5.422	-77.503	-76.604
CE-13	836.43	43°58'06.79"	117°12'08.83"	980276.566	980539.072	1.133	-4.386	-77.929	-76.797
CE-14	859.05	43°58'07.09"	117°12'06.70"	980271.226	980539.072	1.662	-2.747	-78.269	-76.607
CE-15	884.38	43°58'07.40"	117°12'03.91"	980265.330	980539.072	2.191	-0.819	-78.567	-76.376
CE-16	914.31	43°58'07.46"	117°12'00.80"	980258.056	980539.072	2.737	1.136	-79.244	-76.507
CE-17	741.37	43°58'01.83"	117°11'09.09"	980300.924	980539.072	0.212	-9.765	-74.541	-74.330
CE-18	762.06	43°58'03.70"	117°11'21.43"	980296.755	980539.072	0.229	-7.150	-74.145	-73.916
CE-19	772.55	43°58'05.51"	117°11'34.67"	980294.707	980539.072	0.668	-5.960	-73.877	-73.209
CE-20	820.73	43°58'07.75"	117°11'45.07"	980281.810	980539.072	1.129	-3.918	-76.140	-75.011
CE-21	887.24	43°58'07.94"	117°11'50.91"	980265.960	980539.072	2.242	0.688	-77.313	-75.070
CE-22	927.51	43°58'07.61"	117°11'57.22"	980256.004	980539.072	3.283	3.237	-78.307	-75.020
CW-1	753.95	43°58'05.45"	117°12'46.77"	980296.092	980539.072	0.339	-10.313	-76.545	-76.257

STATION NUMBER	ELEVATION (METERS)	LATITUDE	LONGITUDE	OBSERVED GRAVITY (MGALS)	THEORETICAL GRAVITY (MGALS)	TERRAIN CORRECTION (MGALS)	FREE AIR ANOMALY (MGALS)	SIMPLE BOUGER ANOMALY (MGALS)	COMPLETE BOUGER ANOMALY (MGALS)
CW-2	761.73	43° 58'05.41"	117° 12'49.52"	980294.445	980539.072	0.351	-9.561	-76.527	-76.176
CW-3	768.92	43° 58'05.33"	117° 12'52.21"	980292.879	980539.072	0.384	-8.907	-76.506	-76.121
CW-4	789.80	43° 58'05.21"	117° 12'55.28"	980287.627	980539.072	0.410	-7.716	-77.150	-76.732
CW-6	790.33	43° 58'05.13"	117° 13'00.84"	980290.087	980539.072	0.177	-8.172	-76.775	-76.598
CW-8	782.12	43° 58'01.18"	117° 13'05.86"	980289.297	980539.072	0.200	-8.435	-76.995	-76.795
CW-9	788.55	43° 58'01.45"	117° 13'09.38"	980287.591	980539.072	0.223	-8.417	-77.175	-77.952
CW-10	800.83	43° 58'04.59"	117° 13'12.92"	980284.078	980539.072	0.560	-8.138	-77.462	-77.102
CW-11	831.31	43° 58'04.27"	117° 13'16.15"	980276.405	980539.072	0.497	-7.860	-78.264	-77.767
CW-12	824.76	43° 58'04.00"	117° 13'10.90"	980278.320	980539.072	0.997	-6.127	-79.211	-78.214
CW-13	839.02	43° 58'03.75"	117° 13'21.72"	980274.384	980539.072	0.733	-6.227	-78.734	-78.001
CW-14	836.13	43° 58'03.27"	117° 13'25.30"	980274.148	980539.072	1.236	-5.769	-79.530	-78.294
CW-15	821.90	43° 58'02.96"	117° 13'29.00"	980276.531	980539.072	1.481	-6.098	-80.405	-78.924
CW-16	760.60	43° 58'01.98"	117° 13'34.09"	980291.141	980539.072	1.662	-8.080	-81.143	-79.481
CW-17	740.02	43° 58'03.10"	117° 13'39.34"	980296.714	980539.072	0.788	-13.213	-80.080	-79.292
CW-18	716.46	43° 58'02.63"	117° 13'44.42"	980300.474	980539.072	0.688	-13.989	-79.047	-78.359
CW-19	703.66	43° 58'02.65"	117° 13'49.14"	980303.058	980539.072	0.500	-17.499	-80.480	-79.892
CW-20	696.07	43° 58'02.77"	117° 13'54.71"	980304.324	980539.072	0.475	-18.867	-80.728	-80.253
CW-21	688.36	43° 58'03.82"	117° 15'44.22"	980290.804	980539.072	0.361	-19.943	-81.137	-80.775
CW-22	686.84	43° 58'03.52"	117° 15'24.29"	980309.256	980539.072	0.019	-27.042	-88.358	-87.339
CW-23	684.79	43° 58'03.51"	117° 14'59.00"	980305.262	980539.072	0.018	-26.061	-87.243	-87.225

STATION NUMBER	ELEVATION (METERS)	LATITUDE	LONGITUDE	OBSERVED GRAVITY (MGALS)	THEORETICAL GRAVITY (MGALS)	TERRAIN CORRECTION (MGALS)	FREE AIR ANOMALY (MGALS)	SIMPLE BOUGUER ANOMALY (MGALS)	COMPLETE BOUGUER ANOMALY (MGALS)
DS-1	766.30	43° 57'38.15"	117° 12'14.74"	980293.578	980539.072	0.152	-9.017	-79.593	-79.441
DS-2	763.74	43° 57'43.01"	117° 12'15.79"	980294.037	980539.072	0.130	-9.348	-79.688	-79.558
DS-3	763.95	43° 57'53.08"	117° 12'16.81"	980293.776	980539.072	0.377	-9.544	-79.903	-79.525
DS-6	766.37	43° 57'55.20"	117° 12'16.87"	980293.178	980539.072	0.357	-9.333	-79.933	-79.577
DS-7	772.12	43° 57'57.35"	117° 12'16.92"	980291.825	980539.072	0.342	-8.974	-80.085	-79.743
DS-8	777.61	43° 58'59.87"	117° 12'16.98"	98090.508	980539.072	0.355	-8.598	-00.215	-79.859
DS-9	781.14	43° 58'02.05"	117° 12'17.01"	980289.523	980539.072	0.369	-8.492	-80.434	-80.066
DS-10	776.39	43° 58'04.26"	117° 12'16.97"	980290.330	980539.072	0.620	-8.932	-80.437	-79.816
DS-11	785.53	43° 58'06.22"	117° 12'16.97"	980288.382	980539.072	0.872	-8.278	-80.625	-79.753
DS-12	706.17	43° 58'08.15"	117° 12'16.97"	980288.192	980539.072	1.135	-8.271	-80.676	-79.541
DS-13	789.01	43° 58'09.99"	117° 12'16.96"	980287.486	980539.072	1.398	-8.102	-80.769	-79.371
DS-14	797.39	43° 58'11.87"	117° 12'17.09"	980285.483	980539.072	1.486	-7.518	-80.957	-79.471
DS-15	816.13	43° 58'13.54"	117° 12'17.03"	980281.071	980539.072	1.574	-6.146	-81.311	-79.737
DS-16	833.26	43° 58'15.67"	117° 12'17.03"	980277.115	980539.072	1.695	-4.815	-81.558	-79.863
DS-17	838.23	43° 58'17.60"	117° 12'17.01"	980276.393	980539.072	1.817	-4.004	-81.205	-79.388
DS-18	851.89	43° 58'19.91"	117° 12'17.01"	9002773.165	980539.072	2.339	-3.018	-81.746	-79.137
DS-19	872.19	43° 58'22.23"	117° 12'16.93"	980267.673	980539.072	2.862	-2.246	-82.573	-79.711
DN-1	858.71	43° 58'26.64"	117° 12'16.93"	980272.545	980539.072	2.488	-1.531	-80.618	-78.130
DN-2	841.67	43° 58'28.51"	117° 12'16.90"	980275.486	980539.072	2.086	-3.848	-81.366	-79.280
DN-3	820.92	43° 58'30.56"	117° 12'16.88"	980280.367	980539.072	1.684	-5.373	-80.979	-77.894
DN-4	797.63	43° 58'32.64"	117° 12'16.82"	980285.801	980539.072	1.998	-7.125	-80.586	-78.588
DN-5	776.60	43° 58'34.27"	117° 12'16.77"	980290.735	980539.072	2.311	-8.681	-80.205	-77.894
DN-6	756.51	43° 58'36.15"	117° 12'16.73"	980295.642	980539.072	1.830	-9.973	-79.647	-77.817
DN-7	738.16	43° 58'38.16"	117° 12'16.61"	980299.406	980539.072	1.348	-11.871	-79.855	-78.508

STATION NUMBER	ELEVATION (METERS)	LATITUDE	LONGITUDE	OBSERVED GRAVITY (MGALS)	THEORETICAL GRAVITY (MGALS)	TERRAIN CORRECTION (MGALS)	FREE AIR ANOMALY (MGALS)	SIMPLE BOUGUER ANOMALY (MGALS)	COMPLETE BOUGUER ANOMALY (MGALS)
DN-8	713.48	43° 57'39.80"	117° 12'16.68"	980305.125	980539.072	1.242	-13.771	-79.481	-78.240
DN-10	680.41	43° 59'20.84"	117° 12'16.27"	980310.891	980539.072	0.010	-18.210	-80.875	-80.865

STATION NUMBER	ELEVATION (METERS)	LATITUDE	LONGITUDE	OBSERVED GRAVITY (MGALS)	THEORETICAL GRAVITY (MGALS)	TERRAIN CORRECTION (MGALS)	FREE AIR ANOMALY (MGALS)	SIMPLE BOUGUER ANOMALY (MGALS)	COMPLETE BOUGUER ANOMALY (MGALS)
ES-1	718.69	43° 57'13.57"	117° 13'09.05"	980302.673	980539.072	0.323	-14.615	-77.797	-77.473
ES-2	732.61	43° 57'17.50"	117° 13'09.40"	980294.980	980539.072	0.335	-11.839	-78.003	-77.668
ES-3	737.00	43° 57'21.90"	117° 13'10.39"	980294.190	980539.072	0.347	-11.274	-77.825	-77.478
ES-4	780.17	43° 57'25.48"	117° 13'11.97"	980208.736	980539.072	0.574	-9.580	-78.167	-77.593
ES-5	815.16	43° 57'28.90"	117° 13'12.03"	980279.894	980539.072	0.801	-7.624	-79.287	-78.486
ES-6	820.19	43° 57'33.08"	117° 13'12.88"	980279.104	980539.072	1.028	-6.892	-78.967	-77.938
ES-7	815.13	43° 57'36.39"	117° 13'12.86"	980280.592	980539.072	0.766	-6.935	-78.595	-77.830
ES-8	805.31	43° 57'40.47"	117° 13'12.62"	980283.246	980539.072	0.503	-7.310	-78.107	-77.604
ES-9	796.81	43° 57'44.68"	117° 13'11.82"	980285.395	980539.072	0.445	-7.785	-77.835	-77.390
ES-10	789.74	43° 57'48.75"	117° 13'11.64"	980287.041	980539.072	0.386	-8.321	-77.749	-77.363
ES-11	781.42	43° 57'52.72"	117° 13'11.49"	980289.353	980539.072	0.340	-8.577	-77.274	-76.934
ES-12	773.67	43° 57'56.53"	117° 13'11.53"	980290.872	980539.072	0.294	-9.447	-77.463	-77.169
ES-13	792.78	43° 58'01.21"	117° 13'11.18"	980286.435	980539.072	0.453	-7.987	-77.603	-77.230
ES-14	790.04	43° 58'03.51"	117° 13'11.14"	980286.654	980539.072	0.612	-8.614	-78.069	-77.457
ES-15	791.05	43° 58'05.83"	117° 13'11.11"	980286.786	980539.072	0.501	-8.172	-77.715	-77.214
ES-16	791.41	43° 58'08.19"	117° 13'11.08"	980286.874	980539.072	0.390	-7.971	-77.546	-77.157
ES-17	797.23	43° 58'10.55"	117° 13'10.99"	980285.720	980539.072	0.412	-7.328	-77.416	-77.003
ES-18	803.18	43° 58'12.53"	117° 13'10.97"	980284.377	980539.072	0.433	-6.837	-77.447	-77.012
ES-19	811.53	43° 58'14.81"	117° 13'10.86"	980282.472	980539.072	0.495	-6.165	-77.509	-77.014
ES-20	812.90	43° 58'17.28"	117° 13'10.86"	980282.239	980539.072	0.554	-5.975	-77.439	-76.885
ES-21	809.49	43° 58'19.56"	117° 13'10.75"	980283.035	980539.072	0.569	-6.232	-77.397	-76.827
ES-22	803.51	43° 58'21.54"	117° 13'10.75"	980284.625	980539.072	0.584	-6.486	-77.125	-76.541
ES-23	800.28	43° 58'23.73"	117° 13'10.76"	980285.545	980539.072	0.592	-6.563	-76.918	-76.326
EN-1	799.58	43° 58'25.58"	117° 13'10.51"	980285.647	980539.072	0.600	-6.677	-76.971	-76.371

STATION NUMBER	ELEVATION (METERS)	LATITUDE	LONGITUDE	OBSERVED GRAVITY (MGALS)	THEORETICAL GRAVITY (MGALS)	TERRAIN CORRECTION (MGALS)	FREE AIR ANOMALY (MGALS)	SIMPLE BOUGER ANOMALY (MGALS)	COMPLETE BOUGER ANOMALY (MGALS)
EN-2	809.61	43° 58'27.22"	117° 13'09.86"	980283.118	980539.072	0.745	-6.111	-77.287	-76.541
EN-3	816.96	43° 58'29.70"	117° 13'09.93"	980281.079	980539.072	0.891	-5.884	-77.705	-76.814
EN-4	807.96	43° 58'32.11"	117° 13'09.57"	980282.898	980539.072	1.037	-6.839	-77.870	-76.833
EN-5	788.85	43° 58'34.27"	117° 13'09.18"	980287.397	980539.072	1.134	-8.238	-77.588	-76.454
EN-6	823.66	43° 58'36.33"	117° 13'09.30"	980279.289	980539.072	1.204	-5.604	-78.015	-76.811
EN-7	857.37	43° 58'38.46"	117° 13'10.20"	980271.045	980539.072	1.870	-3.445	-78.820	-76.950
EN-8	855.39	43° 58'40.25"	117° 13'10.74"	980271.830	980539.072	1.716	-3.272	-78.472	-76.755
EN-9	834.73	43° 58'41.98"	117° 13'10.74"	980276.649	980539.072	1.563	-4.830	-78.213	-76.650
EN-10	815.25	43° 58'43.73"	117° 13'10.54"	980281.067	980539.072	1.343	-6.422	-78.093	-76.750
EN-11	797.20	43° 58'46.14"	117° 13'10.29"	980285.339	980539.072	1.124	-7.719	-77.803	-76.680
EN-12	814.36	43° 58'48.41"	117° 13'09.90"	980282.249	980539.072	1.980	-5.513	-77.106	-75.127
EN-13	841.67	43° 58'51.08"	117° 13'09.97"	980274.300	980539.072	2.836	-4.834	-78.829	-75.992
EN-14	815.52	43° 58'52.92"	117° 13'09.98"	980280.803	980539.072	2.554	-6.602	-78.297	-75.743
EN-15	783.82	43° 58'55.04"	117° 13'10.08"	980288.375	980539.072	2.272	-8.812	-77.720	-75.449
EN-16	769.74	43° 58'57.35"	117° 13'10.13"	980291.812	980539.072	1.698	-9.720	-77.391	-75.693
EN-17	762.79	43° 59'00.39"	117° 13'09.84"	980293.008	980539.072	1.124	-10.669	-77.729	-76.605
EN-18	753.04	43° 59'02.78"	117° 13'09.96"	980294.992	980539.072	1.205	-11.695	-77.897	-76.692
EN-19	732.31	43° 59'05.07"	117° 13'09.96"	980299.320	980539.072	1.286	-13.563	-77.943	-76.657
EN-20	683.09	43° 59'07.86"	117° 13'09.81"	980311.071	980539.072	0.769	-17.203	-77.255	-76.487

STATION NUMBER	ELEVATION (METERS)	LATITUDE	LONGITUDE	OBSERVED GRAVITY (MGALS)	THEORETICAL GRAVITY (MGALS)	TERRAIN CORRECTION (MGALS)	FREE AIR ANOMALY (MGALS)	SIMPLE BOUGUER ANOMALY (MGALS)	COMPLETE BOUGUER ANOMALY (MGALS)
20-1	680.10	43°58'54.48"	117°12'00.70"	980311.819	980539.072	0.224	-17.377	-77.166	-76.942
20-2	679.16	43°58'54.43"	117°11'42.19"	980311.396	980539.072	0.213	-18.091	-77.790	-77.585
20-3	678.52	43°58'53.97"	117°11'24.99"	980310.747	980539.072	0.202	-18.938	-78.588	-78.386
20-4	677.94	43°58'54.22"	117°11'07.01"	980309.946	980539.072	0.191	-19.917	-79.517	-79.326
F-1	691.89	43°58'54.52"	117°12'34.68"	980311.030	980539.072	0.296	-14.554	-75.372	-75.077
F-2	691.00	43°58'54.48"	117°12'38.11"	980310.621	980539.072	0.348	-14.963	-75.781	-75.434
F-3	691.87	43°58'54.49"	117°12'41.25"	980310.589	980539.072	0.400	-14.976	-75.800	-75.400
F-4	690.55	43°58'54.49"	117°12'44.77"	980310.501	980539.072	0.499	-15.460	-76.177	-75.678
F-5	694.61	43°58'54.49"	117°12'48.14"	980309.541	980539.072	0.594	-15.177	-76.243	-75.644
F-6	697.78	43°58'54.52"	117°12'51.63"	980308.699	980539.072	0.724	-15.041	-76.385	-75.661
F-7	710.92	43°58'54.75"	117°12'54.51"	980304.967	980539.072	0.859	-14.719	-77.210	-76.368
F-8	741.65	43°58'54.55"	117°12'58.42"	980298.693	980539.072	1.057	-11.766	-76.1146	-75.709
F-9	753.44	43°58'54.54"	117°13'01.17"	980295.947	980539.072	1.265	-10.610	-76.055	-75.590
F-10	766.21	43°58'54.59"	117°13'03.86"	980292.740	980539.072	1.195	-9.584	-77.247	-75.644
F-11	775.59	43°58'54.60"	117°13'06.64"	980290.275	980539.072	1.126	-9.452	-77.636	-76.511
F-12	790.71	43°58'54.59"	117°13'10.02"	980286.833	980539.072	1.117	-8.228	-77.742	-76.625
F-13	791.75	43°58'54.70"	117°13'13.54"	980286.617	980539.072	1.109	-8.124	-77.729	-76.620
F-14	800.20	43°58'54.74"	117°13'16.54"	980284.699	980539.072	1.241	-7.409	-77.764	-76.523
F-15	802.08	43°58'54.76"	117°13'19.82"	980284.027	980539.072	1.374	-7.524	-78.039	-76.665
F-16	800.69	43°58'54.77"	117°13'23.22"	980283.936	980539.072	1.502	-7.704	-78.393	-76.891
F-17	709.34	43°58'54.81"	117°13'26.74"	980286.457	980539.072	1.621	-9.027	-78.421	-76.800
F-18	777.42	43°58'54.80"	117°13'30.17"	980289.103	980539.072	1.476	-10.059	-78.465	-76.989
F-19	768.13	43°58'54.81"	117°13'33.42"	980291.454	980539.072	1.330	-10.577	-78.105	-76.855
F-20	762.21	43°58'54.96"	117°13'37.00"	980292.565	980539.072	1.204	-11.291	-78.299	-77.095
F-21	756.27	43°58'54.89"	117°13'40.69"	980298.840	980539.072	1.150	-13.020	-77.749	-76.590

STATION NUMBER	ELEVATION (METERS)	LATITUDE	LONGITUDE	OBSERVED GRAVITY (MGALS)	THEORETICAL GRAVITY (MGALS)	TERRAIN CORRECTION (MGALS)	FREE AIR ANOMALY (MGALS)	SIMPLE BOUGUER ANOMALY (MGALS)	COMPLETE BOUGUER ANOMALY (MGALS)
F-22	735.09	43°58'54.91"	117°13'44.18"	980298.867	980539.072	1.173	-13.360	-77.984	-76.811
F-23	720.18	43°58'54.87"	117°13'47.58"	980301.428	980539.072	1.108	-15.399	-78.712	-77.524
F-24	703.70	43°58'54.89"	117°13'50.34"	980304.734	980539.072	1.164	-15.653	-77.525	-76.361
F-25	690.65	43°58'54.90"	117°13'54.73"	980307.479	980539.072	1.140	-18.462	-79.179	-78.039

APPENDIX B

Station	Gammas	Station	Gammas	Station	Gammas	Station	Gammas
Base	55,742						
B1	55,750	C1	55,517	D1	55,742	E1	55,747
B2	55,751	C2	55,428	D2	55,768	E2	55,746
B3	55,755	C3	55,476	D3	55,778	E3	55,743
B4	55,756	C4	55,589	D4	55,762	E4	55,738
B5	55,739	C5	55,630	D5	55,750	E5	55,748
B6	55,751	C6	55,619	D6	55,757	E6	55,759
B7	55,753	C7	55,639	D7	55,689	E7	55,746
B8	55,746	C8	55,653	D8	55,655	E8	55,751
B9	55,739	C9	55,651	D9	55,641	E9	55,731
B10	55,734	C10	55,647	D10	55,626	E10	55,724
B11	55,731	C11	55,645	D11	55,641	E11	55,715
B12	55,730	C12	55,659	D12	55,636	E12	55,708
B13	55,737	C13	55,611	D13	55,636	E13	55,705
B14	55,732	C14	55,629	D14	55,624	E14	55,695
B15	55,730	C15	55,642	D15	55,650	E15	55,695
B16	55,727	C16	55,645	D16	55,670	E16	55,673
B17	55,735	C17	55,638	D17	55,692	E17	55,681
B18	55,739	C18	55,662	D18	55,726	E18	55,680
B19	55,731	C19	55,656	D19	55,754	E19	55,658
B20	55,733	C20	55,676	D20	55,778	E20	55,670
B21	55,752	C21	55,688	D21	55,770	E21	55,661
B22	55,760	C22	55,687	D22	55,783	E22	55,643
B23	55,764	C23	55,697	D23	55,784	E23	55,660
B24	55,772	C24	55,706	D24	55,789	E24	55,651
B25	55,771	C25	55,715	D25	55,787	E25	55,637
B26	55,771	C26	55,719	D26	55,754	E26	55,628
B27	55,784	C27	55,726	D27	55,740	E27	55,632
B28	55,787	C28	55,719	D28	55,728	E28	55,622
B29	55,789	C29	55,727	D29	55,705	E29	55,621
B30	55,799	C30	55,722	D30	55,704	E30	55,610
B31	55,774	C31	55,720	D31	55,687	E31	55,608
B32	55,767	C32	55,743	D32	55,675	E32	55,593
B33	55,789	C33	55,741	D33	55,667	E33	55,559
B34	55,782	C34	55,748	D34	55,667	E34	55,588
B35	55,796	C35	55,762	D35	55,664	E35	55,590
B36	55,799	C36	55,753	D36	55,658	E36	55,580
B37	55,813	C37	55,755	D37	55,654	E37	------
B38	55,813	C38	55,750	D38	55,653	E38	55,595
B39	55,825	C39	55,758	D39	55,638	E39	55,595
B40	55,841	C40	55,763	D40	55,623	E40	55,566
B41	55,828	C41	55,767	D41	55,624	E41	55,572
B42	55,830	C42	55,763	D42	55,621	E42	55,562
B43	55,823	C43	55,782	D43	55,625	E43	55,547
B44	55,824	C44	55,786	D44	55,627	E44	55,575
B45	55,829	C45	------	D45	55,645	E45	55,552
B46	55,836	C46	55,796	D46	55,655	E46	55,575
B47	55,827	C47	55,802	D47	55,682	E47	55,570
B48	55,855	C48	55,818	D48	55,704	E48	55,567

Station	Gammas	Station	Gammas	Station	Gammas	Station	Gammas
B49	55,870	C49	55,831	D49	55,714	E49	55,570
B50	55,863	C50	55,825	D50	55,709	E50	55,573
B51	55,835	C51	55,831	D51	55,712	E51	55,589
B52	55,850	C52	55,840	D52	55,718	E52	55,750
B53	55,859	C53	55,854	D53	55,706	E53	55,750
B54	55,868	C54	55,872	D54	55,710	E54	55,748
B55	55,865	C55	55,862	D55	55,710	E55	55,753
B56	55,865	C56	55,879	D56	55,707	E56	55,756
B57	55,863	C57	55,926	D57	55,707	E57	55,746
B58	55,860	C58	55,903	D58	55,689	E58	55,760
B59	55,867	C59	55,906	D59	55,675	E59	55,746
B60	55,865	C60	55,895	D60	55,674	E60	55,746
B61	55,871	C61	55,905	D61	55,663	E61	55,737
B62	55,864	C62	55,921	D62	55,659	E62	55,744
B63	55,723	C63	55,889	D63	55,653	E63	55,740
B64	55,732	C64	55,888	D64	55,646	E64	55,695
B65	55,730	C65	55,887	D65	55,630	E65	55,713
B66	55,733	C66	55,873	D66	55,617	E66	55,707
B67	55,735	C67	55,900	D67	55,623	E67	55,698
B68	55,734	C68	55,911	D68	55,635	E68	55,702
B69	55,731	C69	55,858	D69	55,628	E69	55,685
B70	55,731	C70	55,864	D70	55,620	E70	55,681
B71	55,734	C71	55,889	D71	55,620	E71	55,669
B72	55,730	C72	55,877	D72	55,606	E72	55,685
B73	55,734	C73	55,883	D73	55,606	E73	55,681
B74	55,736	C74	55,871	D74	55,608	E74	55,633
B75	55,737	C75	55,875	D75	55,588	E75	55,641
B76	55,748	C76	55,850	D76	55,602	E76	55,639
B77	55,733	C77	55,856	D77	55,593	E77	55,628
B78	55,730	C78	55,843	D78	55,586	E78	55,631
B79	55,720	C79	55,820	D79	55,588	E79	55,619
B80	55,724	C80	55,789	D80	55,567	E80	55,600
B81	55,718	C81	55,772	D81	55,576	E81	55,587
B82	55,734	C82	55,855	D82	55,571	E82	55,600
B83	55,711	C83	55,841	D83	55,559	E83	55,587
B84	55,707	C84	55,815	D84	55,570	E84	------
B85	55,689	C85	55,796	D85	55,585	E85	55,572
B86	55,690	C86	55,797	D86	55,595	E86	55,569
B87	55,654			D87	55,586	E87	55,572
B88	55,659			D88	55,612	E88	55,537
B89	55,648			D89	55,632	E89	55,576
B90	55,620			D90	55,641	E90	55,577
B91	55,616			D91	55,663		
B92	55,602			D92	55,667		
B93	55,584			D93	55,691		
				D94	55,696		
				D95	55,713		
				D96	55,709		
				D97	55,712		
				D98	55,720		
				D99	55,728		

Station	Gammas
D100	55,750
D101	55,744
D102	55,751
D103	55,755
D104	55,756
D105	55,754
D106	55,753
D107	55,760
D108	55,762
D109	55,744
D110	55,743
D111	55,763
D112	55,759
D113	55,761
D114	55,774
D115	55,775
D116	55,794
D117	55,800
D118	55,814
D119	55,833
D120	55,849
D121	55,856
D122	55,872
D123	55,884
D124	55,875
D125	55,878
D126	55,879
D127	55,887
D128	55,873
D129	55,883

Station	Gammas	Station	Gammas
F1	55,616	G1	55,737
F2	55,592	G2	55,731
F3	55,597	G3	55,708
F4	55,592	G4	55,719
F5	55,588	G5	55,733
F6	55,593	G6	55,715
F7	55,576	G7	55,729
F8	55,592	G8	55,734
F9	55,608	G9	55,725
F10	55,621	G10	55,734
F11	55,610	G11	55,739
F12	55,610	G12	55,735
F13	55,621	G13	55,737
F14	55,627	G14	55,750
F15	55,624	G15	55,752
F16	55,614	G16	55,756
F17	55,627	G17	55,753
F18	55,635	G18	55,764
F19	55,635	G19	55,766
F20	55,639	G20	55,764
F21	55,615	G21	55,761
F22	55,632	G22	55,758
F23	55,622	G23	55,756
F24	55,633	G24	55,760
F25	55,638	G25	55,796
F26	------	G26	55,784
F27	55,630	G27	55,788
F28	55,638	G28	55,790
F29	55,652	G29	55,778
F30	55,658	G30	55,783
F31	55,658	G31	55,753
F32	55,672	G32	55,765
F33	55,663	G33	55,764
F34	55,669	G34	55,762
F35	55,682	G35	55,764
F36	55,690	G36	55,782
F37	55,695	G37	55,784
F38	55,698	G38	55,775
F39	55,697	G39	55,782
F40	55,710	G40	55,796
F41	55,708	G41	55,792
F42	55,706	G42	55,779
F43	55,705	G43	55,780
F44	55,723	G44	55,795
F45	55,712	G45	55,782
F46	55,718	G46	55,784
F47	55,719	G47	55,789

F48	55,735	G48	55,798
F49	------	G49	55,810
F50	------	G50	55,807
F51	55,585	G51	55,806
F52	55,593	G52	55,846
F53	55,608	G53	55,817
F54	55,609	G54	55,810
F55	55,617	G55	55,835
F56	55,618	G56	55,842
F57	55,622	G57	55,839
F58	55,609	G58	55,865
F59	55,635	G59	55,856
F60	55,634	G60	55,874
F61	55,649	G61	55,862
F62	55,648	G62	55,822
F63	55,657	G63	55,848
F64	------	G64	55,872
F65	55,657	G65	55,859
F66	55,672	G66	55,850
F67	55,669	G67	55,865
F68	55,689	G68	55,874
F69	55,681	G69	55,863
F70	55,686	G70	55,863
F71	55,685	G71	55,861
F72	55,680	G72	55,880
F73	55,692	G73	55,860
F74	55,690	G74	55,868
F75	55,708	G75	55,859
F76	55,710	G76	55,865
F77	55,708	G77	55,863
F78	55,729	G78	55,852
F79	55,735	G79	55,828
F80	55,732	G80	55,830
F81	55,758	G81	55,831
F82	55,745	G82	55,834
F83	55,756	G83	55,833
F84	55,751	G84	55,828
F85	55,764	G85	55,819
F86	55,775	G86	55,832
F87	55,780	G87	------
F88	55,777	G88	55,841
F89	55,763	G89	55,832
F90	55,769	G90	55,832
F91	55,771		
F92	55,773		
F94	55,774		
F95	55,772		
F96	55,768		
F97	55,770		
F98	55,769		
F99	55,760		

F100	55,754
F101	55,743
F102	55,749
F103	55,742
F104	55,744
F105	55,741
F106	55,737